2006

Mathematical model of arsenic adsorption in a modified zeolite / Microfiltration System

Miles B. Beamguard
University of South Florida

Mathematical Model of Arsenic Adsorption in a Modified Zeolite / Microfiltration System

by

Miles B. Beamguard

A dissertation submitted in partial fulfillment
of the requirements for the degree of
Doctor of Philosophy
Department of Civil and Environmental Engineering
College of Engineering
University of South Florida

Major Professor: Robert P. Carnahan, Ph.D.
Marilyn Barger, Ph.D.
Richard Gilbert, Ph.D.
Julie Harmon, Ph.D.
Audrey Levine, Ph.D.
Mahmood Nachabe, Ph.D.

Date of Approval:
October 5, 2006

Keywords: Arsenite, Cake Layer, Chabazite, Copper, Iron

DEDICATION

This dissertation is dedicated to my friends and family but most importantly to the memory of my good friend Doug Ketchum. I first met Doug in 2nd Grade, where we competed religiously for better math grades. Throughout life we battled to better the other in whatever we did. While I had just started my first semester of graduate school at USF, Doug was moving up the corporate ladder as a trader for Cantor Fitzgerald at the World Trade Center. Although he died on September 11, 2001, our competition lives on and I will always try to accomplish the lofty goals we once set.

ACKNOWLEDGEMENTS

I would like to begin by thanking my major professor, Dr. Robert P. Carnahan, for the wealth of knowledge and guidance he has afforded me over the last five years. The support he has provided me over this time has enabled me to leave my full time position and return to school. While his counseling on the direction of my dissertation was extremely welcomed, his ability to allow me to learn by trial and error made me a more efficient researcher. I truly appreciate his faith in me and his advice when I seem to lose my way. In my work outside of school and from within I have never met a person who has such a busy schedule, but who can still afford the time and energy to provide scholastic guidance and direction in life.

I would also like to thank my committee of Dr. Marilyn Barger, Dr. Audrey Levine, Dr. Mahmood Nachabe, Dr. Richard Gilbert, and Dr. Julie Harmon. Each of you played a fundamental role in my education and direction of my research. Having classes with each of these professors helped to shape my research proposal and provided me an opportunity to get to know their strengths. It is these strengths that I know led to their suggestions to enhance my dissertation and their critical review of my research.

Much appreciation is due to my lab partner Ashutosh Vakharkar, without whom I am sure I would still be in the lab. His patience for my sometimes over-enthusiasm was well beyond that of his age. Many times my haste would have prolonged our work, but his engineering background allowed me to think outside the box while he held true to the job at hand.

Others who deserve appreciation include: Catherine High, for her help in procurement of my materials; Dr. Maya Trotz for the use of her Graphite Furnace AA; the Geology Department for the initial arsenic analysis; Tampa Bay Water for metals analysis and for verification of my methods; and Office of Naval Research (ONR), for funding the main

project, Zeolite Pretreatment for Microfiltration and Ultrafiltration Systems used in Desalination Treatment of Contaminated Water.

Lastly, I would like to thank Jennifer Franklin, my fiancée. By the time this dissertation is published we will have been married and she will truly understand how much of a pain I can be. Her patience with me and her push to have me finish has been unbelievable over the last few months and I truly appreciate her dedication when mine can be lacking. Dr. Carnahan once said to write the dissertation so that even someone who does not understand the engineering behind the project can follow your process and reasoning and feel like they understand the general concept. Through her reading, recommendations, and re-reading of this document, I hope that this goal is accomplished.

TABLE OF CONTENTS

LIST OF TABLES

LIST OF FIGURES

LIST OF NOMENCLATURE

Symbol	Units	Definition
α	µg/L	predicted initial permeate concentration
a	m^2/m^3	zeolite area per bed volume
A	g/s	rate of change in molar mass inside the zeolite
A_m	m^2	membrane area
a_p	mm	particle radius
a_{sat}	m^2	saturated surface area of zeolite
$A_s(\theta_{max})$		correction function accounting for neighboring retained particles
β	1/min	predicted rate of increase in permeate concentration
b	#	Langmuir equilibrium parameter
C_c	%	particle volume fraction in the cake layer = (1 - ε)
C_e	mg/L	concentration of adsorbate in solution (mg/l)
C_E	µg/L	final equilibrium concentration inside the zeolite
C_f	µg/L	feed concentration
C_M	µg/L	instantaneous concentration inside the zeolite
C_p	µg/L	permeate concentration
$C_{z,sat}$	µg/L	saturation concentration in the zeolite
D	#	particle diffusion coefficient which by the Stokes-Einstein equation = $\frac{kT}{6\pi\mu a_p}$
δ_c	mm	cake layer thickness

$\frac{dM_M}{dt}$	g/s	change in molar mass of arsenic inside the zeolite
δ_{sat}	mm	depth of the saturation zone
$E(\tau)$		residence time distribution function
$e^{\frac{-C_M}{\tau}}$	#	acceleration of change in molar mass uptake inside the zeolite
J	$g/m^2/h$	Flux
J_w	$L/(m^2.h)$	Water Flux, with abbreviated units of lmh
k	J/K	Boltzmann Constant
k	m/s	mass transfer coefficient
K_d	#	distribution coefficient
K_L	#	Langmuir constant related to adsorption /desorption energy (l of adsorbent per g of adsorbate)
K_w	$L/(m^2.h)/bar$	pure water mass transfer coefficient
M_c	#	total # of particles per unit area of membrane
m_p	g	total dried mass of cake
M_z	g	Mass of Zeolite in Reactor
n, K_f	#	Freundlich empirical constants dependent on several environmental factors and n is greater than one.
Q	Gal/min or L/min	flow rate
q_e	µg/g	equilibrium adsorption capacity in batch reactor
Q_e	µg/g	adsorption density (mg of adsorbate per g of adsorbent).
q_m	µg/g	maximum adsorption capacity from Langmuir model
Q_{max}	µg/g	maximum adsorption capacity corresponding to complete monolayer coverage (mg of solute adsorbed per g of adsorbent)

$q_{P,i}(\tau,\theta,r)$	g/m^3	solid-phase concentration of organic in the pore of PAC that resided in the contactor for τ and enters at time θ into the UF loop.
$q_{TP,i}(\tau,r)$	g/m^3	solid-phase concentration of organic in the PAC
r	mm	radial distance
ρ_p	g/m^3	density of particle
ε	%	void fraction or solution volume per bed volume
s	m^2	surface area of the zeolite
τ	min	hydraulic retention time
t	min	represents the time from the beginning of the cycle
T	K	Absolute Temperature
T_m	min	mean hydraulic retention time in the UF loop
TMP	psi or bar	transmembrane pressure
t_{sat}	min	time to reach saturation
v	ft/s or m/s	feed velocity
v_{sat}	ft/s or m/s	saturated wave front velocity
y_0	g/s	initial change in molar mass inside the zeolite

MATHEMATICAL MODEL OF ARSENIC ADSORPTION IN A MODIFIED ZEOLITE / MICROFILTRATION SYSTEM

Miles B. Beamguard

ABSTRACT

Carcinogenic health concerns over arsenic in drinking water caused the USEPA to reduce the maximum contaminant level (MCL) from 50 to 10 ppb, effective on January 23, 2006. This has forced many smaller utilities into expensive treatment or discontinuation of water distribution. Researchers throughout the world are working to develop an inexpensive method for arsenic removal to meet this MCL.

Aluminum silicates, or zeolites, are naturally occurring ionic sorbents. Modification of a zeolite may enhance adsorption capacities and ion selectivity. This research investigates the arsenic adsorption capacities of a modified Chabazite. This adsorption, coupled with a hollow fiber, microfiltration membrane substrate, allows for the use of finer zeolite particles. Powdered zeolite creates a cake layer on the filtration surface through which the arsenic solution must filter.

The research goal was to develop an overall mathematical model for the adsorption of arsenic through the adsorption equilibrium isotherms, the cake layer, and the microfiltration operational settings. Baseline adsorption isotherms where performed in distilled water. Solutions containing counter ions were then used to determine any counter-effects. The final isotherms were found using dechlorinated tap water, which is similar to many groundwaters found in the United States. Various runs were used to determine the most efficient modification and loading rate.

Initial characterization of the membrane system defined membrane permeability and inherent arsenic rejection. Variable mass loading in both deadend and crossflow filtration determined that the cake layer was not compressible due to linear pressure increases. This process also determined the maximum cake layer permissible hydraulically on the membrane surface. Membrane system operational characteristics and arsenic dosing were chosen to adhere to these parameters as well as the adsorption isotherms.

Adsorption runs were conducted which varied the flux through the membrane, the arsenic feed concentration, and the cake layer thickness. Through the data collected, a mathematical model based on irreversible adsorption was developed.

This novel approach to arsenic removal and the predictive mathematical model can be used as an effective method for removal of aqueous arsenic, and may provide small water utilities with a cost effective way to meet the recommended new MCL.

INTRODUCTION

On the earth's surface arsenic represents nearly 0.00005% of the total mass making it the 20th most abundant element found in the earth's crust (Gulledge, 1973). While highly prevalent in soil, arsenic can also be found in water. In most natural waters the arsenic usually occurs in two inorganic forms, specifically arsenic trioxide, As(III), and arsenic pentoxide, As(V). As(III) usually exists as a single ionic species while As(V) may exist in two species at a neutral pH and are predominantly in the form of H_3AsO_3 , and $H_2AsO_4^-$ and $HAsO_4^{2-}$, respectively.

Due to its presence in water, the natural method of human exposure is through ingestion. While both arsenic trioxide and pentoxide can result in cancerous and non-cancerous health effects, the oxidation of As(III) within the body poses a serious health concern (NRC, 1999). Following the publishing of these findings the USEPA reclassified arsenic as a Class A carcinogen. The findings suggested that long term exposure to low arsenic levels (less than 50 ppb) contributed to detrimental health effects, including skin, bladder, kidney, and lung cancer, as well as other complications to the epidermal, neurological and cardiovascular systems. While exposure to acute high levels of arsenic can cause more immediate health effects, these are uncommon in the US and it was thus decided to lower the long term exposure (USEPA, 2000).

To lower the chronic exposure to arsenic, the USEPA reduced the MCL of arsenic in drinking water from 50 ppb to 10 ppb. As of January 23, 2006, all public water utilities were to meet this standard, terminate distribution of water exceeding the MCL, or apply for an extension due to implementation of treatment. While larger systems have the capital to add a treatment process to an existing system for polishing, smaller systems with minimal treatment do not. Of the systems affected by the new MCL, 93.6% of these fall into the category of small systems, or systems with less than 10,000 connections. For these systems it is paramount that effective and affordable treatment technologies are developed. To date, arsenic treatment developments have mainly focused on larger

centralized systems or the household point-of-use type system. The implementation of either of these can be both time consuming and financially burdening, but must be done to meet the new MCL.

Some of the technologies which are currently available include: coagulation/precipitation, ion exchange, adsorption processes, and reverse osmosis. While each of these processes is effective in removal of As(V), few have shown to be effective in removal of As(III). Materials that have shown As(III) sorption capacity include activated alumina; iron media (granular ferric hydroxide, iron oxide coated sand, iron pyrites), synthetic ion exchange resins, and fly ash. Zeolites, which are naturally occurring aluminum silicates, have also shown a high affinity for sorption of As(III). It has been shown that by copper or iron treatment of zeolites, the sorption capacity for arsenic may be greatly enhanced (Vakharkar, 2005).

Adsorptive media such as zeolites are normally used in a column configuration through which the contaminated water is passed. These columns, while effective, hydraulically require the use of granular size media. This size is important so that the bed does not have too high of a headloss and so that it is stable both in filtration as well as when it must be regenerated. Use of a smaller grain size would increase the number of available adsorptive sites per surface area for arsenic adsorption; however this is not feasible with a column.

Similar adsorptive materials such as activated carbon have also been used in columns for removal of organics. A higher surface area version of activated carbon is powder activated carbon (PAC) which is usually applied in slurries within a mixing process and must be filtered out at a later stage in the treatment process. An alternative to this adsorptive train was introduced in the 1990's by Aquasource, a membrane manufacturer. Their membrane with a nominal pore size of 0.1 microns could be used to filter out the PAC from water. This allowed the PAC to be fed directly into the feed stream and then removed in one step. This process of filtration for removal of PAC results in the formation of a cake layer on the membrane surface and thereby creates a layer of adsorptive material through which the adsorbate must pass. Based on this methodology, it stands to reason that a powderized zeolite cake layer on a membrane would be an

effective method for treatment of arsenic. If effective, a predictive model would be necessary to ensure that the system would meet the desired effluent and determine the life expectancy of the cake layer.

RESEARCH AND OBJECTIVES

The primary objectives of this research were to develop an effective adsorptive process for arsenic removal and a model which predicts process performance. To accomplish these objectives, successive experiments were conducted to develop an adsorptive media, define membrane system characteristics, and determine arsenic removal using the zeolite/membrane system. Each of these tasks was broken into the following subtasks:

1. Develop adsorptive media
    a. Modify the zeolite using a copper or iron solution
    b. Conduct equilibrium and kinetic studies using the modified zeolites in de-ionized water
    c. Conduct equilibrium and kinetic studies in dechlorinated tap water and ground water which assesses the competitive adsorption capacity for arsenic in the presence of other species
    d. Conduct equilibrium and kinetic studies for arsenic adsorption using modified zeolites in presence of other competing ions like chlorides, hydroxides and sulfates using a matrix of low and high concentrations of the competing species.
    e. Define the governing isotherms and pick the best candidate for further work
2. Define the membrane characteristics
    a. Develop system which was hydraulically similar to a full scale system
    b. Determine initial permeability of the membrane
    c. Develop cake formation characterization through variable mass loading

d. Determine dosing objectives to meet adsorption isotherms previously determined

3. Determine the arsenic removal using the zeolite/membrane system

    a. Determine the impact of flux rate by varying the feed flow rate

    b. Determine the impact of the thickness of the cake layer by varying the amount of zeolite added to the membrane reactor

    c. Determine the impact of arsenic concentration in the reactor by changing the feed concentration

Once the data from the zeolite/membrane experiments were analyzed, existing adsorption models were used to evaluate the data and operational conditions. Trying to fit this data to a known model aided in the understanding of the fundamentals which governed the adsorptive process. These fundamentals, while important to the physical meaning of the process, do not aid the general utility manager in development of a useful tool for removal of arsenic from their water. To accomplish this objective, the model needed to be based on measurable quantities which are available through normal facility operations. These quantities being the arsenic entering their facility, the flow rate through their facility, and the amount of adsorptive material the facility would need to use. Understanding the importance of each of these and their relationship with the overall arsenic removal capacity was necessary to provide a working tool for small systems.

LITERATURE REVIEW

Development of a new method for arsenic removal required background research in several key areas. Those being:

1. Arsenic Occurrence - To determine how prevalent the element exists in nature
2. Arsenic Chemistry - To examine the relevant functional groups
3. Methods and Costs Associated with Arsenic Treatment - To quantify the costs estimated for arsenic removal and to review current and possible methods for arsenic removal
4. Background on Adsorption Isotherms - To understand how arsenic removal through adsorption would be quantified
5. Cake Layer - To review known methods for determining the cake layer thickness where adsorption will occur
6. Membrane with Adsorbent Models - To provide possible systems of equations for modeling the new zeolite/membrane process

Arsenic Occurrence

Arsenic (As) is a metalloid, which has an atomic number of 33. Having many allotropic forms, it is regularly present as yellow, black, or grey solids. Although its presence is not uniform around the world, countries which have levels high enough to cause concern include USA, China, Chile, Bangladesh, Taiwan, Mexico, Argentina, Poland, Canada, Hungary, Japan, and India (Robertson, et al., 1986).

Arsenic in the United States is most prevalent around areas where lumber is produced, but is also seen quite often in areas of agriculture such as Florida where arsenic was used in a cattle dip for screw worms and in central California where it was dispersed in

pesticides. Figure 1 shows the arsenic occurrence found in groundwaters around the country. The figure clearly shows many water sources which exceed the MCL.

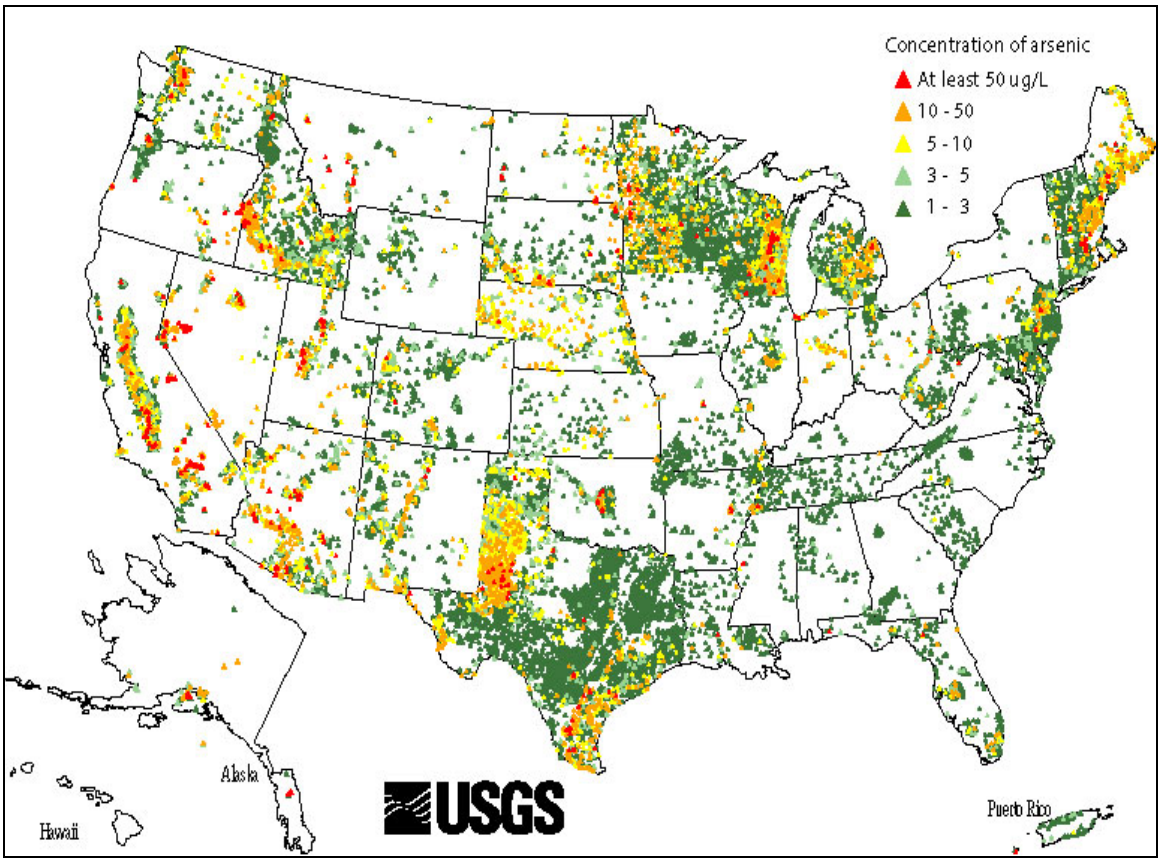

Figure 1 - Occurence of arsenic in groundwater in the United States
(Figure adopted from USGS National Water Quality Assessment, 2001)

Natural inorganic arsenic is found in two oxidation states, arsenite (As(III)) and arsenate (As(V)). In natural waters arsenite usually is present as a nonionic arsenious acid (H_3AsO_3), while arsenate occurs in two anionic forms ($H_2AsO_4^-$ and $HAsO_4^{2-}$) (Clifford and Lin, 1995). Groundwaters, which are oxygen deficient, usually contain the reduced form of arsenic, As(III). In surface waters the arsenite is usually oxidized to arsenate at a relatively slow rate. Treatment of these waters differs due to the different speciation, and in most instances As(III) must first be oxidized to As(V) prior to some type of filtration, coagulation, or adsorption.

Arsenic Chemistry

The most common mineral form of arsenic is arsenopyrite (FeSAs). When this substance is heated the arsenic sublimes and leaves the ferrous sulfide. Once sublimated it is free to enter other phases of the environment; typically mobilizing in groundwater. Understanding the oxidation and reduction reactions of arsenic and how these two species exist in water is paramount to developing remediation treatments (Croal, 2006). Arsenite is slightly soluble in water in the form of arsenious acid ($HAsO_2$). The dissolution reaction for As(III) is as given below:

$$As_2O_3 + H_2O \rightarrow 2HAsO_2 \qquad \text{(Pontius, 1994)}$$

As(V), the oxidized form of arsenic trioxide, forms arsenic acid (H_3AsO_4) in water,

$$As_2O_5 + 3H_2O \rightarrow 2H_3AsO_4 \qquad \text{(Pontius, 1994)}$$

The rate of oxidation of arsenic (III) to arsenic (V) is rapid at high and low pH ranges but proceeds much slower in the neutral pH range (Sorg, 1978). While some microorganisms are able to methylate arsenic into other organic and inorganic compounds, this process is not thermodynamically favored and thus does not play a large role in the alteration of the oxidation states (Pierce, 1980).

Arsenate, As(V), has a net negative ionic charge at neutral pH as seen in Figure 2. By having a charge, many ion exchange processes are able to effectively reduce this form of arsenic. The speciation percentage versus pH is shown in Figure 3. At a neutral pH of 7 approximately 36.5% of the arsenic is present as $H_2AsO_4^-$ and approximately 63.5% as $HAsO_4^{2-}$. Temperature also may impact this speciation.

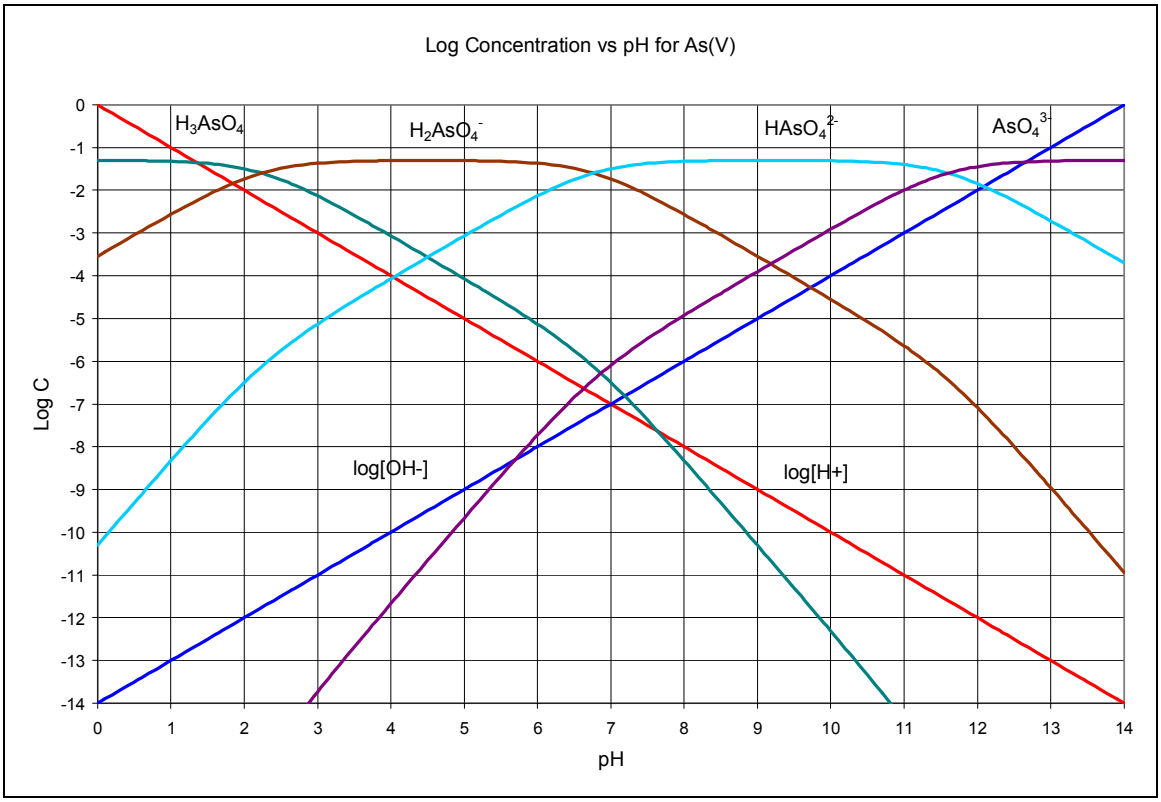

Figure 2 - Log concentration vs. pH for As(V)

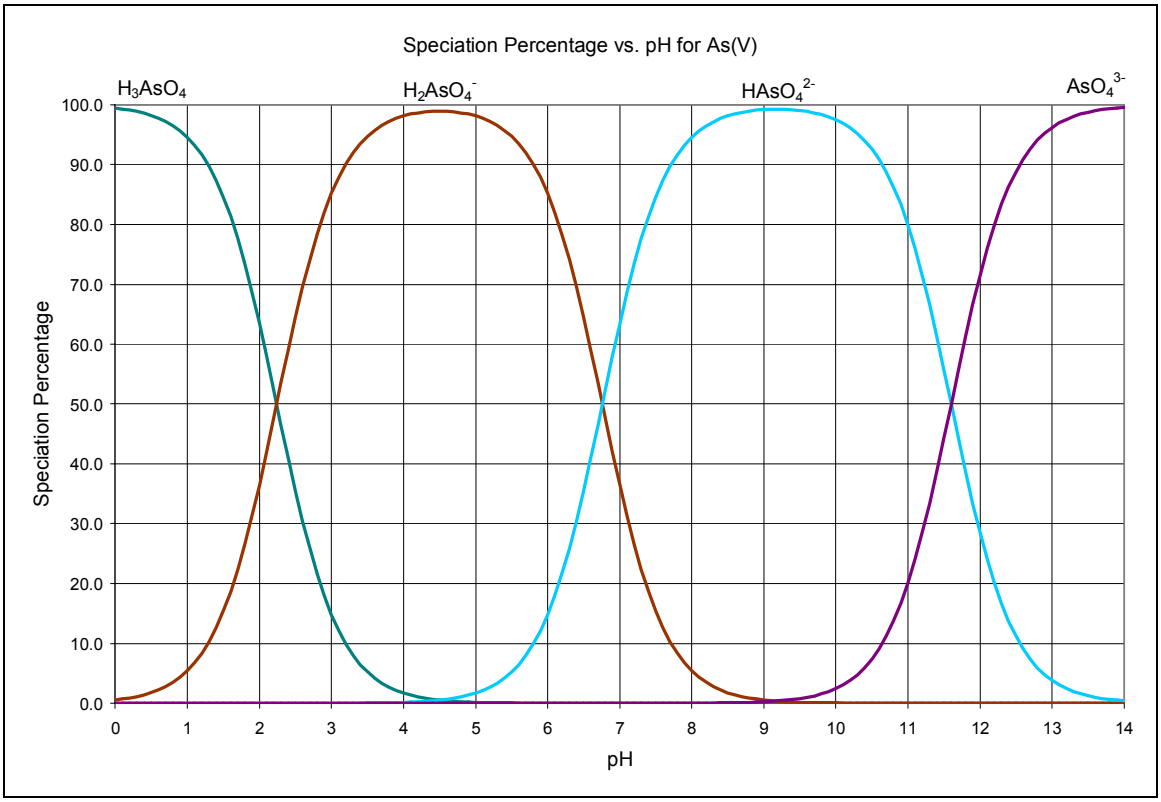

Figure 3 - Speciation percentage vs. pH for As(V)

In Figure 4 and 5 the concentration and the speciation of As(III) is shown, where at a neutral pH of 7 over 99.4% of the arsenic exists as H_3AsO_3 with only 0.58% as the ionic species ($H_2AsO_3^-$).

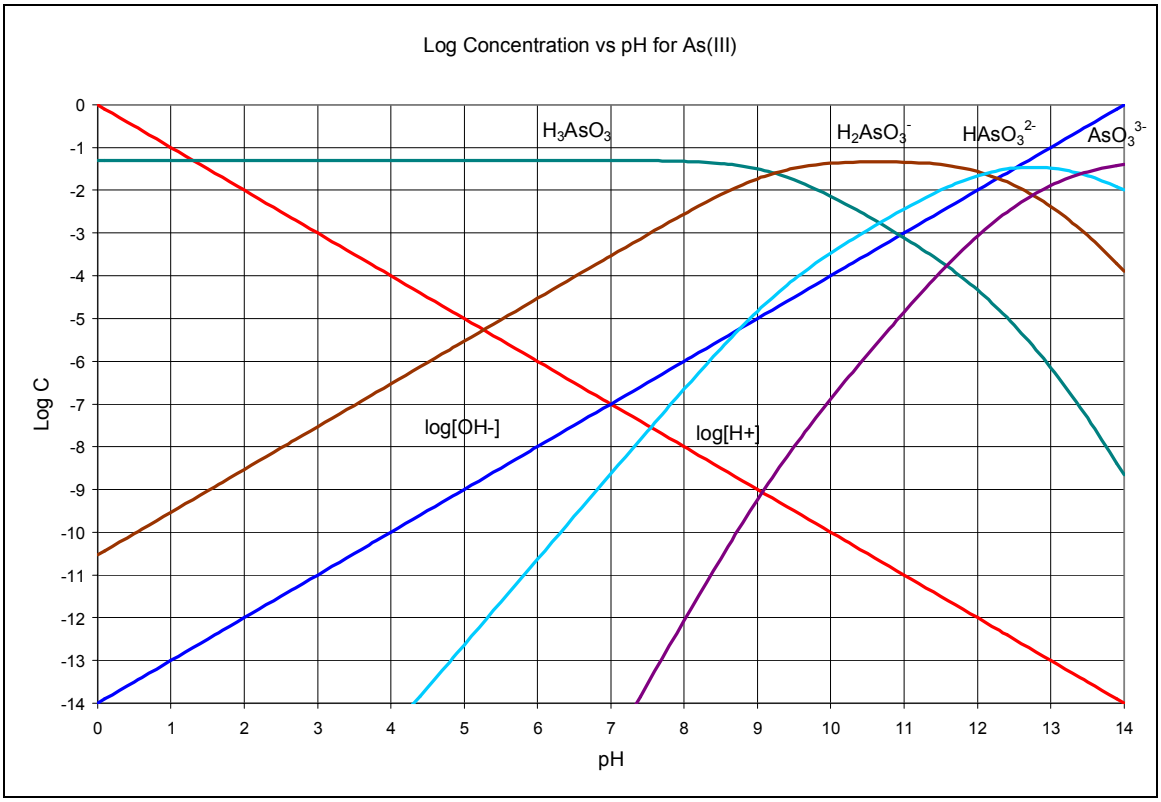

Figure 4 - Log concentration vs. pH for As(III)

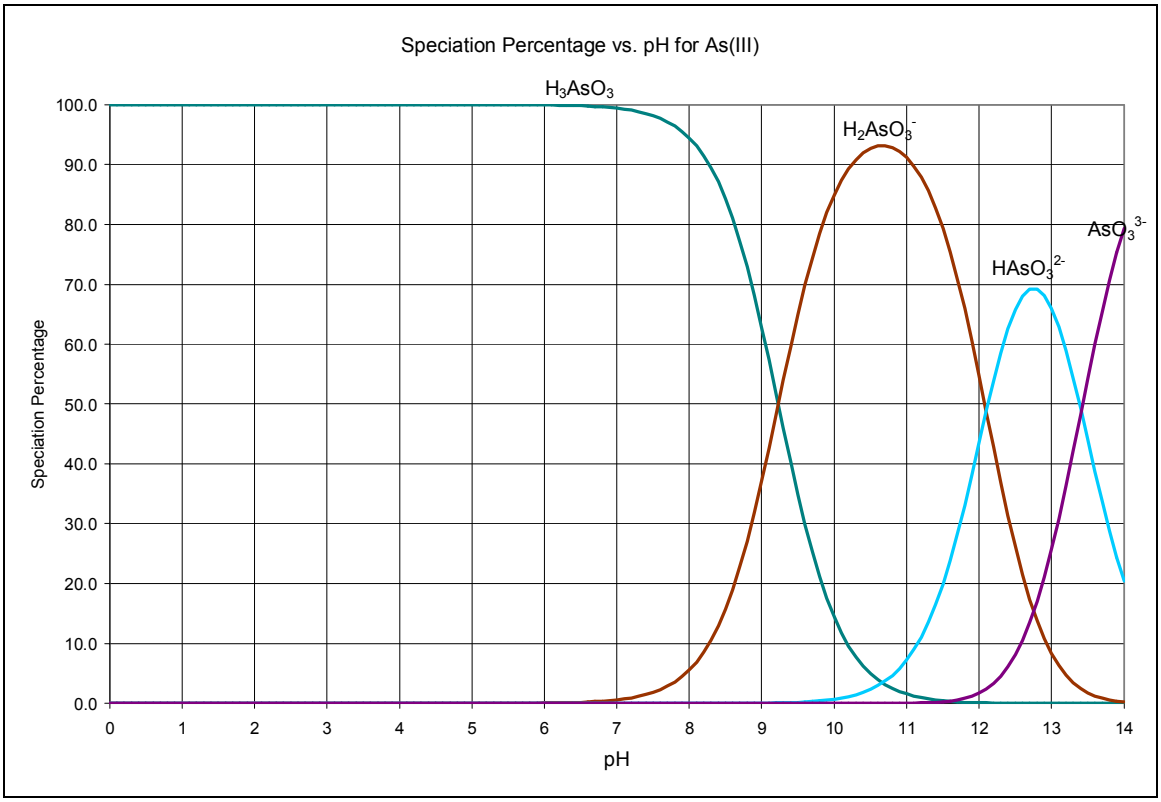

Figure 5 - Speciation percentage vs. pH for As(III)

Without an ionized arsenic species, arsenic is difficult to remove by chemical coagulation or reverse osmosis. With this in mind and based on the speciation of As(III) it is necessary to either first oxidize the As(III) to As(V) or raise the pH of the water to increase ionization. Depending on the buffering capacity of the water, it may be cost prohibitive to raise the pH to 9.23 just to remove 50% of the arsenic. An alternative method is to oxidize As(III) in the water using free chlorine as shown in the following reaction.

$$AsO_3^{3-} + H_2O \rightarrow AsO_4^{3-} + 2e^- + 2H^+$$

$$\underline{HOCl + 2e^- + H^+ \rightarrow Cl^- + H_2O}$$

$$HOCl + AsO_3^{-3} \rightarrow AsO_4^{-3} + Cl^- + H^+$$

This oxidation process results in the addition of chloride to the water and the reduction in pH. Unfortunately the HOCl may also interact with organics and form disinfection by-

products (DBPs) or oxidize other metals resulting in a higher chlorine demand. Other downstream processes, like Reverse Osmosis, may also be chemically incompatible with an oxidant residual.

Methods and Costs Associated with Arsenic Treatment

When the USEPA recently reduced the maximum contaminant level (MCL) of arsenic in drinking water from 50 µg/L to 10 µg/L there was a drastic change in the number of utilities faced with providing treatment. When the MCL was set at 50 µg/L only 0.51% of all Community Water Systems (CWS) were over the standard. With the new MCL, 6.18% of all CWS have water services exceeding the 10 µg/L MCL. This 6.18% or 3034 CWS must implement additional treatment or find alternative water sources now that the 2006 deadline has past (USEPA, 2004). Table 1 charts these 3034 CWS by their number of connections and source water.

Table 1 - Utilities over the 10 µg/L arsenic MCL

Utility Size	<100	101-500	501-1000	1001-3300	3301-10K	10K-50K	50K-100K	100K-1M
Ground Water	874	934	312	424	218	144	19	11
Surface Water	10	18	11	23	16	13	3	4
Total	884	952	323	447	234	157	22	15

Adapted from http://www.epa.gov/safewater/ars/prop_ria.pdf

As can be seen from Table 1, 2936 CWS or 96.7% have ground water supplies which usually indicates the arsenic will probably be present in its reduced state (As(III)). Over 93% of the utilities affected are classified as "Medium water systems" or smaller (less than 10,000 people). Even more disturbing than this is the fact that over 60% of the total number of affected systems fall into the "Very Small water system" classification which

have less than 500 people (USEPA, 2004). This means the largest portion of utilities affected have the smallest group of individuals to defray capital improvement costs. The mean annual household water bill increase in order to meet the new standard implementing current technologies is shown in Table 2 for the same utility sizes previously described.

Table 2 - Annual mean household cost for meeting 10 µg/L arsenic MCL

Utility Size	<100	101-500	501-1000	1001-3300	3301-10K	10K-50K	50K-100K	100K-1M	Total
Cost, $	357.17	246.38	98.35	56.51	37.04	29.13	22.80	18.32	33.65

Adapted from http://www.epa.gov/safewater/ars/prop_ria.pdf

In order to meet the new MCL, small utilities must find alternative sources or more economic ways of removing the arsenic present in their water.

While several technologies which can effectively remove arsenic from water exist, such as reverse osmosis, ion exchange, coagulation/precipitation, and adsorption; for communities without significant resources, adsorption processes seem to be the most practical approach. Adsorption can occur on many mediums such as fly ash, activated alumina, and iron fillings. This process may be centrally located in a plant consisting of a series of columns or a cartridge under the sink as a point of use device. Both of these options represent a financial burden to the community and require an engineering study to develop the chemistry to make the system work.

In order to select a treatment process for the community an engineering firm must establish the design criteria based on the community's specific needs. To do this, they must know their maximum daily flow rate, an average daily flow rate, the historic level of arsenic in their water, the desired finished water quality, and the cost of other consumables (USEPA, 2000).

Coagulation and Precipitation

The most common method for removal of arsenic in the United States is through coagulation and precipitation with metal salts such as aluminum or iron (Buswell, 1943). During this process the arsenic is removed through three main mechanisms (Edwards, 1994):

1. Precipitation: the formation of the insoluble compounds Al (AsO_4) or Fe (AsO_4).
2. Co-precipitation: the incorporation of soluble arsenic species into a growing metal hydroxide phase.
3. Adsorption: the electrostatic binding of soluble arsenic to the external surfaces of the insoluble metal hydroxide.

Of these mechanisms, co-precipitation and adsorption tend to dominate the removal process. Once adsorbed or co-precipitated the complex is either filtered or allowed to settle. Some lighter complexes such as arsenic with hydrous aluminum oxide (HAO) or hydrous ferrous oxide (HFO) may remain suspended in the water. Studies have demonstrated that coagulation and sedimentation alone only removed 30% of the arsenic; while after filtering through a 1.0 micron filter more than 96% of the arsenic was removed (Hering, Sancha, 1999b). Table 3 below presents several coagulation studies with various coagulants and forms of arsenic. While As(V) was removed at a neutral pH, to remove As(III) the pH had to be raised to 11.8 to achieve this level of removal.

Table 3 - Summary of arsenic removal by coagulation studies (Forlini, 1998)

Coagulant	Dosage	Influent Arsenic Concentration (mg/L)	pH	Form of Arsenic	Lowest Achievable Arsenic Concentration	Reference
Hydrated Lime $Ca(OH)_2$	N/A	0.075	11.1	As(V)	0.004 mg/L	McNeil, 1994
Ferric Sulfate $Fe_2(SO4)_3$	10-50 mg/L	0.020	5-8	As(V)	0.001 mg/L	Gulledge, 1973
Alum $Al(OH)_3$	10-50 mg/L	1.6	5-8	As(V)	0.013 mg/L	Gulledge, 1973
Ferric Chloride $FeCl_3$	3-10 mg/L	1.6	7.18 -7.8	As(V)	0.074 mg/L	Scott, 1995
Hydrated Lime $Ca(OH)_2$	1250 mg/L	0.59-0.60	11.8	As(III)	0.060 mg/L	Dutta, 1991

Adsorption Processes and Materials

Adsorption occurs when an adsorbate, which can either be a liquid or gas, accumulates on the surface of an adsorbent, either solid or liquid, and forms an atomic or molecular film. This physical/chemical process is a consequence of surface energy and can occur in a coagulation step or on a fixed media. Since this bonding is on the surface sites of the media, the greater the surface area per gram, the larger the capacity of adsorption media. These adsorbents can be developed from numerous natural and manmade media and vary

in size, chemical composition, regeneration requirements, cost, and affinity for various molecules. Some of these adsorptive materials are describe in detail below.

Ion Exchange

Ion exchange, IX, is a process in which ions are exchanged from a solution phase into an insoluble solid resin or gel. Originally natural zeolites were used as ion exchange materials, but synthetic ion exchange resins are now more common and are typically fabricated from an organic polymer substrate. Most of these polymers are crosslinked polystyrene which is usually accomplished through the addition of divinyl benzene to styrene. Typically these resins are housed in a column where the arsenic laden water is forced to pass. As(V) can be removed through the use of a strong base anion exchange resin (SBR) in either hydroxide or chloride form. Unfortunately, while these resins can effectively remove As(V) in the pH range of 6.5 – 9.0, they are ineffective at removal of As(III) (Clifford et al., 1998). Similar to other processes, specific ions have a selectivity for removal by ion exchange. Competing ions such as sulfates, nitrates, selenium, and fluorides can reduce the amount of As(V) that may be removed as well as increase the frequency of regeneration. Typically the IX columns are placed at the tail end of a plant to reduce competing anions. Due to its effective removal abilities, the USEPA feels that most systems which have low sulfates (<120 mg/l) and low total dissolved solids (TDS) can feasibly implement ion exchange treatment (NWRA 2001).

The use of ion exchange resins must be carefully maintained in order to keep the bed from running to exhaustion. If this occurs or an ion such as sulfate is dramatically increased in the water, arsenic can re-release into the water at levels greater than the initial feed stream. Typical resins have a greater affinity for sulfate removal and since typical waters contain sulfate concentrations greatly exceeding that of arsenic, careful monitoring of its concentration must be upheld. The preferential ions for the resin exchange are listed below:

$$SO_4^{2-} > HAsO_4^{2-} > NO_3^-, CO_3^{2-} > NO_2^- > Cl^-$$

Once the IX bed is exhausted it must be regenerated. The waste from this process contains extremely high levels of arsenic. Due to the difficulty in disposal of this waste, USEPA does not consider ion exchange for Point of Use/Point of Entry (POU/POE) compliance to the MCL (Kempic J.B. et.al, 2000). While ion exchange is highly effective, studies are still being conducted to improve this process such as indefinite regeneration, As(V) selective resins, and continuous counter current ion exchange. Due to the lack of As(III) removal, ion exchange resins were not suitable as an adsorptive media for this research.

Activated Alumina

Activated alumina (AA) is manufactured by dehydroxylating aluminum hydroxide to form a highly porous media which can have a surface area of over 200 m^2/g. It is used primarily as a desiccant but has also been shown to effectively remove arsenic from water (Wikipedia, 2006). Currently AA is considered the best sorbent for arsenic removal however it preferentially removes fluoride ions.

Similar to IX, the AA is used in packed columns where the contaminated water is passed through in down flow or upflow modes. The pH of the water is maintained between 5.5 and 6.0 to increase its affinity for arsenic.

Competing ions also affect AA in a similar manner as IX; however, the selectivity of these ions is quite different as seen below.

$$OH^- > H_2AsO4^- > Si(OH)_3O^- > F^- > HSeO_3^- > TOC > SO_4^{2-} > H_3AsO_3$$

Like IX, AA is efficient at removal of As(V) but at pH levels below 9.2 it is fairly poor at removing As(III). Raising the pH to above 9.2 is counterproductive as the AA prefers hydroxide to As(III), therefore pre-oxidation of As(III) to As(V) is necessary for effective treatment. Figure 6 demonstrates how this increase in pH dramatically reduces filter run

times. Based on the pH requirements as well as the greater selectivity for fluorides and sulfates, AA was an unacceptable media for further research.

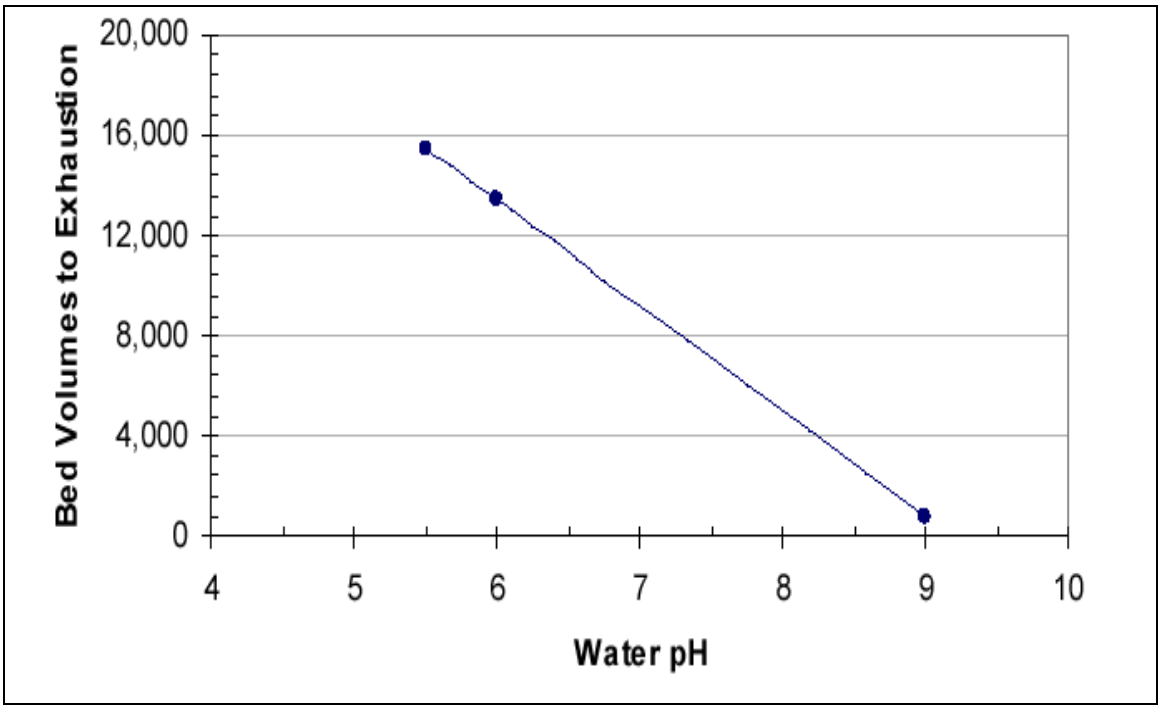

Figure 6 - Effect of pH on activated alumina performance (USEPA, 2000)

Granular Ferric Hydroxide

Granular Ferric Hydroxide (GFH) which was developed at the Technical University of Berlin, Department of Water Control is a promising adsorptive media for arsenic removal. According to a recent study by Banerjee, et al. (2002), the removal of arsenic by GFH was not pH dependent in the range 5 to 7.5. Figure 8 also shows that at a arsenic concentration of approximately 80 µg/L and a GFH concentration of 500 mg/L approximately 100% of both As(III) and As(V) is removed.

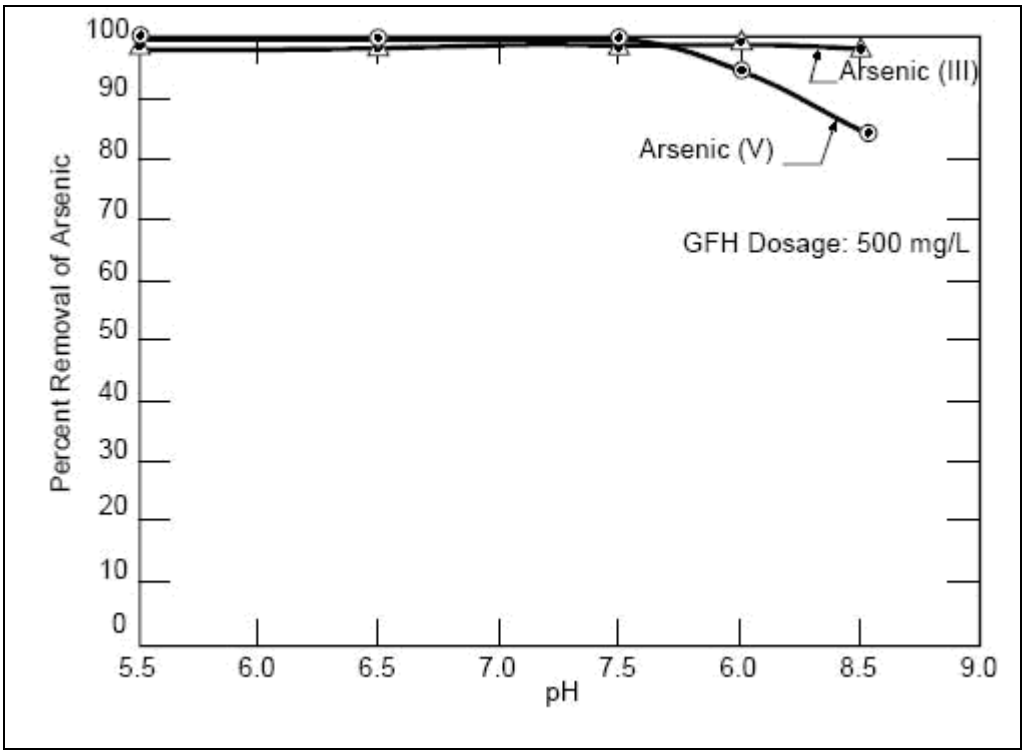

Figure 7 - Effect of pH on arsenic removal by GFH (Banerjee et al. 2002)

Banerjee et al. concluded that GFH was capable of reducing the concentration of arsenic in water below new MCL of 10 µg/L. They also found that the adsorption rate was dependent on reaction pH, media dosage, particle size, and water quality.

Another study by Simms (2000) reported that a 5.3 MGD GFH plant located in the United Kingdom reliably and consistently reduced the average influent arsenic concentrations of 20 µg/L to less than 10 µg/L for 200,000 Bed Volumes (BV) (over a year of operation) at an empty bed contact time (EBCT) of 3 minutes. The arsenic adsorbs onto the surface of the grains of ferric hydroxide forming a ferric-arsenic complex. The operating costs of this system are about $0.10 – $0.25 per thousand gallons treated depending on the influent arsenic concentration.

The greatest deterrent to widespread use of GFH is the media cost. At nearly $4000/ton it is much more expensive then AA. This cost is mitigated however due to the longer runtimes and smaller reactor volumes of GFH versus AA. Another benefit as noted by

Banerjee et al. is that As(III) does not need to be oxidized to As(V) for removal, which results in a reduced chemical cost.

Iron Oxide Coated Sand and Iron Oxide Coated Fiberglass

Iron oxide coated sand and iron oxide coated fiberglass were developed as another media for metal adsorption. Both use fixed bed reactors and are effective for arsenic removal. When arsenic laden water reaches the media, hydroxides on the surface are exchanged for the arsenic. Joshi and Chaudhuri found the oxidation state of arsenic plays a role in its removal, As(V) appears to be more easily removed than As(III). Benjamin et al. (1998) also demonstrated that iron oxide coated sand sorbed As(V) faster than As(III). Kumar et al. (2001) developed IOCFG as an alternative to IOCS and found that 13 times more iron was need to coat the sand in order to achieve the same arsenic removal. While both of the processes have merit, their widespread use has not been witnessed.

Pyrite Fines

Pyrite (FeS_2) is an isometric crystals which once powderized has a high surface area and shows an adsorption capacity for arsenic. Arsenic adsorption studies found that a 10 g/L concentration of pyrite removed 95% of As(III) from solutions when the pH was raised from 7 - 9. It was also capable of removing 98% of As(V) from solutions having pHs ranging from 4 to 7. Both of these processes require very short contact times required to achieve equilibrium (Zoboulis, 1993). Due to the requirement of a higher pH for removal of As(III) Pyrite Fines were not considered for further research.

Zeolites

The term zeolite comes from the Greek words “zeo” (to boil) and “lithos” (stone) (Guisnet, 2002). The first known documentation for a physical or chemical properties of a zeolite was made by Eichhorn around 1880 and was related to the cation exchange capability of the zeolite. In 1945 Barrer introduced the first commercial application of zeolites in which he used Chabazite as a molecular sieve (Breck, 1979). Advances over

the last 50 years have lead to significant breakthroughs in the basic knowledge of zeolites' physical and chemical properties and their potential applications.

It is now known that zeolites are hydrated aluminum silicates of the form (Shim et al. 1999):

$$[(Li, Na, K)_a\ (Mg, Ca, Sr, Ba)_d(Al_{(a+2d)}Si_{(n)(a+2d)}O_{2a})mH_20]$$

These colorless to red minerals are alterations of volcanic tuffs exposed to saline environments (Megamin, 2003, and Virta, 1996). In the US the primary deposits are in Arizona, California, Idaho, Nevada, New Mexico, Oregon, Texas, Utah, and Wyoming. Along with the major zeolites of chabazite, clinoptilolite, mordenite, and phillipsite, other silica or volcanic glasses as well as minerals may be present. Many times the zeolite content will be nearly 100% if the process of alteration has been nearly completed. Of the zeolites mined in the US, chabazite and clinoptilolite make up nearly 52,800 tons annually. Clinoptilolite is primarily mined in California, Nevada, New Mexico, Oregon and Texas while chabazite is mined in Arizona (Virta, 1996).

Zeolites differ in chemical composition and structure that dramatically alter their applications and results. Due to these variations, a zeolite may contain a charge or be neutral. Most of the naturally occurring zeolites have negatively charged frameworks. These frameworks are composed of the three most common elements found in the Earth's crust, aluminum, silica and oxygen. Zeolites are more stable when their external frameworks are balanced by cations, which are normally monovalent or divalent ions such as Na^+ and Ca^{2+} (Seff, 1996). Due to the many varied configurations and chemical properties, any practical application which intends to use zeolites should first undergo extensive tests on a representative sample of the actual zeolite supply to ensure it meets specifications (Armbruster, 2001).

Since chabazite was first discovered to have ion exchange capability, tremendous strides have been made in development of the many current uses and potential applications. These can mainly be summarized into three main categories; Adsorption, Ion Exchange,

and Catalysis. The following table which categorizes zeolite applications was taken from (Breck, 1979) and reproduced.

1. Adsorption
    a. Regenerative
        i. Separations based on sieving
        ii. Separations based on selectivity
    b. Purification
    c. Bulk separations
    d. Non-regenerative
        i. Drying
        ii. Windows
        iii. Refrigerators
    e. Cryosorption
2. Ion exchange
    a. Regenerative processes
        i. NH_4^+ removal
        ii. Metals separations, removal from waste water
    b. Non-regenerative processes
        i. Radioisotope removal and storage
        ii. Detergent builder
        iii. Artificial kidney dialysate regeneration
        iv. Aquaculture - NH_4^+ removal
        v. Ruminant feeding of non-protein nitrogen
        vi. Ion exchange fertilizers
3. Catalysis
    a. Hydrocarbon conversion
        i. Alkylation
        ii. Cracking
        iii. Hydrocracking
        iv. Isomerization

b. Hydrogenation and dehydrogenation
c. Hydrodealkylation
d. Methanation
e. Shape-selective reforming
f. Dehydration
g. Methanol to gasoline
h. Organic catalysis
i. Inorganic reactions
    i. H_2S oxidation
    ii. NH_3 reduction of NO
    iii. CO oxidation
    iv. $H_2O \rightarrow O_2 + H_2$

4. Other applications involve replacing the balancing cation with HDTMA. In this configuration the zeolite has the potential to possibly adsorb ground water contaminants such as PCE.
5. Another example in the waste industry is the removal of ammonium from waste water. Upon removal, the zeolite is regenerated with NaCl/KCl and an Ammonium-Phosphate is left. This media can then be used as fertilizer.
6. NASA currently uses zeolite for treatment of waste water in space.
7. When Chernobyl had a catastrophic failure, the Soviet Union brought in 500,000 tons of zeolite to try and abate the movement of radiation into water sources.
8. Also potential zeolites if charged with Silver could allow for ion exchange of *E. coli.* (Armbruster, 2001).
9. Zeolitic membranes as seen below can improve the fashion in which gases are separated (Exter, 1996).

One of the most heavily mined zeolite in the United States is clinoptilolite. With a structure similar to that of heulandite, clinoptilolite has approximately 15 to 20 m^2 of surface area per gram (Ouki, 1999). This naturally pale green zeolite has a silica to

aluminum ratio of 6. While the internal structure has a net negative charge, clinoptilolite balances this predominantly by adding Na^+ and K^+ (Megamin, 2003). The most common form of clinoptilolite has the chemical formula of:

$(Na,K)_6Si_{30}Al_6O_{72}*nH_2O$

Normally clinoptilolite is found in locations where it is at 60-90% purity making mining and process relatively easy. For this reason mining of this zeolite has been increasing at a rate of 10% a year and typically sells for $50 to $300/ton depending on the purity and quantity. The basic framework of heulandite and clinoptilolite are similar and a representation of this is shown below (Armbruster, 2001).

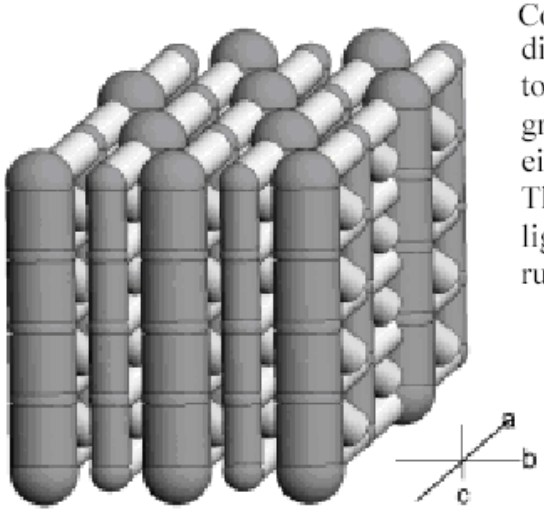

Columnar model of the two-dimensional channel arrangement parallel to (010) in HEU frameworks. The dark gray columns parallel to [001] represent eight- and ten-membered ring channels. These channels are cross-linked by the light gray eight-membered ring channels running parallel to [100] and [102].

Figure 8 - Basic framework of heulandite (Armbruster, 2001)

The various polymorphs of alumina and silica form rectangular pores of approximately 3.0 x 7.6 Angstroms in size (Chon, 1996). This structure does not provide the same large internal cavity as other zeolites such as chabazite. Below are a picture of a clinoptilolite crystal, another structural representation of its framework, and an Atomic Force Microscopy (AFM) image.

Figure 9 - Clinoptilolite crystal from http://mineral.galleris.com

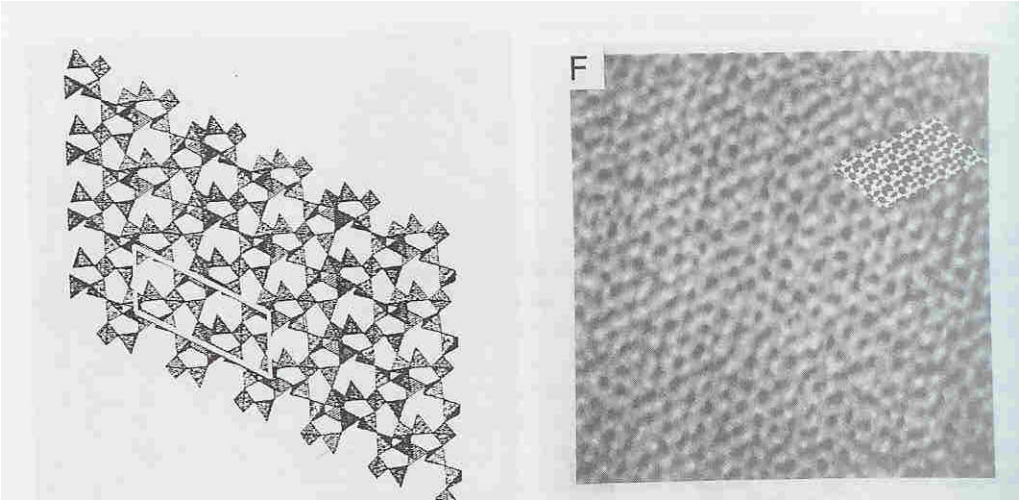

Figure 10 - Clinoptilolite structure and AFM (Occelli, 1994)

Another heavily mined zeolite in the US is chabazite. The structural framework of chabazite is pictured below (Guisnet, 2002).

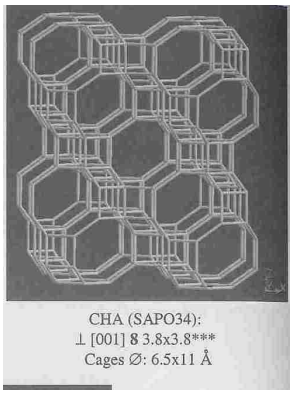

Figure 11 - Structural framework of chabazite (Guisnet, 2002)

As can bee seen from the structure, chabazite is a caged zeolite. This caged structure provides a pore size of approximately 3.8 by 3.8 Angstroms (Chon, 1996). Throughout extensive testing this caged structure has shown a large capacity for ion exchange. For example it has a far greater iron removal capability than greensand or clinoptilolite even after several regenerations. In column studies, it has been shown that this ion exchange capability for iron and manganese dominates oxidation and adsorption as the flow rates through the media increase (Aiello, 1979). Many feel this high ion exchange capability is a result of the high silica content of chabazite and the relatively large cavity to pore size ratio (Harris, 1994); however clinoptilolite has a Si/Al ratio of 6 while chabazite is only 4. Chabazite, as seen in Figure 12, is normally a clear to white crystal.

Figure 12 - Chabazite crystal from http://mineral.galleris.com

Under a scanning electron microscope these crystals are look much more uniform and regular (Kirkov, 1994).

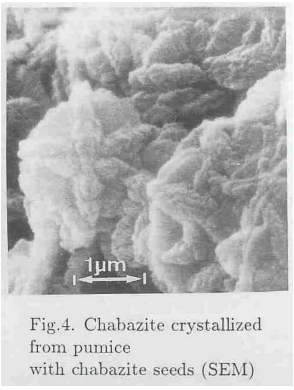

Fig.4. Chabazite crystallized from pumice with chabazite seeds (SEM)

Figure 13 - SEM of chabazite (Kirkov, 1994).

These regular crystals, which normally have a Si/Al ratio of 3.5 to 4.5, hydrate spontaneously under ambient conditions. Upon dehydration it was shown that chabazite maintained its framework. To maintain its charge balance the normally negatively charged zeolite normally in the calcium form. It has been demonstrated that the enthalpy of hydration becomes less exothermic as the water content in the zeolite decreases (Shim, 1999).

One of the most common uses of zeolites is the removal of iron from water and wastewater. Ouki tested this removal ability on waters containing high levels of metals to determine which metals were more likely to be removed (Ouki, 1999). Ouki used both chabazite and clinoptilolite with particle sizes of less than 150 microns. 0.5 g of each zeolite was placed into 100 ml of a solution containing seven metals. The concentration of metals in this solution ranged from 1 to 30 mg/L. These solutions were maintained at a pH of 5 and equilibrium calculations were performed at time 1 to 240 minutes as well as after 24 hours. His results showed that chabazite had a larger ion exchange capacity than clinoptilolite for the selected metals. He estimates that greater than 90% of the removal was achieved during the first five minutes of contact for the chabazite, while the clinoptilolite took approximately 15 minutes to achieve the same level of removal. The data also suggested that 10 mg/L was the optimum metal concentration based on the 0.5 mg of zeolite. These results can be seen in the following graphs:

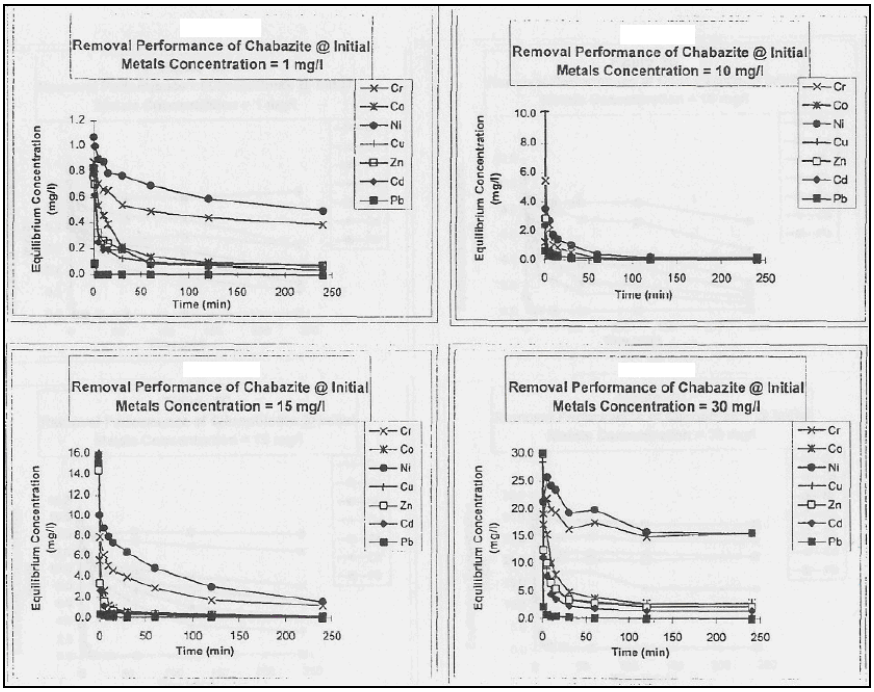

Figure 14 - Metals removal from water using chabazite (Ouki, 1999)

For chabazite the order of rejection best follows: Pb>Cd>Zn>Co>Cu>Ni>Cr.

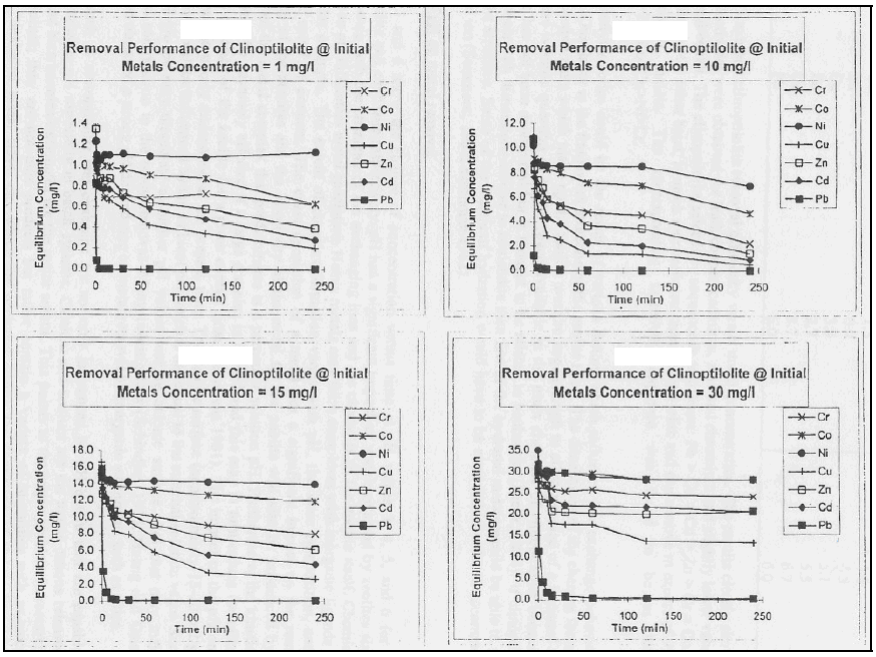

Figure 15 - Metals removal from water using clinoptilolite (Ouki, 1999)

For clinoptilolite the order of rejection best follows: Pb>Cu>Cd>Zn>Cr>Co>Ni (Ouki, 1999).

Although metal removal as described previously occurs as a cation exchange mechanism, arsenic remains undissociated, so a molecular complex sorption mechanism must be used for arsenic removal (Gonzalez and Mattusch, 2001). Pretreatment of the zeolite with Copper or Iron can enhance the adsorption capacity of the zeolite for arsenic. Literature review suggests only one report concerning arsenic removal using the natural zeolites clinoptilolite and chabazite (Carnahan, Forline, Bonnin, 2001).

Membrane Separation

The term Reverse Osmosis, RO, is derived from its counterpart osmosis. Osmosis is a thermodynamic property and a measure of the colligative property of the solution. It is characterized by the natural tendency of a solvent to move from an area of low concentration to an area of high concentration. When a semi-permeable polymeric membrane is placed between two solutions of different concentrations, a pressure will be seen as the two waters try to equilibrate. This pressure is called the osmotic pressure. Applying a pressure greater than the osmotic pressure to the higher total dissolved solids (TDS) side will force water to diffuse into the lower TDS side causing the net osmotic pressure to further increase. Osmotic pressures vary considerably from fresh waters to seawater and consequently the pressures needed to filter water. Operating pressures as low as 30 psi can exist for some low TDS waters while pressures approaching 1000 psi are commonplace in seawater applications.

Since the creation of RO, several other membrane technologies have been developed. Figure 7 relates the size of common materials ranging from sand to dissolved salts to its filtration counterpart. While RO is able to remove nearly everything from water the pressures are sometimes too high for the necessary level of treatment. Nanofiltration (NF), with an approximate pore size of 10^{-9} meters, was developed to operate at less than 200 psi. They can remove nearly all divalent salts and organics and are primarily used to soften waters.

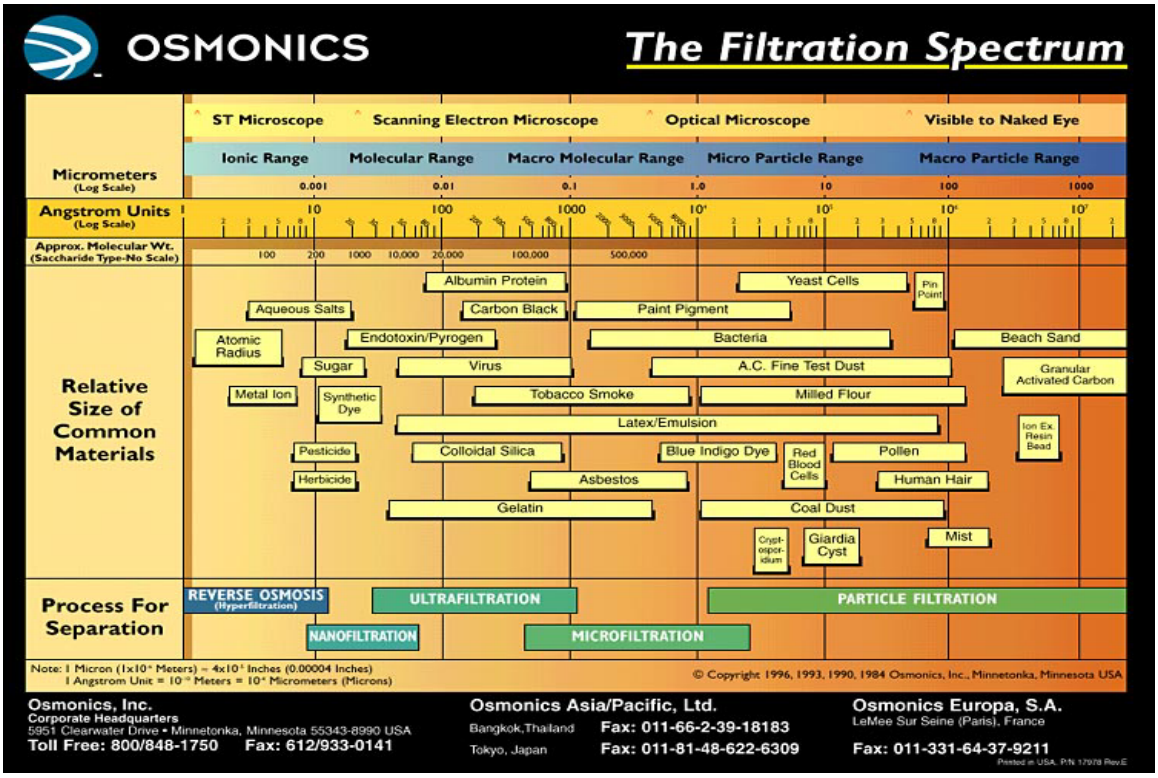

Figure 16 - Membrane separation compared to size of common materials (Osmonics, 2004)

Membranes themselves differ from manufacturer to manufacturer with each having a nominal molecular weight cutoff (MWC). Those with a low MWC are able to separate solutions of monovalent ions at a greater degree than those with higher MWC. A typical MWC for an RO membrane is approximately 100 Dalton. A Dalton is a representative measure of a single molecule based on its molar weight (MW). For example, water whose MW is approximately 18 g/mole, is referenced as 18 Dalton. Sodium, MW = 23 Dalton, hydrates with 6 water molecules and therefore has a total MW of 131 Dalton. Unlike cations such as Sodium, anions do not hydrate as much. Chloride, for example only hydrates with 3 water molecules providing it with a MW of 89.5 Dalton. Due to this MW it passes through an RO membrane more readily. Likewise As(V) being charged also binds with water and is rejected nearly completely by a tight RO membrane. As(III), being uncharged, does not hydrate well and consequently is too small to be rejected completely by the RO membrane. In studies arsenic removal was found to be independent of pH and competitive ions, but somewhat dependent upon temperature.

Removal efficiencies were in range of 75% for As(III) and 95% for As(V) (Kang, Kawasaki, et.al, 2000).

Leaching of arsenic into the finished water is not expected since RO membranes do not typically sorb arsenic. Also oxidation and pH adjustment are not required for arsenic removal, thereby making the system user friendly. Based on these factors, RO has merit as a point-of-use technology; however, due to their inherent costs, low water recovery rates, and higher operating pressures, it is typically more cost effective to place the RO process at a centralized location.

Ultrafiltration (UF) and microfiltration (MF) have pore sizes of 10^{-8} meters and 10^{-6} meters, respectively. These membranes are typically used to remove particulate matter. As seen in Figure 7, each process has a range of sizes that it excludes. This is owed to the casting of the membrane and polymer itself. Due to the pore size and overall lower operating pressures when compared to NF and RO, MF and UF represent applicable separation processes for the removal of the developed adsorptive material. For this reason they were chosen for further research.

Microfiltration and ultrafiltration are hollow fiber polymer membranes that remove primarily suspended solids from water. Polymers used for production of these membranes include cellulose acetate derivatives (CA), polypropylene (PP), polysulfone (PS), polyether sulfone (PES), and polyvinylidene fluoride (PVDF). MF, with a nominal pore size of 0.1 µm, was first introduced by Memtec in the early 1980s and was first installed into a drinking water plant in 1987. UF, which has a nominal pore size of 0.01 µm was developed by Suez Lyonnaise des Eaux in the 1980s and saw its first US plant placed into production in 1988. Since their inception, the proliferation of MF and UF into the US water treatment market has been exponential as depicted in Figure 17.

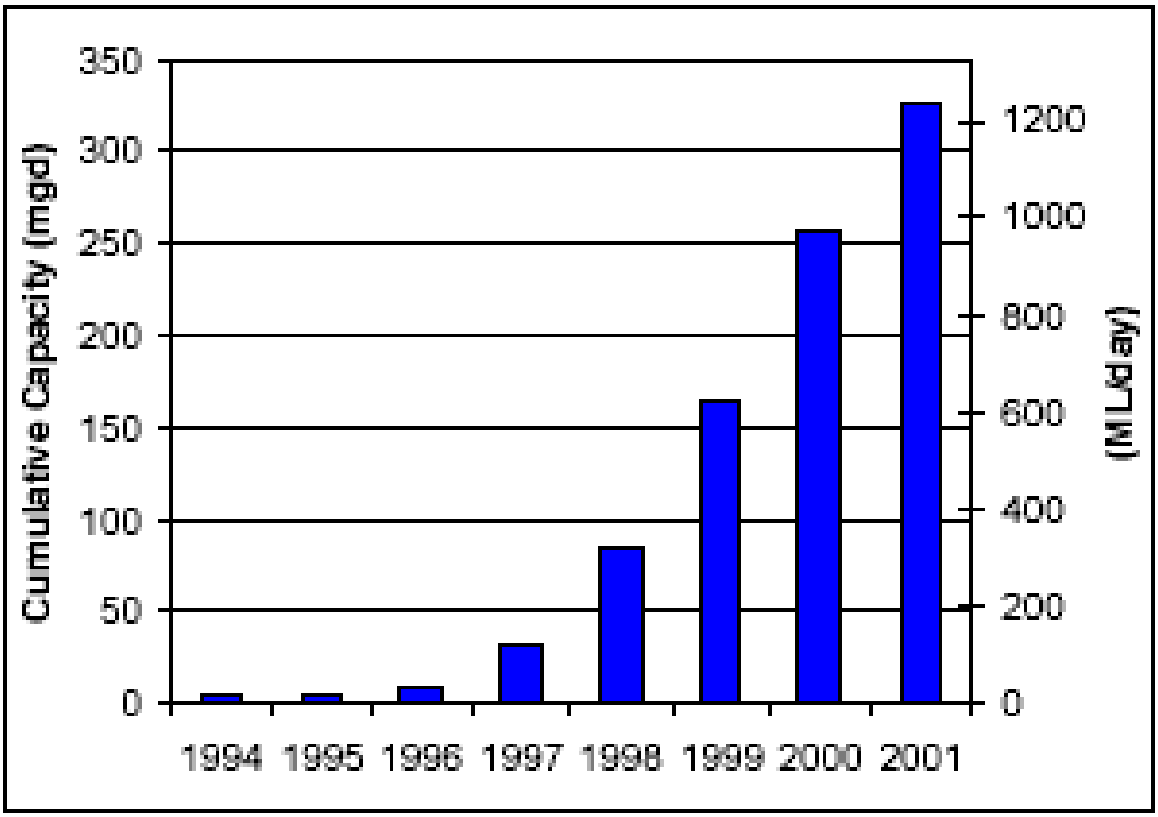

Figure 17 - MF and UF installed capacity in USA (Lozier, J., CH2M-Hill, 2001)

New regulations for Cryptosporidium and Giardia set by the EPA in the 1990s are probably the greatest reasons for this large increase in capacity. Since both Cryptosporidium and Giardia are greater than 0.1 μm in size they are rejected by the MF and UF membranes.

MF and UF can operate in dead-end mode where all water entering the membrane leaves as permeate or in cross-flow mode where a portion of the water not passing through the membrane is mixed with the feed water again. Typically cross-flow is implemented when the level of suspended solids is high or when a greater contact time is needed before permeation. Permeation can occur with flow from the inside to the outside of a fiber (inside-out) or from the outside into the inside of the lumen (outside-in). Outside-in is preferential in high solids loading due to reduced risk of plugging of the heads of the fibers. The configuration for MF and UF systems can vary substantially, but the majority fall into two categories, pressurized and submerged.

A scanning electron microscope (SEM) view of a UF membrane is seen below in Figure 18. This membrane feeds water through the inside of the fiber and permeates out through its walls. The membrane pores are asymmetrical in an effort to reduce the headloss incurred during permeation. This membrane is also double walled around this porous area which allows the membrane to be backwashed. During this process water is passed through the membrane in the opposite direction of normal permeation to remove the buildup of filtered material.

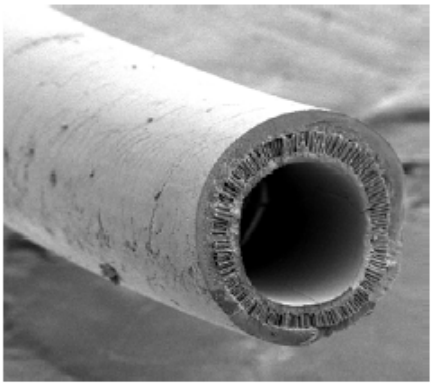

SEM picture of Ultrafiltration Hollow fiber

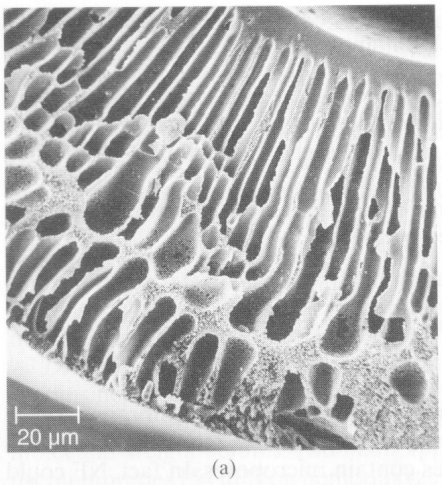

Figure 18 - Cross section of UF membrane under SEM (Mallevialle, 1996)

MF and UF, due to their pore size, which are several orders of magnitude greater than an arsenic molecule, are not inherently able to the contaminant from water. Studies (Vagliasindi, 1998) have been conducted by feeding a ferric coagulant or a ferric hydroxide fine into the feed which have demonstrated removal, but operational conditions governing the process were not well documented.

As a separation process with an absolute pore size, MF and UF can be used to remove fine particulates such as a powderized zeolite which is placed into the membrane housing or reactor. This allows for an extremely fine powder which has a high surface area to be retained on the membrane surface. This rejection of fines results in a cake layer forming on the surface of the membrane. Once formed any adsorbate entering the system must pass through the zeolite cake layer before entering the permeate stream.

Background on Adsorption Isotherms

Adsorption is an essential method for contaminant removal, but understanding of the physiochemical properties governing the reaction is needed to optimize the process. By evaluating the kinetics and equilibrium of a reaction an operational guideline may be produced. Kinetic studies determine the rate at which the process approaches equilibrium and is used to determine the adsorption coefficient and the reaction constant, while equilibrium studies give the capacity of the adsorbent (Ho, 1995) for specific contaminants. While there are many experimental isotherms used in practice, the Freundlich and Langmuir isotherms are the most predominant in water treatment (Muhammad, Parr et al., 1998).

Freundlich Isotherms

In 1894, Freundlich and Küster developed their isotherm which was initially used to describe the equilibrium of gaseous adsorbates and was later applied to liquid systems in 1906. This equation is often expressed by:

$$Q_e = K_f C_e^{1/n} \text{ (Casey, 1997)}$$

where:

Q_e is the adsorption density (mg of adsorbate per g of adsorbent).

C_e is the concentration of adsorbate in solution (mg/l).

K_f and n are the empirical constants dependent on several environmental factors and n is greater than one.

The equation can be linearized by taking the logarithm of both sides:

$$\text{Log } Q_e = \text{Log } K_f + 1/n \text{ Log } C_e$$

If a plot of Log C_e vs. Log Q_e results in a straight line, then the Freundlich Isotherm is an accurate description of the adsorption process. The inverse slope and the intercept of this

line represent the two equilibrium constants n and K_f which denote the sorption intensity and the sorption capacity, respectively (Weber et al., 1991). Large values of n denote that large changes in equilibrium concentration will not affect the adsorption on the adsorbent. If n is equal to 1, the partitioning between the solid and liquid phase is linear and Freundlich coefficient (K_f) can be viewed as a distribution coefficient K_d. Although the Freundlich model applies to high adsorbate concentrations well, it is excellent at predicting lower concentration reactions.

Langmuir Isotherms

In 1916 Irving Langmuir published a new isotherm which was derived from a kinetic mechanism. It is based on the following four assumptions:

- The adsorbent surface is uniform
- Adsorbed molecules do not interact with others
- All adsorption occurs by the same mechanism
- At final adsorption a monolayer is formed and molecules can not be deposited on top of this monolayer

The Langmuir isotherm can be described by the following equation:

$$C_e/Q_e = 1/(Q_{max}.K_L) + C_e/Q_{max}$$

where:

Q_e is the adsorption density at the equilibrium solute concentration C_e (mg of adsorbate per g of adsorbent)

C_e is the concentration of adsorbate in solution (mg/l)

Q_{max} is the maximum adsorption capacity corresponding to complete monolayer coverage (mg of solute adsorbed per g of adsorbent)

K_L is the Langmuir constant related to adsorption /desorption energy (l of adsorbent per g of adsorbate)

Plotting C_e/Q_e versus C_e should yield a linear line if the assumption of a Langmuir isotherm is correct. From the intercept and slope of this line the Langmuir constants of the maximum adsorption capacity, Q_{max}, and the adsorption energy, K_L, can be determined, respectively.

Cake Layer

Literature review of cake formation inside of a membrane reactor led to several studies including:

Faibish (Faibish et al., 1998) studied removal of colloidal suspensions using a cross flow membrane. From their work they developed the following equation for estimating cake layer thickness which led to a means of projecting flux decline:

$$\delta_c = \left(\frac{\frac{4}{3}\pi a_p^{\,3}}{1-\varepsilon} \right) M_c \qquad \text{Equation 1}$$

Where:

δ_c = cake layer thickness

a_p = particle radius

ε = cake porosity or void fraction

And M_c = total # of particles per unit area of membrane

Choi (Choi et al., 2000) developed a more basic model for estimating the thickness of the cake using microspheres in a microfiltration process. In this model they assumed a homogeneous cake layer and were able to simplify their expression for cake layer thickness to:

$$\delta_c = \left(\frac{m_p}{\rho_p (1-\varepsilon) A_m} \right) = \text{volume of cake per area of membrane} \qquad \text{Equation 2}$$

Where:

m_p = total dried mass of cake

ρ_p = density of particle

And A_m = membrane area

Work by Hong (Hong et al., 1997) in removal of colloidal suspensions using a cross flow system, included a diffusion term in the cake layer thickness model.

$$\delta_c = \left(\frac{\frac{4}{3}\pi a_p{}^3 D}{C_c k T A_s(\theta_{\max})} \right) \left(\frac{\Delta P - J R_m}{J} \right) \qquad \text{Equation 3}$$

Where:

D = particle diffusion coefficient using the Stokes-Einstein equation = $\frac{kT}{6\pi\mu a_p}$

$A_s(\theta_{\max})$ = correction function accounting for neighboring retained particles

C_c = particle volume fraction in the cake layer = (1 - ε)

k = Boltzmann Constant

T = Absolute Temperature

The correction function can be calculated as follows:

$$A_s = \frac{1 + \frac{2}{3}\theta^5}{1 - \frac{3}{2}\theta + \frac{3}{2}\theta^5 - \theta^6} \qquad \text{Equation 4}$$

Then using Happel's Cell Model

$\theta = (1 - \varepsilon)^{\frac{1}{3}}$

With an assumed maximum random sphere distribution provides:

$\varepsilon = 0.36$

$\theta_{\max} = 0.86$

$A_s(\theta_{\max}) = 123.22$

Substituting these values into Equation 3, Hong simplified the original cake layer model to the following:

$$\delta_c = \left(\frac{0.0018 a_p^{\ 2}}{(1-\varepsilon)\mu}\right)\left(\frac{\Delta P - JR_m}{J}\right) \qquad \text{Equation 5}$$

Membrane with Adsorbent Models

Reddad (Reddad et al., 2003) studied the adsorption of cadmium and lead onto a natural polysaccharide in a membrane reactor. They found that the equilibrium conditions were best described by the Langmuir isotherm equation as shown below:

$$q_e = \frac{q_m b C_e}{1 + b C_e} \qquad \text{Equation 6}$$

Where:

q_e = equilibrium adsorption capacity in batch reactor

q_m = maximum adsorption capacity from Langmuir model

b = Langmuir equilibrium parameter

C_e = metal concentration at equilibrium

Matsui (Matsui et al., 2000) studied the removal of organic compunds by PAC using a UF system. The system was assumed to be hydraulically similar to a CSTR. This model states:

$$C_{Organics,In} = C_{Organics,Out} + \frac{3C_{PAC}}{R_{PAC}} \int_0^{\infty} \left(\int_0^{R_{PAC}} q_{TP,i}(\tau, r) r^2 dr \right) E(\tau) d\tau \qquad \text{Equation 7}$$

Where:

$q_{TP,i}(\tau, r)$ = solid-phase concentration of organic in the PAC

r = radial distance

τ = hydraulic retention time

C_{PAC} = PAC concentration

R_{PAC} = PAC average radius

and $E(\tau)$ = residence time distribution function

Applying a pore surface diffusion model (PSDM) to this model with the initial and boundary conditions of:

$q_{TP,i}(\tau, r) = 0$ for $\tau = 0$ and $C_{TP,i}(\tau, r) = C_{T,i}$ for t>0 and r = R results in:

$$\frac{\partial q_{TP,i}(\tau,r)}{\partial \tau} = \frac{1}{\rho}\frac{D_{P,i}}{r^2}\frac{\partial}{\partial r}\left(r^2\frac{\partial C_{TP,i}(\tau,r)}{\partial r}\right) + \frac{D_{S,i}}{r^2}\frac{\partial}{\partial r}\left(r^2\frac{\partial q_{TP,i}(\tau,r)}{\partial r}\right) \qquad \text{Equation 8}$$

Where:

$C_{TP,i}(\tau, r)$= concentration of organics in the pore of PAC with a detention time of τ

$D_{P,i}$ = pore diffusion coefficient of organic

$D_{S,i}$ = surface diffusion coefficient of organic

If the PAC is added continuously, a mass balance on the system provides the following system model:

$$T_m\frac{dC_{Orgaincs,Loop}}{dt} = C_{Organics,Out} - C_{Organics,Loop} - \frac{3}{QR^3}\int_0^t\int_0^\infty\left(\frac{\partial}{\partial t}\int_0^R q_{P,i}(\tau,\theta,r)r^2dr\right)Q_c(\theta)E(\tau)d\tau d\theta$$

Equation 9

Where:

T_m = mean hydraulic retention time in the UF loop

Q = flow rate

Q_c = cross-flow rate

$q_{P,i}(\tau,\theta,r)$ = solid-phase concentration of organic in the pore of PAC that resided in the contactor for τ and enters at time θ into the UF loop.

Li (Li et al., 2003) also investigated the use of PAC for removal of organic matter using microfiltration as the separation process. Contrary to Reddad, Li based his model on a Freundlich Isotherm. His model derivation begins with the Freundlich Isotherm:

$$q = KC_{eq}^{1/n} \qquad \text{Equation 10}$$

Incorporating multi-solutes for competitive adsorption and then rearranging to find the equilibrium concentration of a single solute results in:

$$C_{eq,i} = \frac{q_i}{\sum_{j=1}^{N} q_j}\left(\frac{\sum_{j=1}^{N} q_j n_j}{n_i K_i}\right)^{n_i} \qquad \text{Equation 11}$$

For a system containing two solutes, s and t, the equilibrium concentrations can be written as:

$$C_{eq,s} = \frac{q_s}{q_s + q_t}\left(\frac{q_s n_s + q_t n_t}{n_s K_s}\right)^{n_s}$$
$$C_{eq,t} = \frac{q_t}{q_s + q_t}\left(\frac{q_s n_s + q_t n_t}{n_t K_t}\right)^{n_t} \qquad \text{Equation 12}$$

Rearranging and solving for q results in:

$$q_s = \frac{K_s\left(1+\frac{q_t}{q_s}\right)^{1/n_s}}{1+\frac{n_t}{n_s}\frac{q_t}{q_s}} C_{eq,s}^{1/n_s}$$

$$q_t = \frac{K_t\left(1+\frac{q_s}{q_t}\right)^{1/n_t}}{1+\frac{n_s}{n_t}\frac{q_s}{q_t}} C_{eq,t}^{1/n_t}$$

Equation 13

A mass balance on the system provides:

$$C_{0,s} = C_{eq,s} + q_s C_c$$
$$C_{0,t} = C_{eq,t} + q_t C_c$$

Equation 14

Where:

$C_{0,s}$ = initial concentration of solute s

$C_{eq,s}$ = equilibrium concentration of solute s

q_s = the kinetic coefficient of solute s

C_c = concentration of adsorbent

$C_{0,t}$ = initial concentration of solute t

$C_{eq,t}$ = equilibrium concentration of solute t

q_t = the kinetic coefficient of solute t

Li states that if the concentration in the liquid phase is much less than that adsorbed then:

$$\frac{q_s}{q_t} \cong \frac{C_{0,s}}{C_{0,t}}$$

Equation 15

If you substitute this into the original equations for q you arrive at:

$$q_s = \frac{K_s\left(1+\frac{C_{0,t}}{C_{0,s}}\right)^{1/n_s}}{1+\frac{n_t}{n_s}\frac{C_{0,t}}{C_{0,s}}} C_{eq,s}^{1/n_s}$$

$$q_t = \frac{K_t\left(1+\frac{C_{0,s}}{C_{0,t}}\right)^{1/n_t}}{1+\frac{n_s}{n_t}\frac{C_{0,s}}{C_{0,t}}} C_{eq,t}^{1/n_t}$$

Equation 16

If you divide each solutes' q by the equilibrium concentration term you arrive at the competitive adsorption Freundlich coefficient.

$$K'_s = \frac{K_s\left(1+\frac{C_{0,t}}{C_{0,s}}\right)^{1/n_s}}{1+\frac{n_t}{n_s}\frac{C_{0,t}}{C_{0,s}}}$$

$$K'_t = \frac{K_t\left(1+\frac{C_{0,s}}{C_{0,t}}\right)^{1/n_t}}{1+\frac{n_s}{n_t}\frac{C_{0,s}}{C_{0,t}}}$$

Equation 17

If the initial concentration of one is much greater than the other, ie. $C_{0,s} >> C_{0,t}$, then this can be simplified to:

$$K'_t = K_t \frac{n_t}{n_s}\left(\frac{C_{0,s}}{C_{0,t}}\right)^{(1-n_t)/n_t}$$

Equation 18

METHODS AND MATERIALS

Materials

Table 4 summarizes the equipment used in the modification of the zeolite, the jar testing for kinetic and equilibrium tests, microfiltration studies, and analysis.

Table 4 - Materials list

Material	Specification	Quantity	Resource
Zeolite	Na - chabazite, -40 Mesh	20 lb.	GSA Resources
Arsenic	Arsenic Trioxide, 99.9%	100 g	Fisher Scientific
Jar Testers	Compact Laboratory Mixers, 1L	2	ECE Engineering
UV Spectrophotometer	Hach DR4000	1	Hach
pH Meter	Oaktron Ion 510 Series	1	Cole-Parmer
AA	PSA Excalibur AFS	1	University
Distiller	Corning MP-3A	1	University
Pan Balance	Mettler AE 260, 100 g max	1	University
Oven	Blue M Stabil-Therm Gravity Oven	1	University
Sieves	Soiltest, 100, 200, and 400 mesh	1	University
Syringes	BD 20ml Syringes	160	Cole-Parmer
Arsenic Sample Vials	Passport IP2, 30ml, HDPE	72	Cole-Parmer
Membrane	Hydranautics, 0.85 m^2	1	Hydranautics
Membrane Vessel	2” Clear PVC	3 ft	Barnes Industrial
Membrane Skid	0.254 gpm Automatic Skid	1	AES Engineering

A more comprehensive description of the chabazite and chemicals used in the modification and jar testing studies is listed below:

Chabazite Zeolite: The chabazite, a -400 mesh sodium zeolite, was purchased from GSA Resources, Tucson, Arizona. The chabazite was obtained in 20 lbs container. The material safety data sheet (MSDS) for the chabazite is listed in Appendix C.

Arsenic: The laboratory grade arsenic was granular and was purchased from Fisher Chemicals Co, in form of arsenic trioxide (As_2O_3) (99.9%). A stock solution of As(III) was prepared using "Standard Methods for Water and Wastewater, 19th Edition, 1995". The method used to prepare this stock solution and the analysis of arsenic is provided in Appendix A.

Copper Chloride: Copper (I) chloride, which was used to modify the chabazite, was purchased from Acros Organics Co., in form of copper (I) chloride (95%). The modification concentration was 0.01 M.

Ferrous Chloride: Ferrous chloride, which was used to modify the chabazite, was purchased from Fisher Chemicals Co., in form of iron (II) chloride tetrahydrate ($FeCl_2.4H_2O$). The modification concentration was 0.1 M.

Ferrous Sulfate: Ferrous Sulfate, which was used to modify the chabazite, was purchased Acros Organics Co., in form of iron (II) sulfate heptahydrate reagent ACS ($FeSO_4.7H_2O$). The modification concentration was 0.1 M.

Methods

The experimental methods for this research can be subdivided into the following tasks:

1. Modification of the Zeolite
2. Kinetic and Equilibrium studies
3. Sampling Procedure and Analytical Methods
4. Microfiltration Baseline Qualification
5. Microfiltration with Zeolite Studies

Modification of the zeolite, kinetic and equilibrium studies were performed in conjunction with Ashutosh Vakharkar and may also be found within his Master's Thesis entitled *Adsorption Studies For Arsenic Removal Using Modified Chabazite* (Vakharkar, 2005).

Modification of the Zeolite

The modification chemicals were prepared separately in polycarbonate batch reactors using DI water at concentrations of 0.01 M, 0.1 M, and 0.1 M for Copper (I) Chloride, Iron (II) Chloride, and Iron (II) Sulfate, respectively. The solutions were allowed to mix at 300 rpm for a period of 30 minutes to ensure a complete dissolution. High purity sodium chabazite, an aluminum-silicate zeolite which has been dried, reactivated using a sodium solution, and then allowed to equilibrate with air was purchased in 20 lbs drum from GSA Resources. Zeolite was weighed using a Mettler AE 260 Delta Range Analytical Balance, Figure 19, and added to the batch reactors at a concentration of 5 g/L. The batch reactor, Figure 20, was then covered and allowed to mix for a period of 24 hours at a rate of 300 rpm.

Figure 19 - Mettler AE 260 Delta Range Analytical Balance

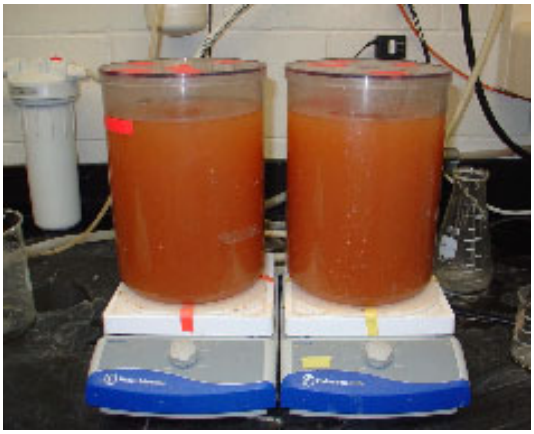

Figure 20 - Batch reactors for pretreatment of chabazite using various reagents

Upon completion of the 24 hour modification period, the solutions were rinsed with DI water and then sieved through a 400-mesh sieve, Figure 21. This modified zeolite was then added to a Pyrex drying tray, Figure 22, and placed in a Blue M Stabil-Therm Gravity Oven, Figure 23, at a temperature of 103^{o} C for a period of 2 hours. Once dried the final modified zeolite was weighed, labeled, and stored in desiccators for future use.

Figure 21 - 400 mesh sieve

Figure 22 - Modified chabazite in Pyrex drying tray

Figure 23 - Blue M Stabil Therm Gravity Oven used for drying of treated chabazite

Comparative pictures, Figures 24-26, of the non-modified and modified zeolite for each of the chemicals are presented below.

Figure 24 - Chabazite before and after copper (I) chloride modification

Figure 25 - Chabazite before and after iron (II) chloride modification

Figure 26 - Chabazite before and after iron (II) sulfate modification

Kinetic and Equilibrium Studies

Kinetic Studies

The kinetic studies were carried out in ECE Compact Laboratory Mixers. For these tests, 100 µl of standard arsenic trioxide solution was added to 3 jars filled with 1 liter of de-ionized/dechlorinated tap water/pre-chlorinated groundwater. 0.5 g of the treated chabazite was measured using a Mettler AE 260 Delta Range analytical balance and added to each of three 1 L jars, (A, B, and C) of the laboratory mixer.

Figure 27 - Kinetic studies jar tester configuration

The kinetic tests were run for a period of 6 hours at speed of 180 rpm. During this 6-hour test run, 20 ml sample was pulled from jar A for arsenic analysis. At the same time, 20 ml was taken from Jar B and injected into jar A to maintain the same solid /solution ratio. Similarly, 20 ml was transferred from jar C to jar B for the same reason. Sampling frequency for the kinetic runs was as follows:

1. 5 mins interval for the first 30 min.
2. 10 mins interval from 30 to 60 min.
3. 15 mins interval from 60 to 120 min.
4. 1 hr interval from 120 to 360 min.

Equilibrium Studies

The batch equilibrium studies involved using identical volumes and concentration of arsenic exposed to different quantities of adsorbent. For equilibrium tests, each of the 6 jars was prepared at an initial As(III) concentration of 100 µg/L using de-ionized water, dechlorinated tap water, or unchlorinated ground water. Sequential amounts of copper or iron treated chabazite (0.25, 0.5, 0.75, 1.0, and 2.0 g/L)

were measured using a Mettler AE 260 Delta Range analytical balance and added to the jars. One jar served as a control in order to detect any adsorption of arsenic on to the jars. Simultaneous runs for Cu treated and Fe treated zeolites were conducted at a speed of 180 rpm. The batch equilibrium tests were performed for 6 hrs period with samples taken at time 0 min (prior to zeolite addition) and time 360 mins.

Long Term Equilibrium Studies

Long term equilibrium studies for adsorption were performed for a period of 90 days. For long term equilibrium studies, 100 µl of arsenic trioxide solution was added to 12 dark colored glass bottles containing 1 L of dechlorinated tap water. Different amounts of copper or iron treated chabazite (0.25, 0.5, 0.75, 1.0, and 2.0 g/L) were measured and added to the dark colored bottles. One bottle served as a control in order to detect any adsorption of arsenic on to the glass bottle. These sample bottles were stored in a refrigerator at a temperature of $4^{O}C$. and were shaken every 10 days. The initial and final pH of the solution was measured.

Sampling Procedure and Analytical Methods

All samples (20 ml) were filtered using a 0.45 µm Fisher brand Nylon filter into a Nalgene passport IP2 Narrow mouth HDPE bottles. The bottles were acidified with 200 µl of concentrated HCl acid to obtain a pH of 2.5-3 and then stored at $4^{o}C$ until arsenic analysis could be performed. These samples were then analyzed for arsenic species using Atomic Absorption Spectroscopy.

Initial analysis was performed using the Atomic Adsoprtion (AA) machine from the Geology department. The calibration curve for the AA is shown below in Figure 29.

Figure 28 - Geology Lab AA

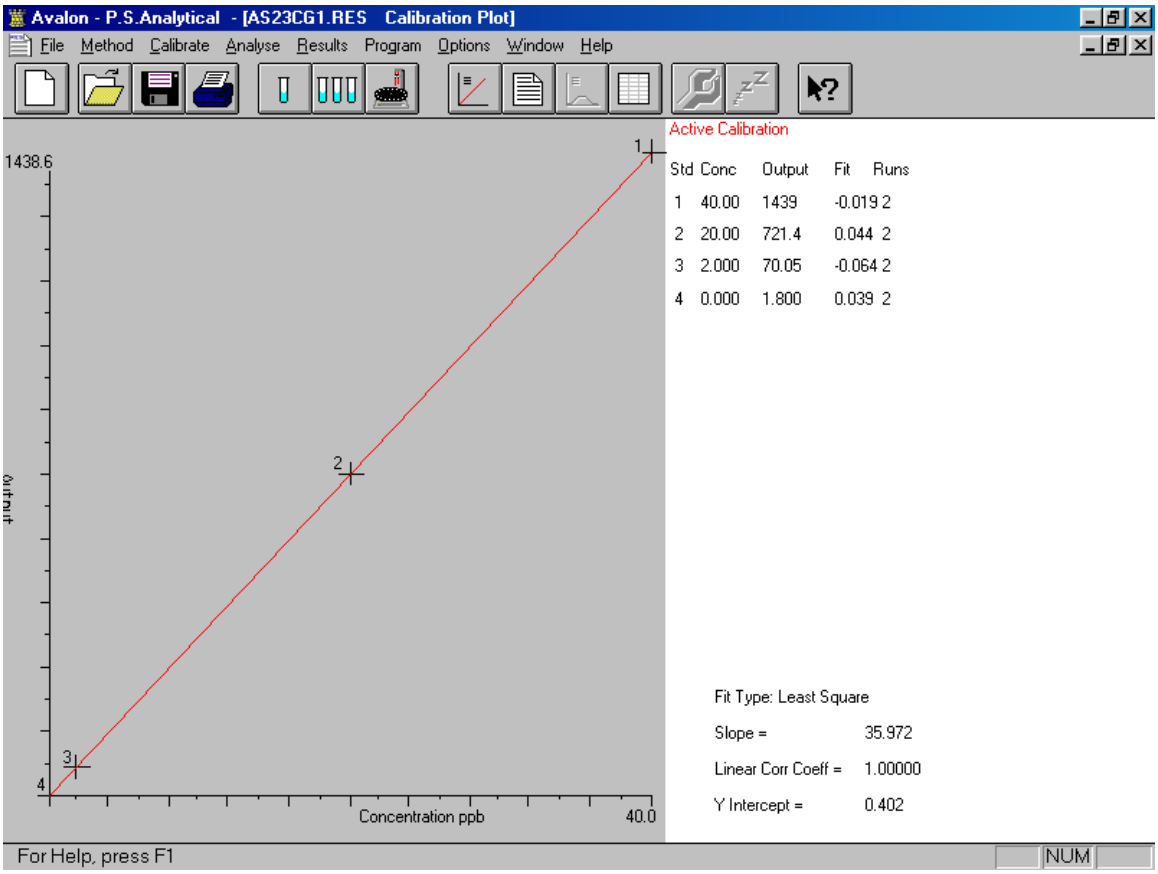

Figure 29 - Calibration curve for Geology Lab AA

Subsequent samples, following initial runs, were conducted on the Graphite Furnace Atomic Adsorption Spectrophotometer housed in Dr. Trotz's lab at USF.

Figure 30 - Varian SpectrAA Zeeman Graphite Furnace

Microfiltration Baseline Qualification

The membrane system, Figure 31, was built by American Engineering Services and implemented a single outside-in membrane element. This element implements a microfiltration membrane from Hydranautics which has a surface area of 0.85 m^2. This system was capable of running at varying flux rates, cross flow rates, and cycle times. Setpoints specified by the membrane manufacturer and common to low pressure membrane systems were used to ensure that the system performed in a similar manner to a full scale plant.

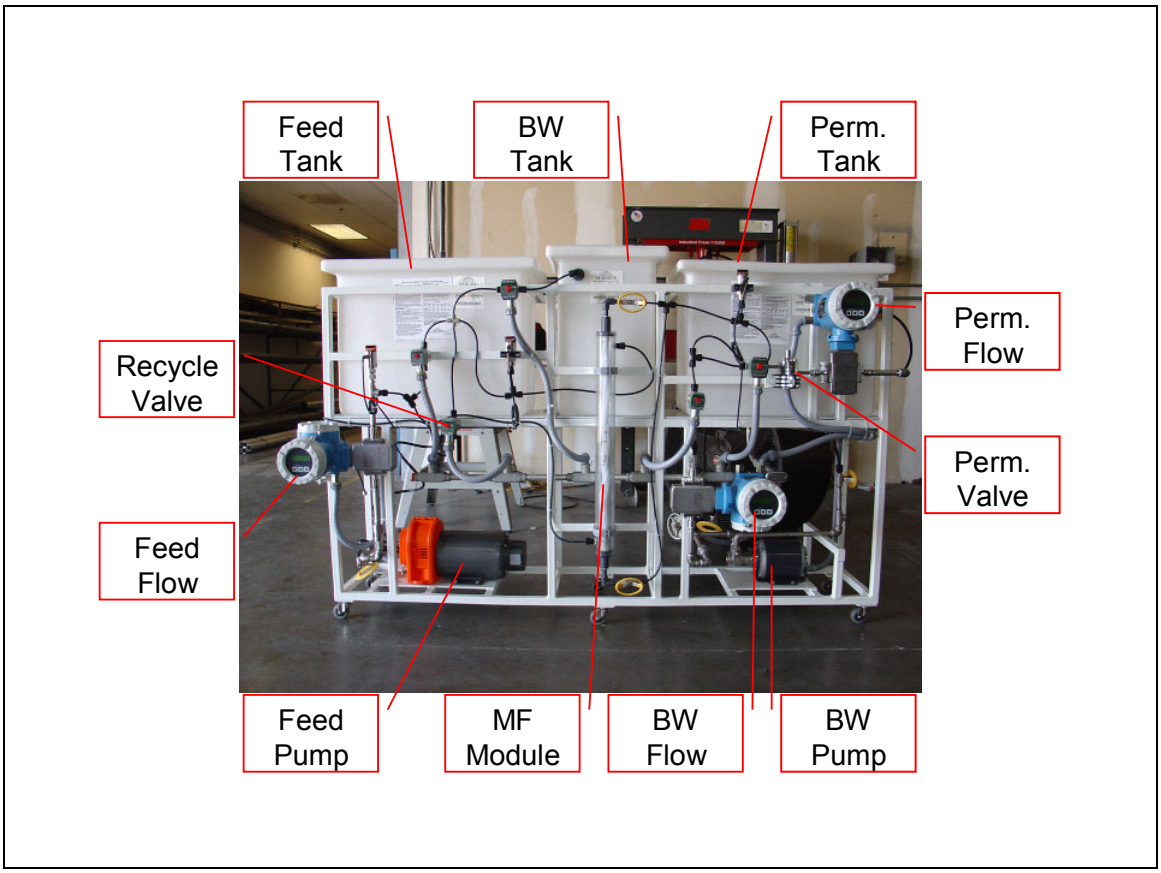

Figure 31 - Membrane system

Initially the pure water mass transfer coefficient (Kw) for the membrane was established by reducing the water flux rate in consecutive cycles and measuring the resulting transmembrane pressure. A single cycle flux decline test is shown in Figure 32 while a multiple cycle is shown in Figure 33. These tests are performed by allowing the system to stabilize at a flux, measuring the operational pressures, and then lowering the flux and repeat this process. A multiple cycle indicates that a backwash was performed prior to the reduction of the flux rate. By plotting the Temperature Corrected Flux against the Transmembrane Pressure (TMP) and evaluating the slope of the line which best intersects these points Kw may be determined. This resulted in a Kw of approximately 11 and 10 gfd/psi for the single and multiple cycle flux decline tests, respectively.

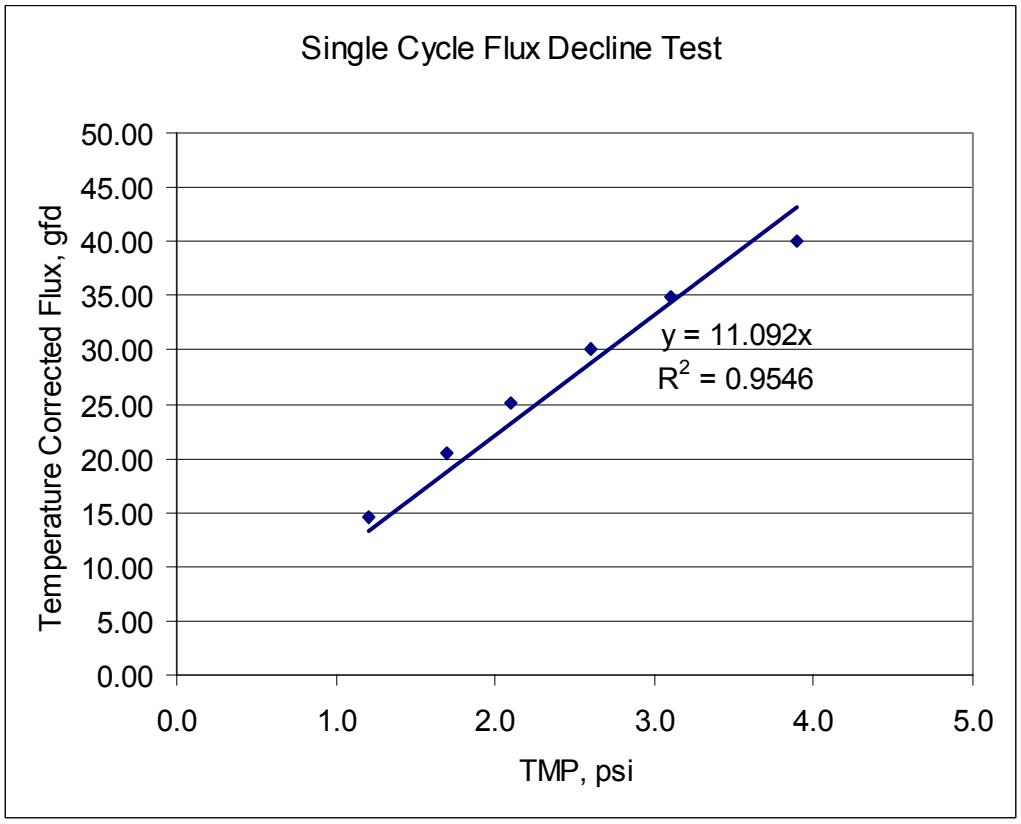

Figure 32 - Single cycle flux decline test

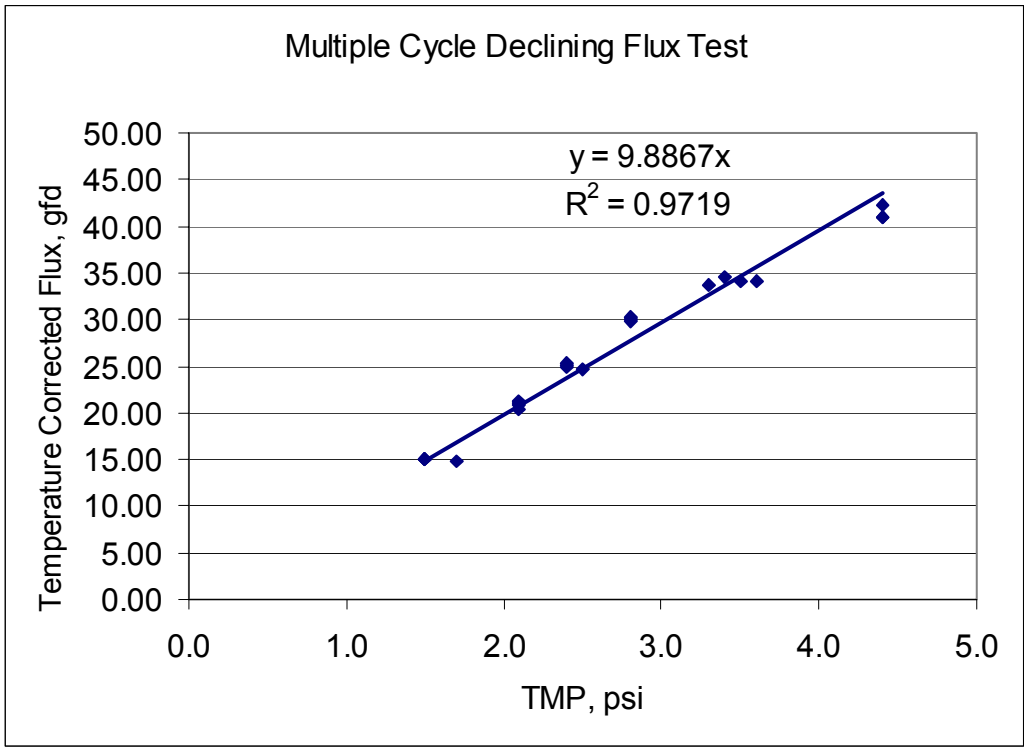

Figure 33 - Multiple cycle declining flux test

Following the pure water test, the water was dosed from a stock solution of arsenic and samples were taken of the feed and permeate water streams to determine the inherent membrane rejection without the zeolite addition. As seen in Figure 34, there membrane was not able to reduce the arsenic entering the permeate stream.

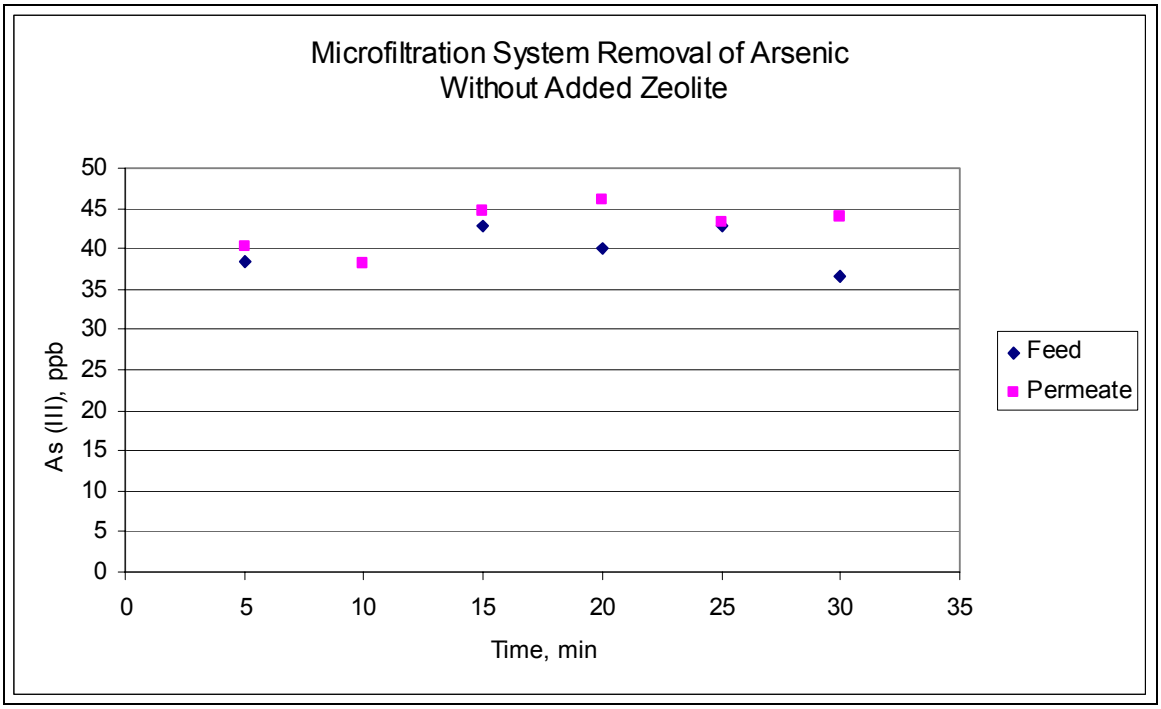

Figure 34 - Inherent membrane rejection of arsenic

Following this determination, studies were conducted to determine the effect of the addition of the zeolite and its impact on the cake layer formation and the resulting increase in TMP. These mass loading studies were conducted by dosing a continuous stream of a slurry of modified zeolite into the feed stream and resulting operational conditions. A picture of the membrane reactor is shown in Figure 35 and 36 which demonstrate the membrane as it is initially receiving the zeolite and then just prior to backwash as the cake layer has reached its thickest.

Figure 35 - Initial cake deposition

Figure 36 - Final cake deposition

The results from the cake studies were used to determine the amount of cake which could be added to the reactor without significantly impacting the overall membrane

performance. As can be seen in Figure 37, the K_w or permeability was reduced by nearly 0.8 gfd/psi with the addition of 0.5 g/L of zeolite.

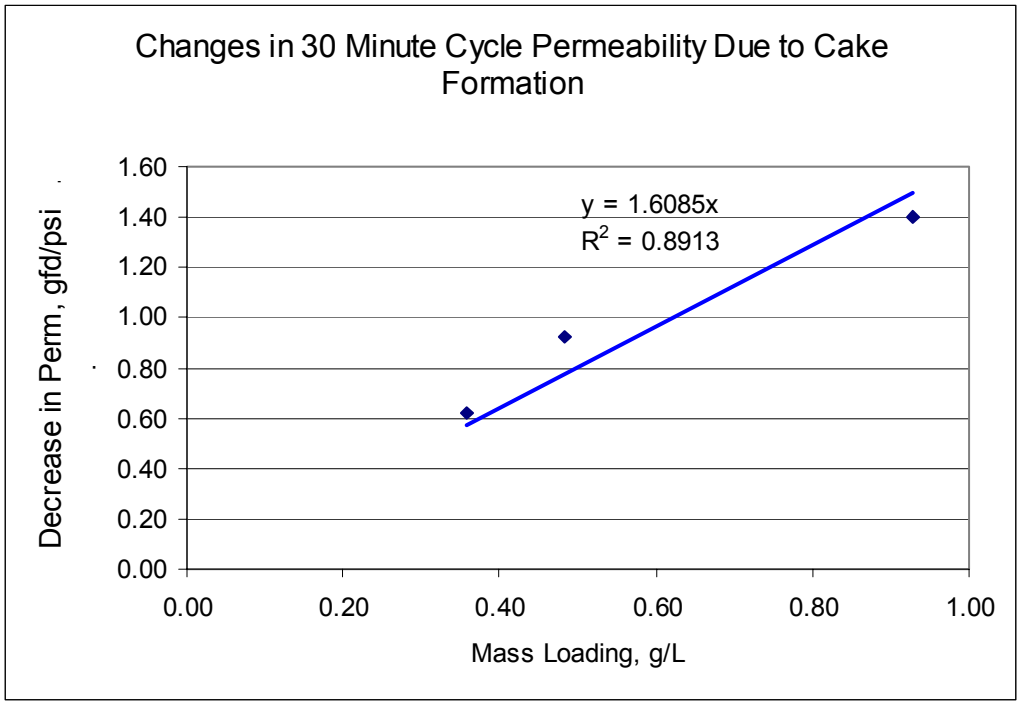

Figure 37 - Permeability changes due to cake layer formation

Microfiltration with Zeolite Studies

Based on the equilibrium and cake layer studies as well as the operational parameters governed by maintaining a scalable system, the experimental matrix for the arsenic removal using the ferrous sulfate modified zeolite on the microfiltration substrate was defined in Table 5.

Table 5 - Operational matrix for modified zeolite/membrane substrate studies

		Zeolite Mass, g			
		11.78	23.56		
Arsenic Feed Concentration, µg/L	140	I	VII	34 (0.482)	Water Flux Rate, l/(m^2*h), (L/min)
	140	II	VIII	51 (0.723)	
	80	III	IX	34 (0.482)	
	80	IV	X	51 (0.723)	
	30	V	XI	34 (0.482)	
	30	VI	XII	51 (0.723)	

By adding either 11.78 or 23.56 g of ferrous sulfate modified zeolite to the membrane reactor prior to starting the flow of arsenic and maintaining a flux rate of either 34 or 51 L/(m2.h) (liters per square meter per hour) the zeolite concentration ranged from 0.25 g to 1.0 g per liter of water filtered, Table 6.

Table 6 - Zeolite mass per volume of filtered water in reactor

Flux Rate, L/(m^2.h)	Zeolite Addition, g	Zeolite Mass per Volume of Filtered Water, g/L
34	11.78	0.5
51	11.78	0.25
34	23.56	1.0
51	23.56	0.5

Once the system was started, the arsenic was dosed using a LMI pump into the feed stream to reach feed concentrations ranging from 30 to 140 µg/L. This process was the same for all 12 operational matrix settings. Feed samples were collected at the beginning of the cycle, while permeate samples were collected at 5 minute increments following the hydraulic retention time to the sampling port which was estimated at 2 and 3 minutes for the flux rates of 34 and 51 L/(m^2.h), respectively.

Once a cycle was completed, the system was backwashed and then the membrane reactor was disassembled, thoroughly rinsed with DI water and reassembled. This was done to ensure that the system did not have any arsenic or zeolite left behind from previous runs.

RESULTS AND DISCUSSION

The results are presented in the following sequential subtopics:

1. Modification of Zeolite
2. Freundlich and Langmuir Isotherm Equilibrium Studies
3. Arsenic Removal Using a Zeolite/Membrane Reactor
4. Development of Mathematical Model Describing This System

Modification of Zeolite

Modification of the zeolite with ferrous chloride, cuprous chloride, and ferrous sulfate was accomplished using the batch reactor as described in the Methods and Materials section. 5 g of chabazite was added to each liter of 0.1 or 0.01 N solution for a total of 20 grams. The solubility of copper chloride prohibited a 0.1 N solution. In order to determine the amount of uptake of the modification ions, samples of the cuprous chloride and ferrous sulfate solution prior to addition of chabazite as well as those before rinsing and after each rinse were analyzed and the results of which are shown in Table 7. For the uptake calculations in mg of ion per gram of zeolite, the original mass was used to determine the original uptake prior to rinsing. Following rinsing, the final dried mass was used to determine the loss due each successive rinse. This assumes that all of the mass is lost during the initial rinse and none in subsequent rinsing, an assumption which seems valid based on visual inspection of the rinse supernatant where the zeolite was not found to subsequently pass through the mesh screen.

Table 7 - Modification of zeolite ionic results

	Cuprous Chloride		Ferrous Sulfate	
Time	Copper	Chloride	Ferrous	Sulfate
Before, mg/L	419.50	252.00	540.80	1010.00
Before, mmol/L	6.60	7.11	9.68	10.52
After, mg/L	29.27	392.00	182.50	1276.00
After, mmol/L	0.46	11.06	3.27	13.29
% Uptake, (-x.x) = loss	93.02	(-55.56)	66.25	(-26.34)
mg/g	19.51	(-7.00)	17.92	(-13.30)
mmol/g	0.31	(-0.20)	0.32	(-0.14)
After 1 Rinse	31.67	8.66	25.25	28.70
mg/g left	15.11	(-8.20)	15.35	(-16.21)
mmol/g	0.24	(-0.23)	0.27	(-0.17)
% lost	22.54	(-17.18)	14.31	(-21.91)
After 2 Rinse	9.35	0.73	5.18	2.56
mg/g left	13.81	(-8.30)	14.83	(-16.47)
mmol/g	0.22	(-0.23)	0.27	(-0.17)
% lost	8.59	(-1.24)	3.43	(-1.60)
After 3 Rinse	10.25	0.45	4.88	0.90
mg/g left	12.39	(-8.37)	14.33	(-16.56)
mmol/g	0.19	(-0.24)	0.26	(-0.17)
% lost	10.31	(-0.75)	3.34	(-0.55)

Metallic ion uptake onto the zeolite is shown in the % Uptake row. According to laboratory data, 93% of the available copper was taken up by the zeolite, while only 66% of the iron ions were adsorbed. This corresponds to 19.5 and 17.9 mg per gram of zeolite for copper and iron respectively. Interestingly, the mmol/g uptakes onto the zeolite are nearly identical at 0.31 and 0.32 mmol/g of copper and iron, respectively. Chlorides and sulfates were actually released by the zeolite as the copper and iron were taken up. For electro-neutrality, it must be assumed that hydroxide ions are also adsorbed onto the zeolite. This assumption was verified through a decrease in pH in the solution of approximately 0.7 pH units.

Rinsing of the modified zeolites resulted in a greater loss of copper than iron per gram of zeolite. The final concentrations of copper and iron on the zeolites were 12.4 and 14.3 mg/g, respectively. This equates to a 0.19 mmol/g copper modified zeolite and a 0.26 mmol/g iron modified zeolite.

Freundlich and Langmuir Isotherm Equilibrium Studies

Three different modified zeolites were used in adsorption studies to determine the most effective adsorbent. This work was done in collaboration with Ashutosh Vakharkar and may be viewed in entirety within his Master's Thesis; however a summary of these results are listed below with the method for determination listed in Appendix B.

Integral method, due to its simplicity over more complicated graphical differential methods, was used for determining the kinetic order of reaction. This method fits elementary reactions such as:

A → Products or A+B → Products

Equilibrium data was analyzed using Langmuir and Freundlich isotherm equations. While Langmuir isotherms describe adsorption capacity as a monolayer, Freundlich isotherms describe solid-liquid heterogeneous reactions.

Kinetic and Equilibrium Studies in De-ionized Water

Kinetic Studies

Kinetic studies were conducted in de-ionized water at an arsenic concentration of 100 ppb and a zeolite concentration of 0.5 g/L for a period of 6 hours. This was used to determine the baseline kinetics without the effect of competing ions.

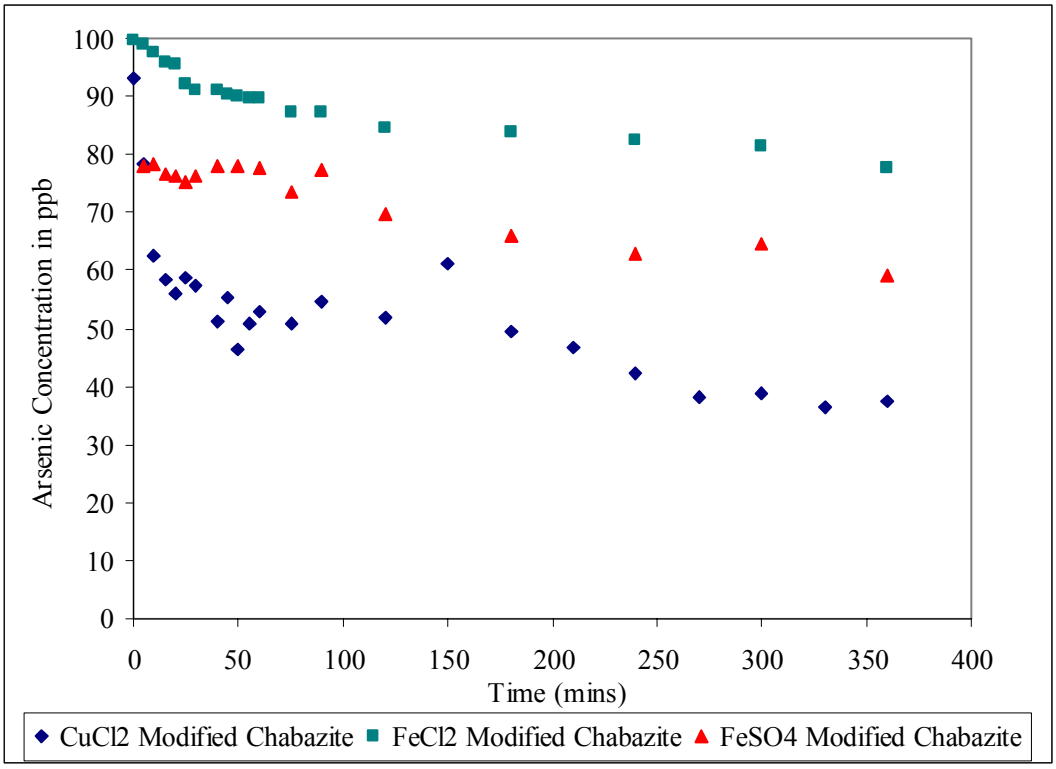

Figure 38 - Kinetic runs for As(III) removal using a modified chabazite in DI water

The kinetic runs demonstrate how fast the reaction proceeds towards equilibrium and may be used to determine the order of the reaction and the adsorption coefficient. The quantitative results of these runs are shown in Table 8.

Table 8 - Kinetic studies on DI water with concentrations of As(III) at 100 ppb and zeolite at 0.5 g/L

Type of chabazite	Initial concentration of arsenic (ppb)	Removal at 30 mins		Removal at 360 mins	
		Concentration (ppb)	% Removal	Concentration (ppb)	% Removal
Copper (I) chloride modified chabazite	100	58	42 %	38	62 %
Ferrous chloride modified chabazite	100	91	9 %	78	22 %
Ferrous sulfate modified chabazite	100	76	24 %	59	41 %

Based on this data, the copper modified chabazite had the fastest rate for arsenic adsorption in DI water. A fit of these data points resulted in a second order regression represented by $dC_A/dt = kC_A^2$. Based on a comparison of the ferrous modified chabazite, the chloride ion seems to hinder the adsorption kinetics when compared to the sulfate ion. Therefore the use of a particular anion does influence adsorption kinetics.

Table 9 - Order of reaction and rate constants for modified chabazite in DI water

Type of chabazite	Rate constants (liter/mol.min)	Rate equation
Copper (I) chloride modified chabazite	3e-05	$r_A = 3e\text{-}05C_A^2$
Ferrous chloride modified chabazite	7e-06	$r_A = 7e\text{-}06C_A^2$
Ferrous sulfate modified chabazite	1e-05	$r_A = 1e\text{-}05C_A^2$

Equilibrium Studies

Since the copper chloride and ferrous sulfate modified zeolites proved to have the fastest kinetics, equilibrium studies were then conducted to determine their maximum adsorption capacities. Data gathered from the 6 hour equilibrium runs were fitted to both Freundlich and Langmuir isotherm equations. The Langmuir isotherm equation, as seen in the figure below, provides the maximum adsorption capacity for monolayer coverage of the modified chabazite.

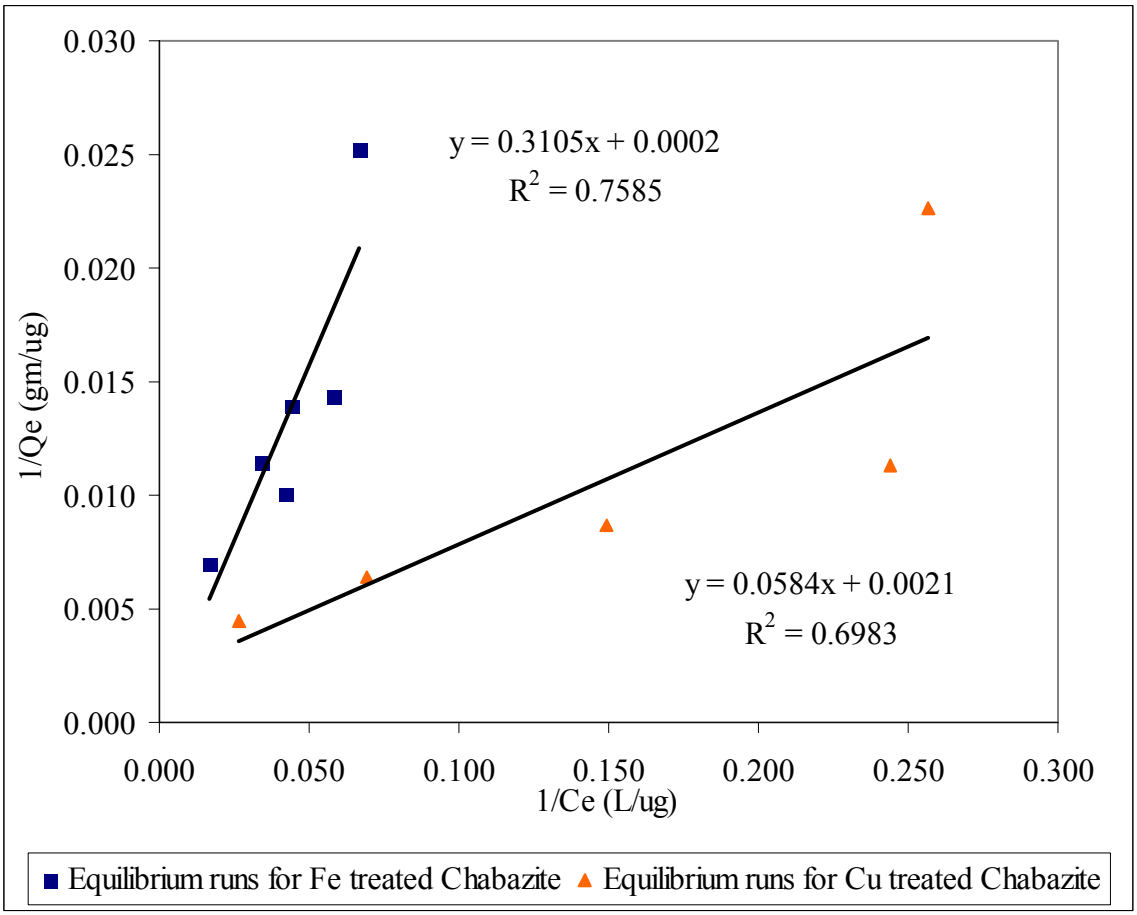

Figure 39 - Langmuir adsorption isotherm for modified chabazite in DI water

A linear model of Freundlich isotherm, which provides the adsorption affinity, was fitted by plotting Log Q_e and Log C_e in Figure 40.

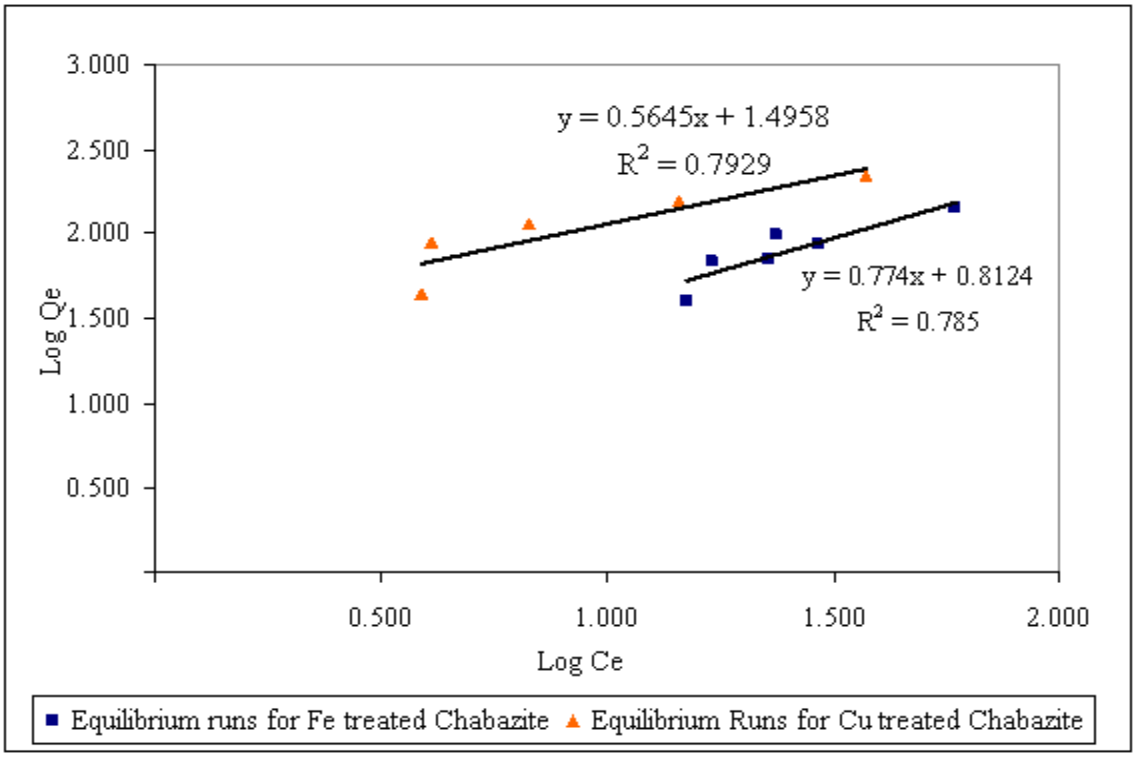

Figure 40 - Freundlich adsorption isotherm for modified chabazite in DI water

The maximum adsorption capacities and the Langmuir constants, K_L, were determined from the intercept and slope of the zeolite's linearized Langmuir isotherm. The Freundlich isotherm provides the maximum adsorption, k, and the adsorption intensity, 1/n, by analyzing the intercept and slope, respectively.

Table 10 - Langmuir and Freundlich isotherm constants in DI water

Type of modified chabazite	Langmuir constants			Freundlich constants		
	Q_{max} (ppb/g)	K_L	R^2	k	n	R^2
Copper (I) modified chabazite	477	0.058	0.70	31.31	1.77	0.80
Ferrous (II) modified chabazite	5000	0.31	0.76	6.49	1.29	0.79

Due to the solubility of copper, the copper modification of the zeolite took place at a lower concentration, 0.01N, which was only 10 percent of the normality of the ferric treatments, 0.1N. Table 10 indicates that the maximum adsorption capacity may be directly related to this as the ferrous zeolite had a capacity for arsenic over 10 times that of the copper.

Based upon the analysis provided in Table 10, the equilibrium data fits Freundlich isotherms to a higher degree than Langmuir isotherms. Analyzing this data also shows that the Freundlich constants of k and n are higher for the copper chloride modified chabazite. As mentioned previously, this may indicate that the adsorptive bond is stronger than that of the iron modified zeolite.

Kinetic Studies for Determination of Effect of Stoichiometric Ratio

In order to determine the effect of the stoichiometric ratio, cations:anions, two comparisons are made. The first compares the same anion with different cations and the second the same cations with a different anions. Ashutosh Vakharkar presents more of this data in his master's thesis, but a summary is included here for reference.

1. Kinetic studies using chabazite modified with same anions of different cations (Cu:Cl::1:1) versus (Fe:Cl::1:2) in dechlorinated tap water. The results, presented in Figure 41 and Table 11, demonstrated that the arsenic removal is nearly identical.

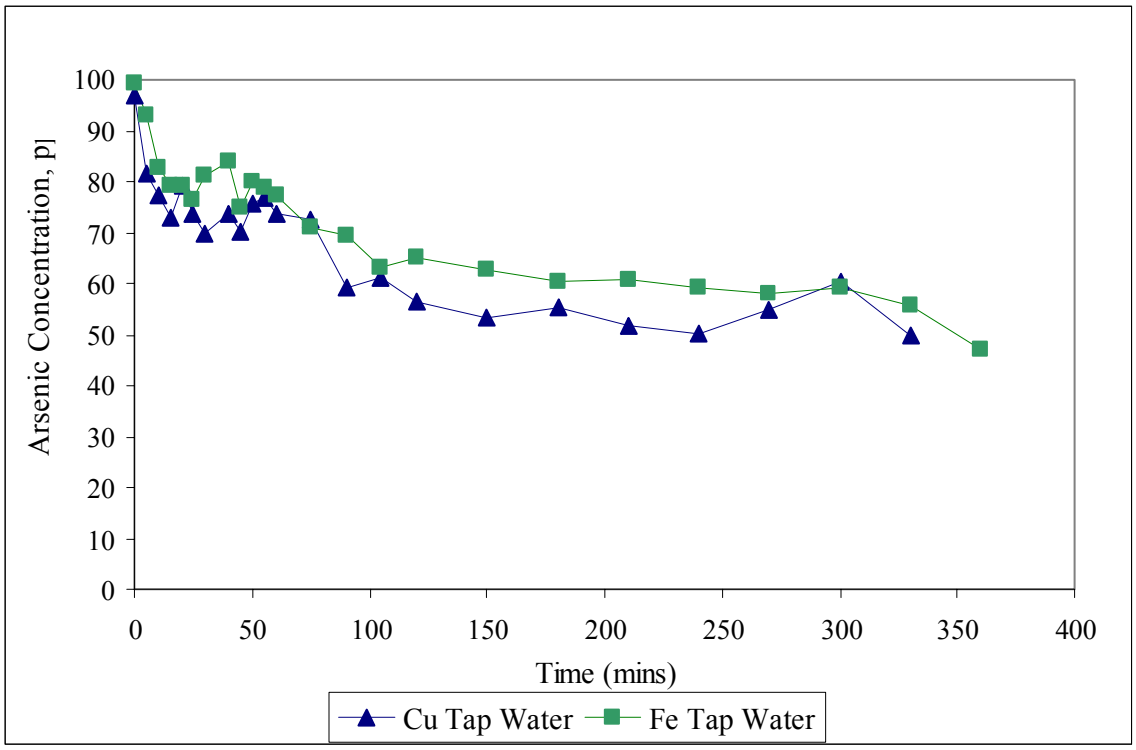

Figure 41 - Kinetic runs for As(III) adsorption using chloride salts of two metal ions in dechlorinated tap water

Table 11 - Kinetic results using chabazite modified with same salt of different metals with 0.5 g/L of modified chabazite

Type of chabazite	Initial concentration of arsenic (ppb)	Removal at 30 mins		Removal at 360 mins	
		Concentration (ppb)	% Removal	Concentration (ppb)	% Removal
Copper (I) chloride modified chabazite	100	70	30 %	46	54 %
Ferrous chloride modified chabazite	100	76	24 %	48	52 %

Table 12 summarizes the arsenic removal of the copper (I) and iron(II) modified chabazite which fit a second order regression, $dC_A/dt = kC_A^2$.

Table 12 - Reaction order and rate constants for chabazite modified with same salts of different metals

Type of chabazite	Rate constant (liter/mol.min)	Rate equation
Copper (I) chloride modified chabazite	2e-05	$r_A = 2e\text{-}05C_A^2$
Ferrous chloride modified chabazite	4e-05	$r_A = 4e\text{-}05C_A^2$

The reaction rate constant for copper modified zeolite is twice that of the ferrous modified zeolite. In a ferrous chloride solution the ratio of chloride to ferrous is 2:1, while in cuprous chloride it is 1:1. This ratio seems to play a significant role in the rate of arsenic adsorption by the modified chabazites.

2. Kinetic studies using chabazite modified with different salts of same metal were conducted using $FeSO_4$ and $FeCl_2$. The results for kinetic studies, presented in Figure 42, indicate that the kinetics are similar for the first 30 minutes; however, while the ferrous sulfate modified zeolite continued to adsorb arsenic, the ferrous chloride modified zeolite had nearly reached equilibrium. These results are summarized in Table 13. Concentrations were measured using the Zeeman GFAA.

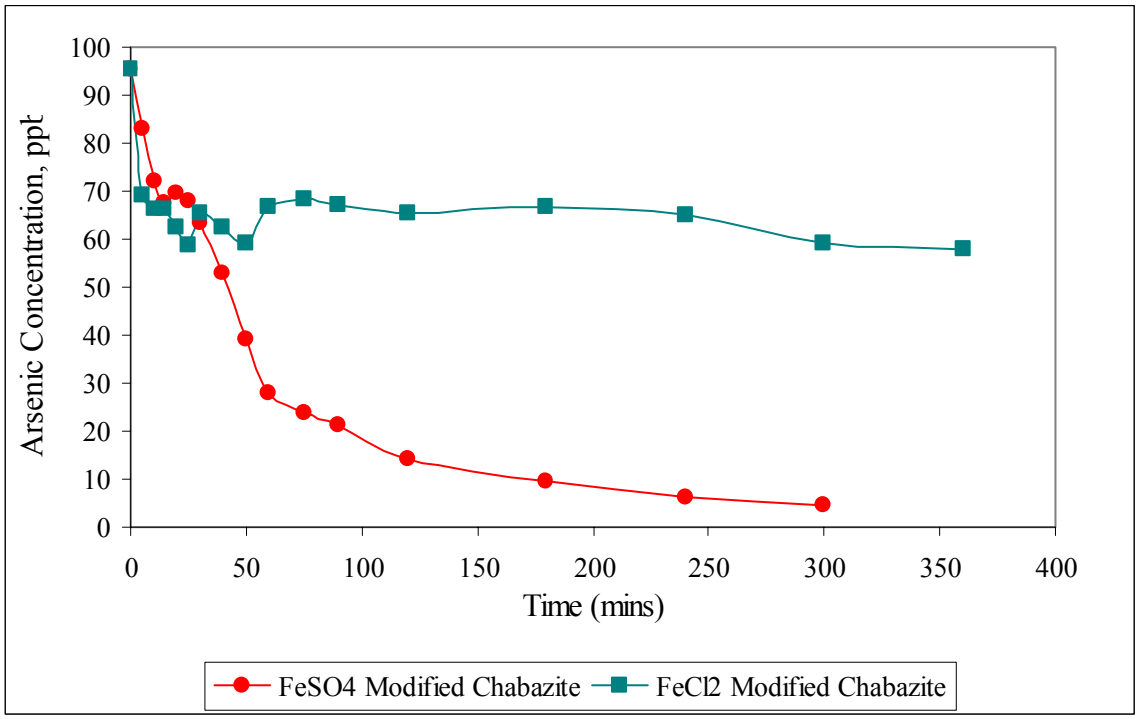

Figure 42 - Kinetic studies for As(III) using different salts of same metal in dechlorinated tap water

Table 13 - Results from kinetic studies using chabazite modified with different salts of same metal at 0.5 g/L of modified chabazite

Type of chabazite	Initial concentration of arsenic (ppb)	Removal at 30 mins		Removal at 360 mins	
		Concentration (ppb)	% Removal	Concentration (ppb)	% Removal
Ferrous chloride modified chabazite	100	63	37 %	57	43 %
Ferrous sulfate modified chabazite	100	65	35 %	5	95 %

Linear regression of the reaction kinetics for the ferrous sulfate modified zeolite proved to be a good fit, R^2 of approximately 85%, to a second order reaction. The ferrous chloride modified zeolite was neither a good fit for either a first or second order reaction.

The ratio of ferrous to the anion in ferrous sulfate is 1:1 whereas the ratio in ferrous chloride is 1:2. Earlier work on ionic uptake and release indicated that more chlorides are released by the natural zeolite into the water than sulfates. This coupled with the kinetic data infers that the chloride species in the modification slurry hinders the release of the zeolites' chloride thereby preventing the zeolite from taking up ferrous and hydroxide ions. This process is further justified by the change in pH values before and after modification. While the pH of the chloride solution was reduced by 0.14 pH units, the sulfate solution decreased by 0.7 pH units. This indicates that much more hydroxide was removed from solution. Following this logic, it is assumed that a greater quantity of the metal in the modification slurry was adsorbed onto the sulfate modified zeolite. This indicates that if the arsenic removal is dictated by chemisorption, the anion used in the modification does play a critical role in the adsorption of the media.

Relationship Between Mass of Zeolite and Arsenic Removal

Equilibrium studies provide an idea of the amount of zeolite which must be fed into the membrane reactor to achieve adequate removal of the arsenic. Figure 43 depicts the relationship between the various masses of different zeolites and their removal efficiency.

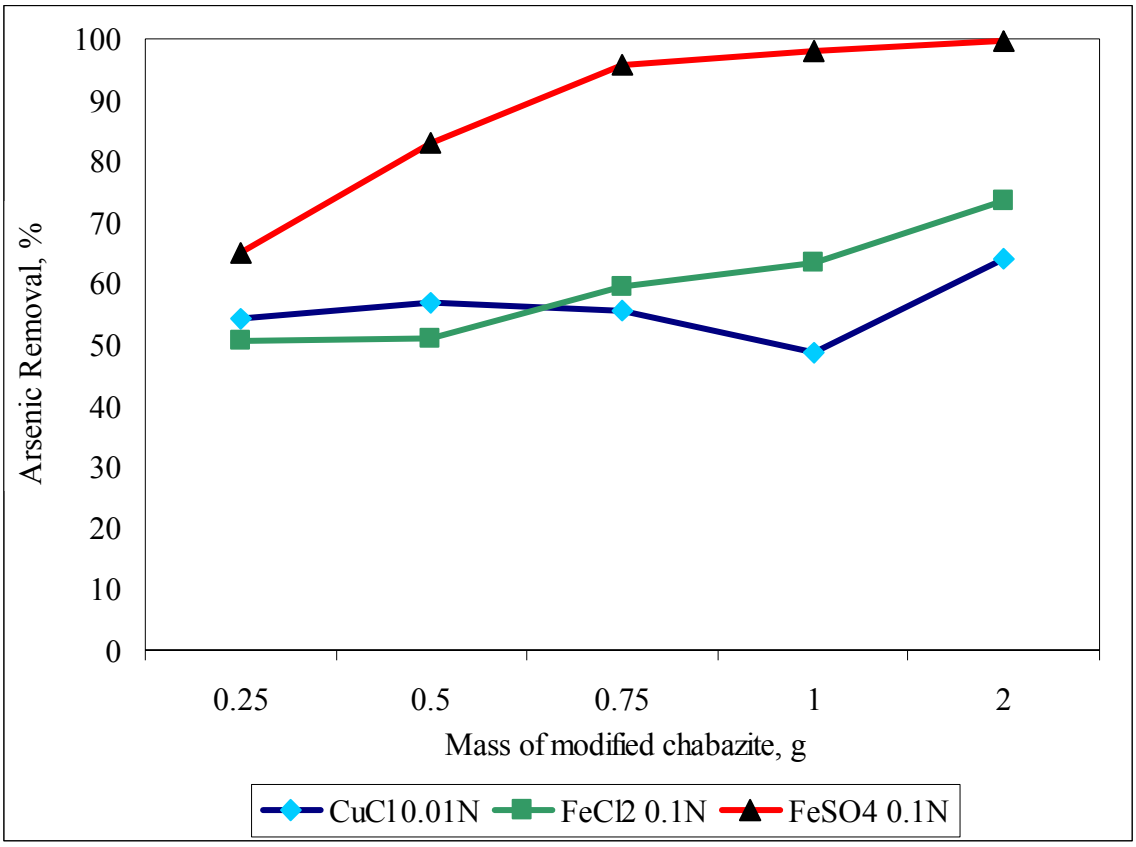

Figure 43 - Relationship between As(III) removal and mass of zeolite

It is clear from this figure that the ferrous sulfate modified zeolite has the highest adsorptive capability. While nearly all of the arsenic is removed at 2 g/L, there is no significant change after 1 g/L and very little after 0.75 g/L. Between 90 and 95% of the 100 ppb of the arsenic in solution is removed between these two values. Based on this data, the ferrous sulfate modified zeolite was chosen to use in the membrane reactor at a concentration of up to 1 g/L.

Uptake and Leaching Studies

Uptake and leaching studies were conducted to ensure that the modified zeolite was chemically stable. Tap water was analyzed both before and after the addition of the modified zeolite for cations typically found in tap water, as seen in Table 14.

Table 14 - Uptake data for metals used in modification of chabazite

Metals analyzed	Ca	Cu	Fe	Mg
Tap water (mg/L)	77.16	0.78	0.14	3.74
Cu treated chabazite (mg/L)	73.17	0.46	0.06	3.97
Uptake (Leaching)	3.99	0.31	0.08	(0.24)
% Uptake (Leaching)	5.17	40.34	57.66	(6.34)
Tap water (mg/L)	77.16	0.78	0.14	3.74
Fe treated chabazite (mg/L)	70.93	0.31	0.07	3.71
Uptake (Leaching)	6.23	0.47	0.07	0.03
% Uptake (Leaching)	8.07	60.70	50.36	0.80

It was observed that none of the metals, except for 0.24 mg/L of Manganese in the copper modification, leached in the solution. On the contrary, the modified zeolite actually adsorbed some calcium, less than 10%, but a much higher uptake of copper and iron, from 40 to 60%. From these results we can conclude that the copper and iron used for modification have a strong bond to the zeolite and are therefore safe to use for further work.

Previous work performed by Carnahan et al. (2001) demonstrated that when arsenic was adsorbed onto the zeolite, the waste material did not leach it back into the water. This work was done using the TCLP (Toxicity Characteristic Leaching Procedure) test and proved that the media can be landfilled.

Results from Long Term Equilibrium Studies Using Different Modified Chabazite in Dechlorinated Tap Water

Long-term equilibrium studies (90 days) were conducted using all three modified chabazites. The resulting data was fitted to both Langmuir and Freundlich Isotherms. Table 15 presents the correlation coefficients obtained by these fits.

Table 15 - Langmuir and Freundlich correlation coefficients obtained for long term equilibrium studies

Type of modified chabazite	Langmuir isotherm R^2	Freundlich isotherm R^2
Copper (I) chloride modified chabazite	0.30	0.13
Ferrous chloride modified chabazite	0.58	0.40
Ferrous sulfate modified chabazite	0.96	0.97

Table 15 clearly shows that zeolites modified with a chloride salt did not fit either isotherm successfully. Those studies using ferrous sulfate modified chabazite however showed excellent correlation coefficients of 0.96 and 0.97 for Langmuir and Freundlich isotherms, respectively. Figures 44 and 45 illustrate these isotherms for the ferrous sulfate modified chabazite in dechlorinated tap water.

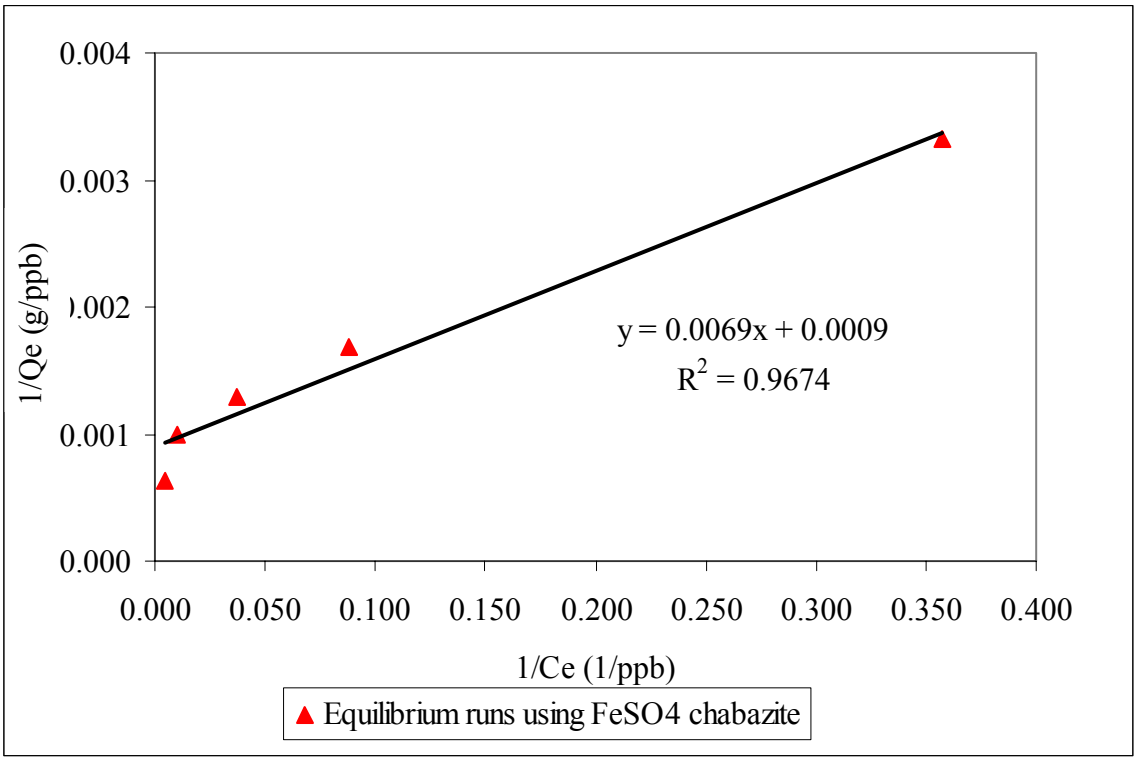

Figure 44 - Langmuir isotherm for long term equilibrium studies using ferrous sulfate modified chabazite in dechlorinated tap water

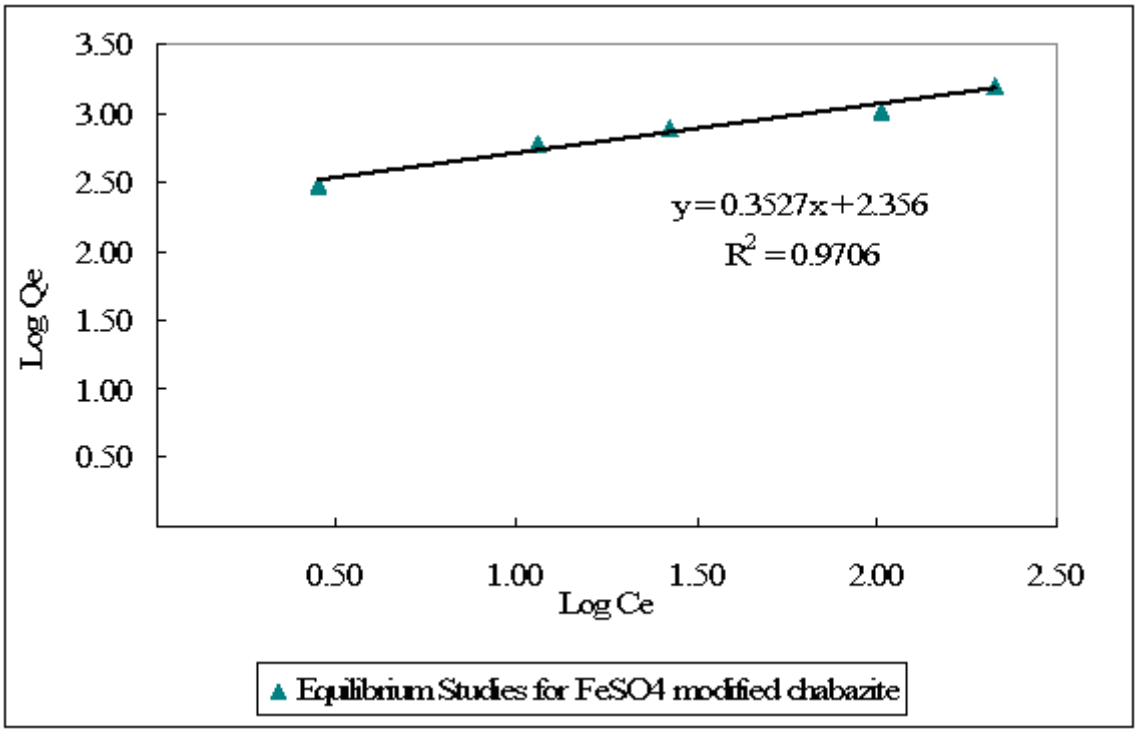

Figure 45 - Freundlich isotherm for long term equilibrium studies using ferrous sulfate modified chabazite in dechlorinated tap water

Table 16 - Langmuir and Freundlich isotherm constants for ferrous sulfate modified chabazite in dechlorinated tap water

Type of modified chabazite	Langmuir constants		Freundlich constants	
	Q_{max} (ppm/g)	K_L (liter/mg)	K	n
Ferrous sulfate modified chabazite	11.11	0.131	226.98	2.83

Results from Kinetic Studies for Arsenic Adsorption in Various Source Waters

Various source waters were gathered in order to determine the impact of these competing ions on the adsorption of arsenic onto the modified zeolite. These waters were DI, prechlorinated water from The University of South Florida (USF) potable wells, dechlorinated tap water from the USF distribution system, and a higher sulfide

groundwater which comes from the USF irrigation wells. These waters had conductivity values of 7.05, 512, 523, and 594 µS/cm, respectively. For these studies, the ferrous sulfate modified chabazite was used and the resulting kinetic results are found in Figure 46 and Table 17.

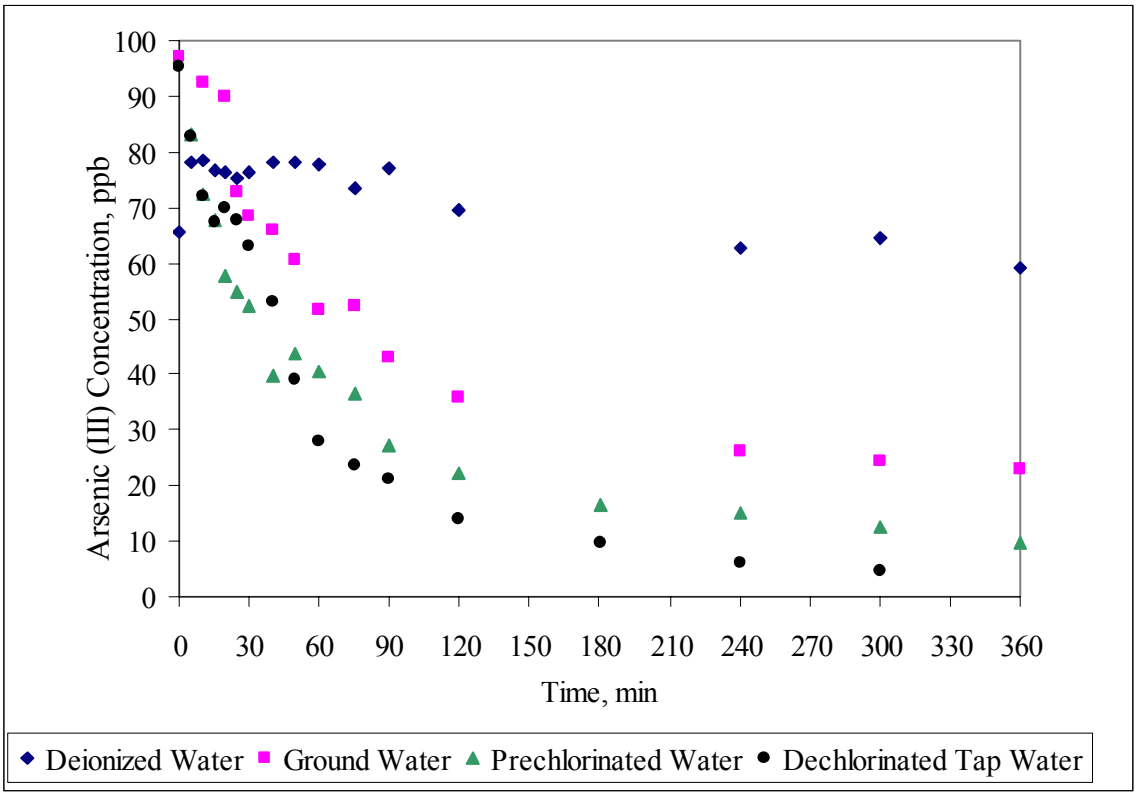

Figure 46 - As(III) adsorption kinetics for different source waters

Table 17 - Results from kinetic studies using different source waters with 0.5 g/L of zeolite

Type of source waters	Initial concentration of arsenic (ppb)	Removal at 30 mins		Removal at 360 mins	
		Concentration (ppb)	% Removal	Concentration (ppb)	% Removal
Dechlorinated tap	100	63	37 %	5	95 %
Prechlorinated tap	100	52	48 %	9	91 %
Ground	100	68	32 %	23	77 %
De-ionized	100	76	24 %	59	41 %

The order of reaction and the rate constants for various source waters, which were found through integral method, are summarized in Table 18 given below. These all followed a second order reaction.

Table 18 - Order of reaction and reaction rate constants for kinetic studies with ferrous sulfate modified chabazite in various source waters

Type of source water	Rate constants (liter/mol.min)	Rate equation
Dechlorinated tap	7e-04	$r_A = 7e\text{-}04 C_A^2$
Prechlorinated tap	2e-04	$r_A = 2e\text{-}04 C_A^2$
Ground	1e-04	$r_A = 1e\text{-}04 C_A^2$
De-ionized	1e-05	$r_A = 1e\text{-}05 C_A^2$

Figure 46 demonstrates similar kinetics for dechlorinated, prechlorinated and ground water, with the affinity for removal decreasing slightly in that order. It is also clearly seen that the DI water hindered the adsorption of arsenic. Ionic availability therefore seems to play a key role in the media's ability to adsorb arsenic. An investigation into a larger TDS range is provided later to verify these findings. Literature suggests that these results are indicative of inner sphere surface complexes. Inner sphere complexes occur when the anion in this case As(III) adheres directly to the metal (Fe) forming an FeAs complex. Outer sphere complexes develop when a water molecule is present between the anion and the cation. Adsorption via outer sphere complexes is reduced when ionic strength increases. On the contrary, adsorption through inner sphere complexes has little negative impact by increases in ionic strength and may actually increase capacity as ionic strength increases (Goldberg, 2000).

Effects of Competing Ions on Adsorption

Due to the availability of dechlorinated tap water and its resemblance to prechlorinated tap water, dechlorinated tap water was used for all further studies. The baseline studies were done with this water while competing ions were added using salts, commonly found in drinking water, which would easily dissociate.

Since it is assumed that the arsenic removal is by chemisorption, it was assumed that competition for adsorption would be due to increased anionic species. The anions chosen for this study, chloride and sulfide, readily exist in typical groundwaters and are easily dissociated.

Chloride Competition

Kinetic studies were carried out at the declorinated tap water baseline of 38 mg/L and increased levels of 145 and 245 mg/L using KCl as a source for chloride. Samples which were taken during the kinetic runs were analyzed for both As(III) and chlorides. Figure 47 indicates that the chloride concentration in all three waters did not change over time. The initial increase in chlorides in the first 5 minutes was due to the addition of the arsenic solution which uses HCl in its

preparation. Figure 48 demonstrates that the initial arsenic adsorption is similar for all three waters, but towards the end of the 6 hours the water containing the highest TDS achieved the greatest adsorption. This coincides with the theory of inner sphere complexes.

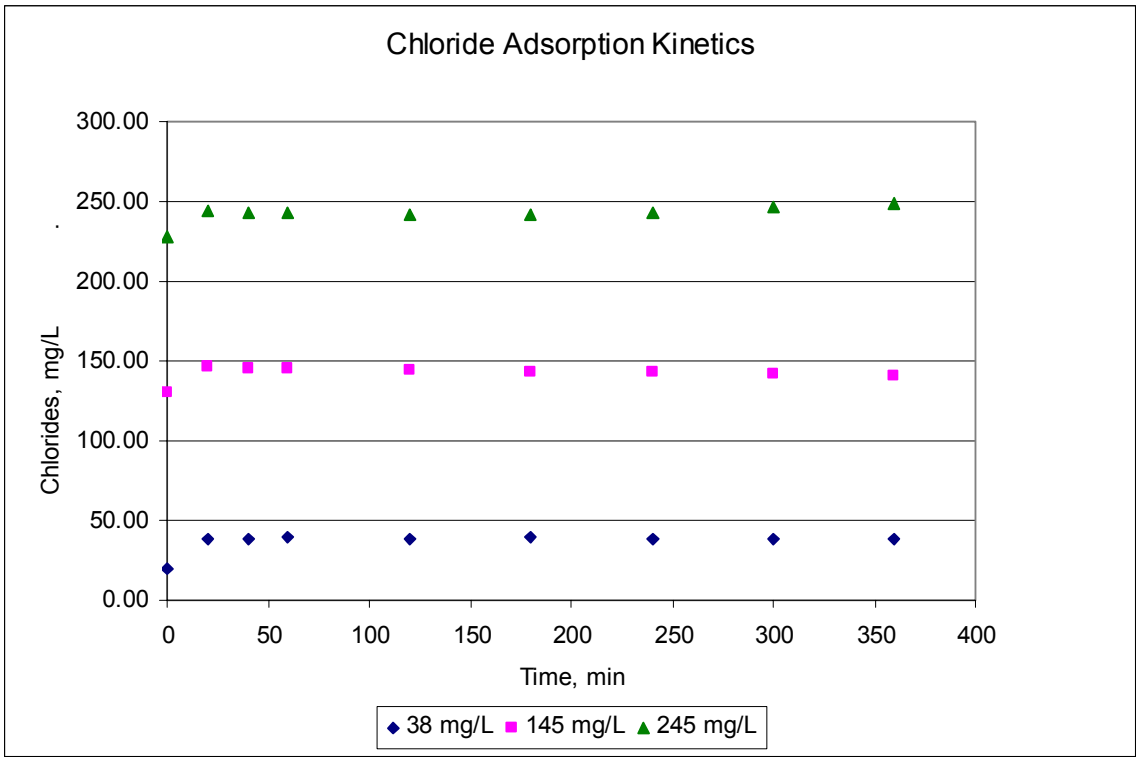

Figure 47 - Chloride concentration used in As(III) competitive kinetic studies

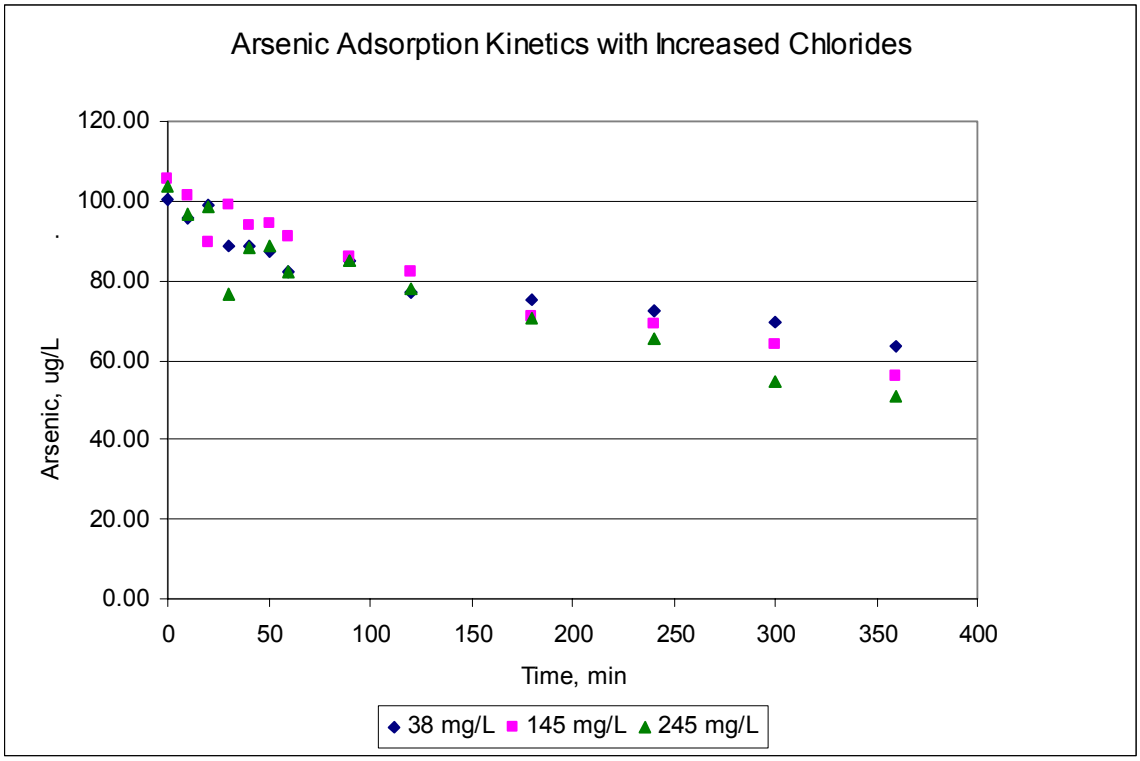

Figure 48 - As(III) adsorption kinetics with chloride competition

To ensure that this theory was valid experiments were conducted over a broader conductivity range. This ranged from the natural water with a conductivity of 631 to 1803 and 3220 µS/cm waters, elevated again through the use of KCl. These results, as seen in Figure 49, were not as conclusive as the previous, yet still the highest conductivity water yielded the greatest adsorption. It is possible that a chloride threshold exists in this region of conductivity.

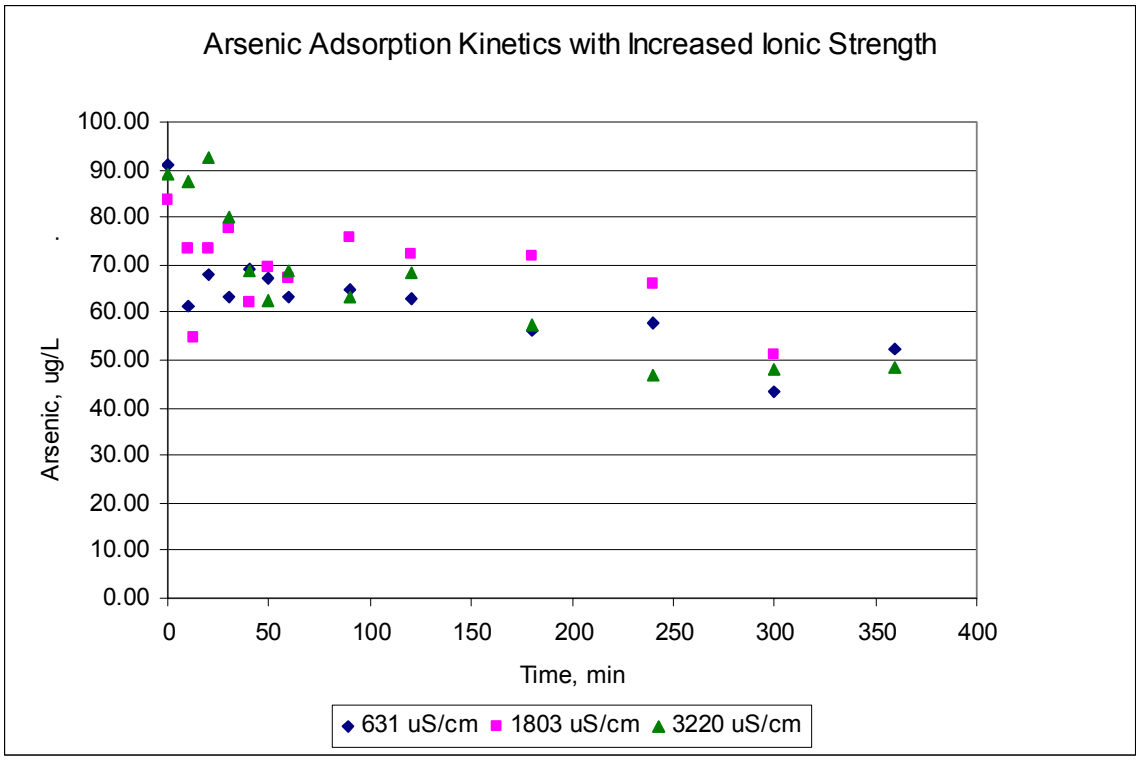

Figure 49 - As(III) adsorption kinetics with increase ionic strength

Sulfate Competition

Sulfate, a species which is commonly found in groundwaters, was also tested to verify its impact on the zeolite's arsenic adsorption. The dechlorinated tap water which was used had a sulfate concentration of 85 mg/L. Potassium sulfate was used to increase this to concentrations of 165 and 274 mg/L. Figure 50 shows a significant initial drop in the arsenic level. Although immediate complexation of the arsenic at the elevated sulfate levels may be possible, a more likely explanation is an interference with the GFAA. After consulting Varian, the manufacturer of the GFAA, and searching literature for similar instances, no explanation of any interference was found.

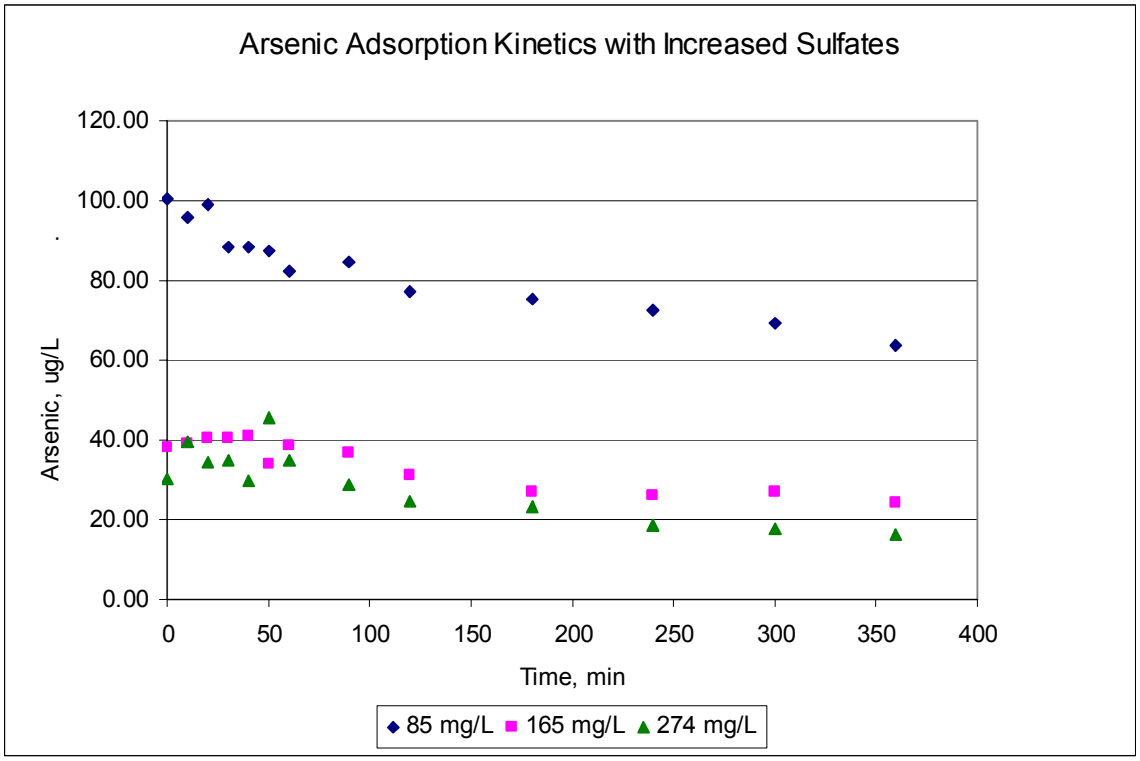

Figure 50 - As(III) adsorption kinetics with increased sulfates

To verify these findings, a study was conducted without the zeolite present. Eight jars were dosed with sulfate concentrations ranging from 0 to 405 mg/L and 86 ppb of arsenic, allowed to mix for 5 minutes at 180 rpm and then sampled. All samples were acidified and then analyzed using the same Varian GFAA and procedure as had been implemented in the previous sulfate runs.

The results from this experiment depicted in Figure 51 show a linear decrease in arsenic concentration. This clear indication of an interference prompted additional experiments with additional analysis methods.

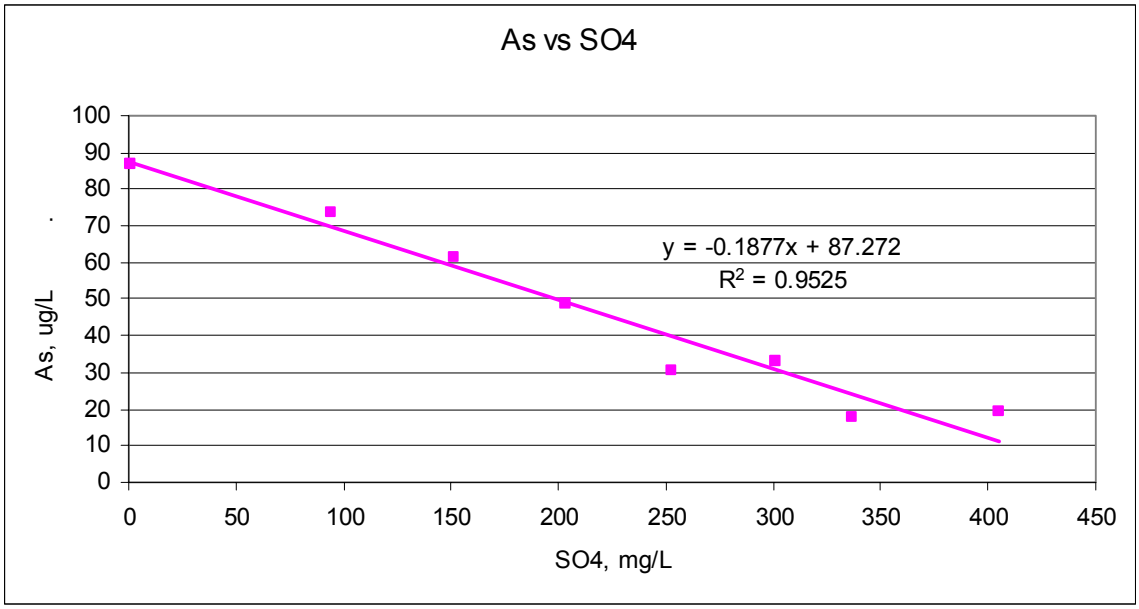

Figure 51 - Sulfate interference with arsenic analysis

Prior analysis of arsenic in this research had been conducted using the GFAA with peak calibration and analysis. Sulfate/arsenic samples were again created and 3 methods were used in analysis: GFAA Peak Height Method, Hach Colormetric Method, and GFAA Peak Area Method. As seen in Figure 52, the Colormetric and Peak Area Methods both yielded the anticipated constant arsenic concentration, while the Peak Height Method decreased in a similar method as witnessed previously. Due to this phenomenon, Peak Area Method was used for all subsequent sample analysis.

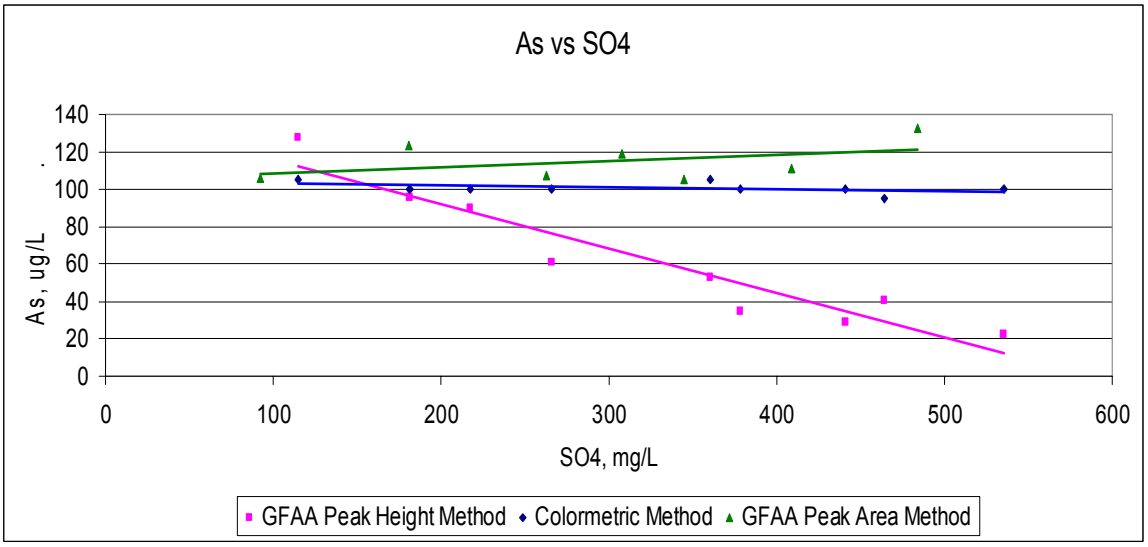

Figure 52 - Sulfate interference on arsenic analysis - method comparison

Arsenic Removal Results from Zeolite/Membrane Reactor

Once the membrane system had been characterized and operational parameters, which were inline with the previous adsorption studies and conventional membrane facilities, had been developed, the zeolite/membrane reactor was prepared for arsenic adsorption studies. The same ferrous sulfate modified zeolite, which was characterized in the previous kinetic and equilibrium studies, was used as the adsorbent media on the membrane substrate. The system was operated under the varying conditions of flux rate, arsenic feed concentration, and ferrous sulfate zeolite concentration, and water samples were collected of both the feed and permeate streams. As can be seen in Figure 53, the water quality from all 12 cases when viewed simultaneously exhibit similar behavior but there exists some discrepancy between their slope, initial arsenic passage, and time to begin sloping.

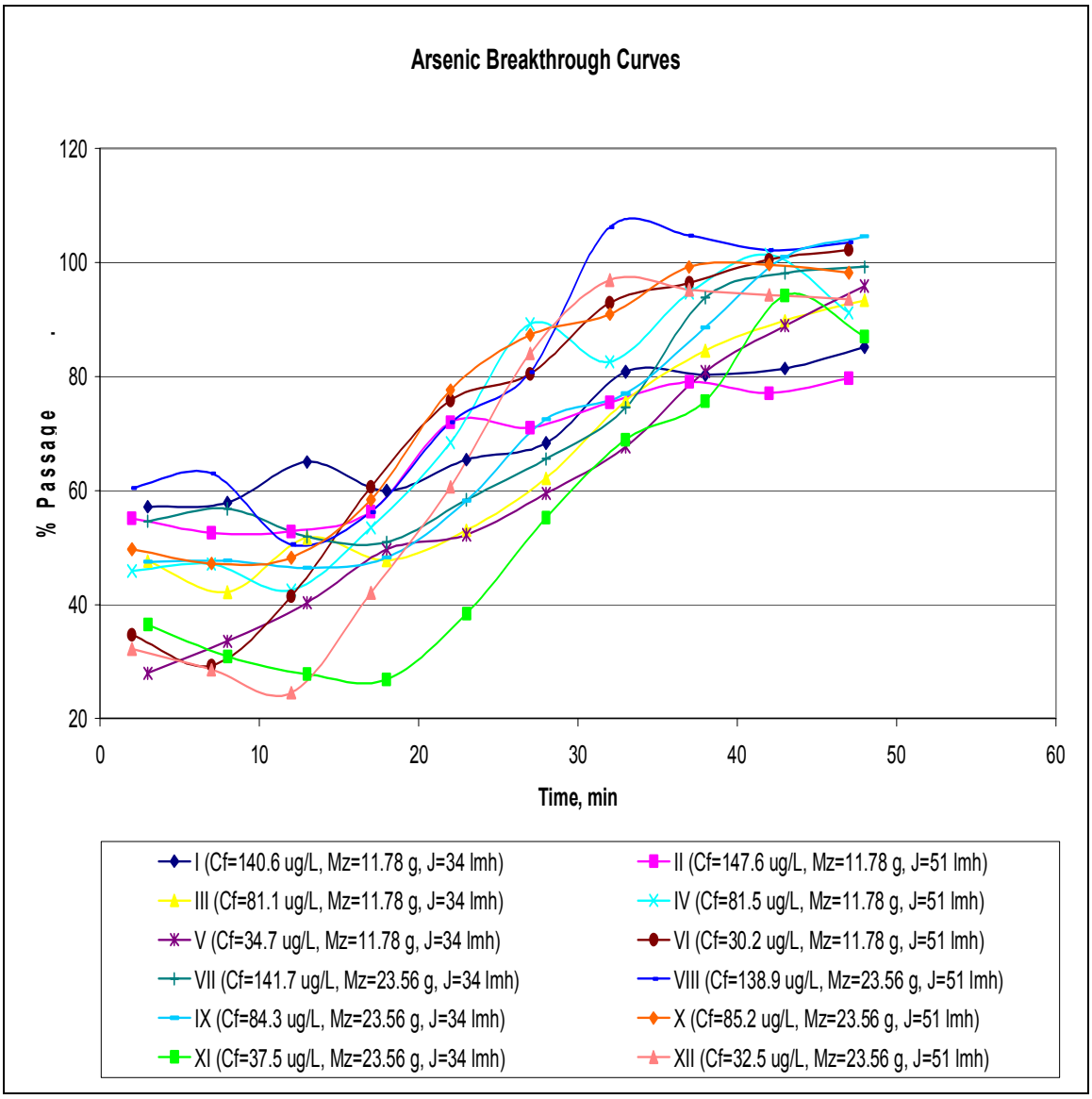

Figure 53 - Arsenic breakthrough curves for zeolite/membrane reactor, where C_f = As(III) feed concentration, M_z = mass of zeolite in reactor, J = water flux through membrane in L/(m^2.h) or lmh

To better understand these phenomena and to decide which factors most influence the reaction, a graph of the arsenic uptake per gram of zeolite was plotted against the total arsenic feed concentration which had entered the system. It is easily seen that two groups of lines with different slopes exist, one for the systems having on 11.78 g of zeolite (I – VI) and one for those having 23.56 g (VII – XII). Each group has a similar slope for the first 500 µg of arsenic added and then they begin to differ based on flux rate and initial concentration.

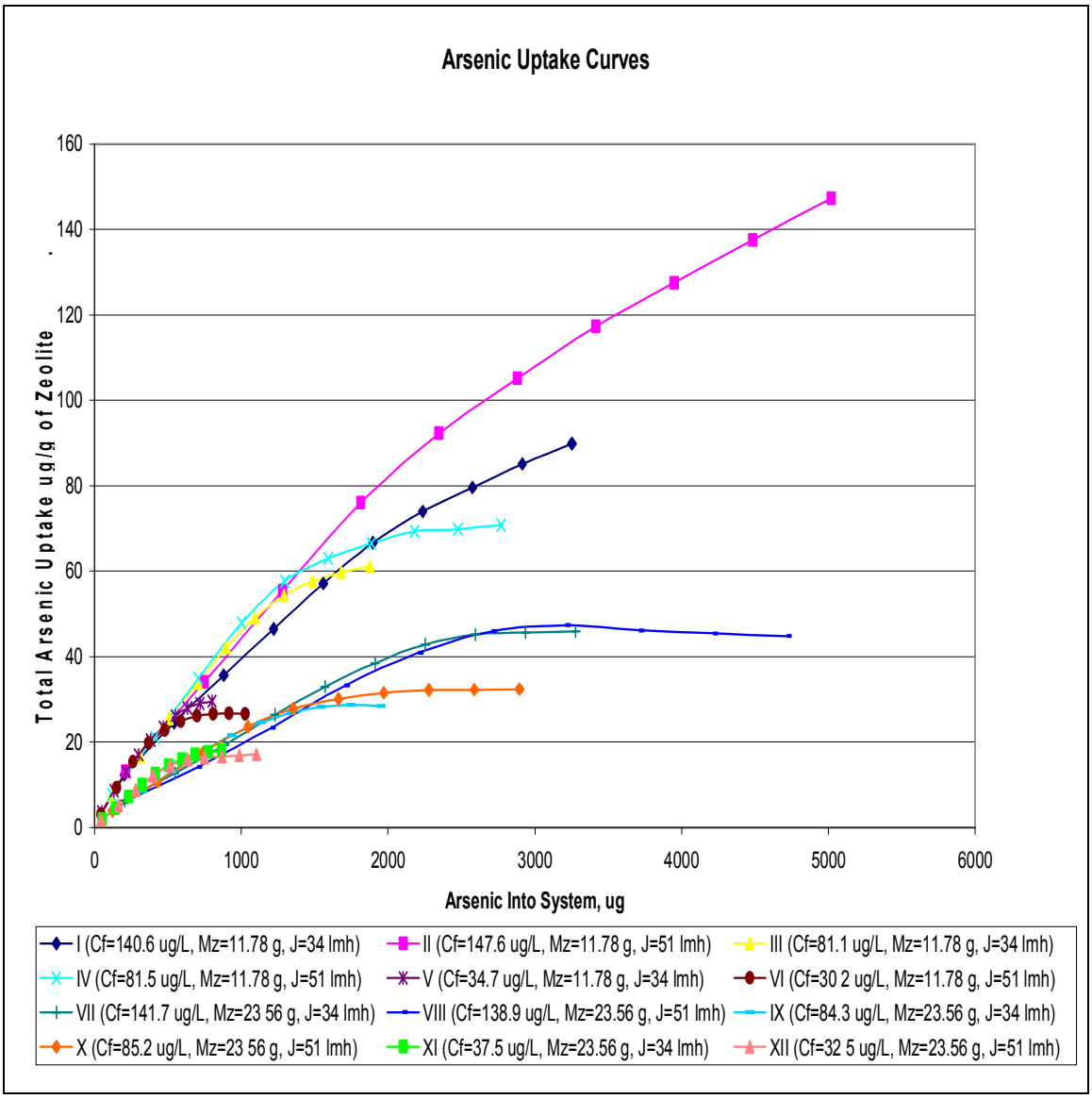

Figure 54 - Arsenic uptake per gram of zeolite versus total arsenic into the system

If the amount of arsenic adsorbed in a 5 minute time period is graphed versus the arsenic into the system as seen in Figure 55, these cases separate considerably. Those cases which had similar initial arsenic concentrations and flux rates (I and VII, II and VIII, III and IX, etc.) are similar in their trends while considerable differences occur when these values are changed. Based on this, it is presumed that under these conditions the mass of zeolite of 11.78 g or 23.56 g, does little to impact the overall uptake.

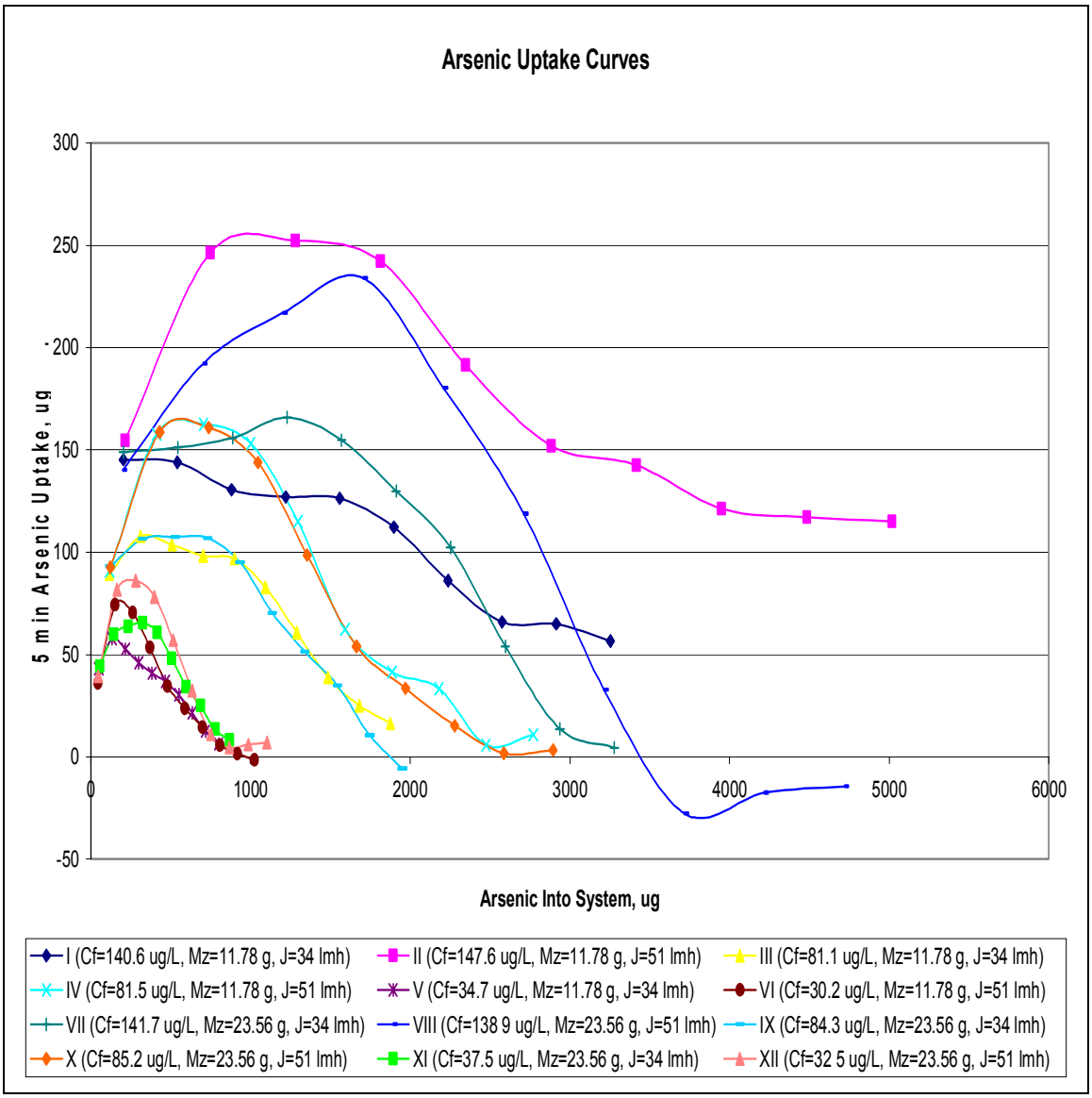

Figure 55 - Arsenic uptake in 5 minutes versus the arsenic dosed into the system

Appendix C contains many comparative graphs which demonstrate the major differences between the operational conditions and their resulting arsenic passage. Based on these graphs it was clear that the initial arsenic concentration and flux rate had the greatest impact on the arsenic adsorption and hence the passage into the permeate stream.

Development of Mathematical Model Describing this System

While the data sets, as described previously, demonstrate several trends, the correlation of these trends with the operational conditions that govern them is paramount to developing a fundamentally useful system. These models must accurately predict either the rate of uptake onto the zeolite or the change in arsenic permeate concentration in order for them to be applied by an engineer. Of the models previously mentioned in the literature review which dealt with cake layers on membrane substrates, the Langmuir model by Reddad and the Freundlich model by Li were most similar to the operational conditions which existed in these experiments. The model Matsui (Matsui et al., 2000) used in his experiments was developed using a continuous feed dose of the adsorbent material. Since our system was batch fed at the onset of the cycle, this model was not applicable.

Langmuir Model of Zeolite/Membrane System

A Langmuir Model similar to the work performed by Reddad (Reddad et al., 2003) was initially used to fit the data. His model states that:

$$q_e = \frac{q_m b C_e}{1 + b C_e}$$

q_e = equilibrium adsorption capacity in batch reactor

q_m = maximum adsorption capacity from Langmuir model

b = Langmuir equilibrium parameter

C_e = metal concentration at equilibrium

Using the conditions which exist in our system, the following equation was derived.

$$\frac{dM_m}{dt} = s\left(-aC_m + b\left(\frac{gC_e}{1 + gC_e}\right)\right)$$

Where: $\frac{dM_M}{dt}$ is the change in molar mass of arsenic inside the zeolite

s is the surface area of the zeolite

C_M is the instantaneous concentration inside the zeolite

C_E is the final equilibrium concentration inside the zeolite

And a, b, and g are fitting parameters

Using this equation, the following figure was developed which graphs the empirical change in molar mass to that of the model prediction. While the correlation, seen in Figure 56, is nearly a 1:1 fit and the R^2 value is 0.93, each of the first 6 runs (I –VI) have significantly different fitting parameters, a, b, and g, which could not be related to operational conditions. These values are seen in Table 19. Without this correlation the model would be impossible to predict under varying circumstances.

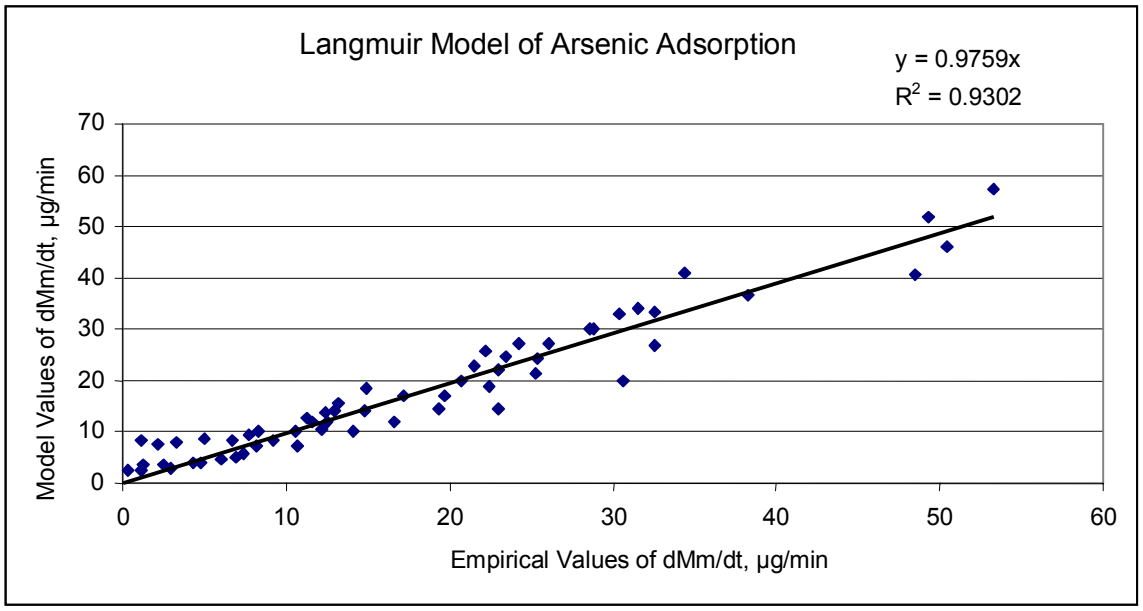

Figure 56 - Langmuir model of arsenic adsorption in zeolite/membrane reactor

Table 19 - Curve fitting parameters for Langmuir adsorption model

Run	a	b	g
I	0.154	256	1.15
II	0.151	354	1.37
III	0.192	300	1.26
IV	0.306	426	1.42
V	0.228	625	0.710
VI	0.389	518	1.35

Freundlich Model of Zeolite/Membrane System

Li (Li et al., 2003) used a Freundlich model to predict removal of organics through the use of PAC in a membrane reactor. Similar to this model the Freundlich model for this system was:

$$\frac{dM_M}{dt} = s\left(-aC_M + bC_E{}^g\right)$$

Where: $\frac{dM_M}{dt}$ is the change in molar mass of arsenic inside the zeolite

s is the surface area of the zeolite

C_M is the instantaneous concentration inside the zeolite

C_E is the final equilibrium concentration inside the zeolite

And a, b, and g are fitting parameters

As can be seen from Figures 57 through 62, the model does fit some of the cases fairly well, but did not model the non-linear curve change seen in cases like III and IV also the curve fitting parameters again proved to have little in common with the operational conditions of the system . Due to this, a Non-Linear Curve Fit was also tried.

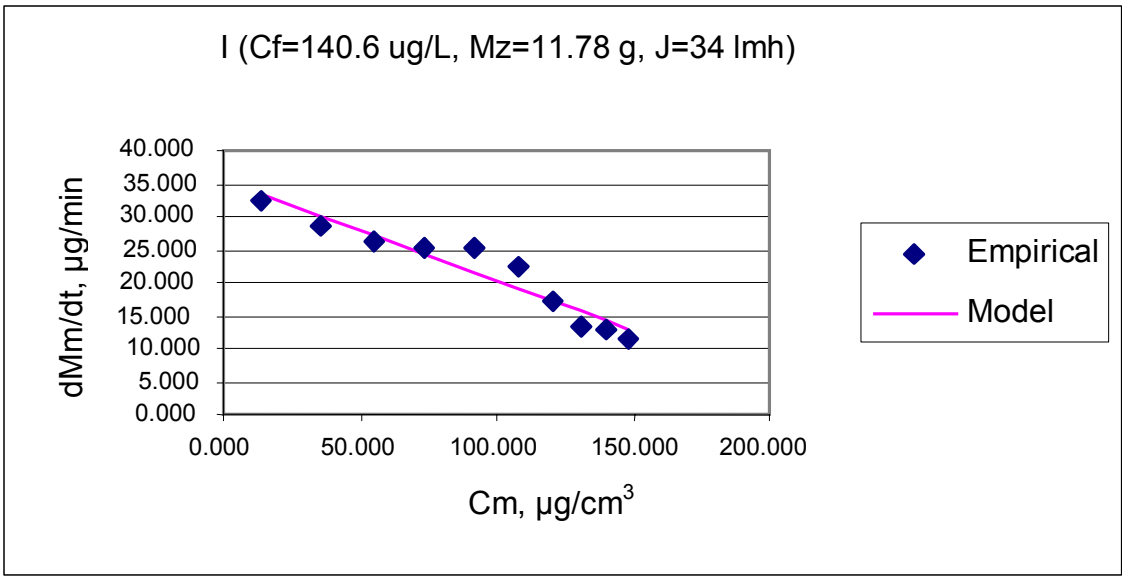

Figure 57 - Freundlich model of case I (140.6 ug/L of arsenic, 11.78 g of zeolite, and a water flux rate of 34 L/(m^2 h))

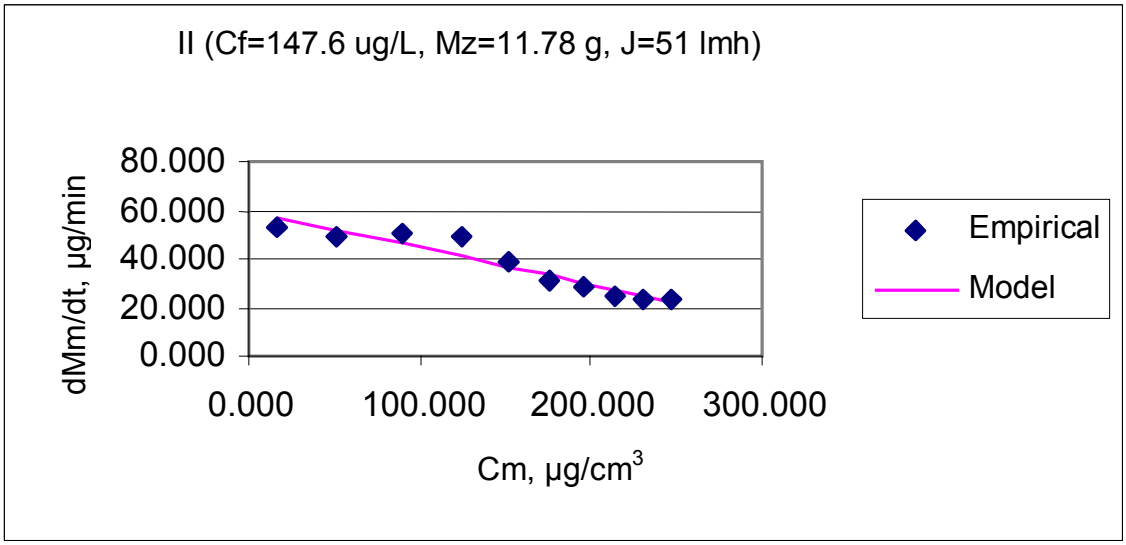

Figure 58 - Freundlich model of case II (147.6 ug/L of arsenic, 11.78 g of zeolite, and a water flux rate of 51 L/(m^2 h))

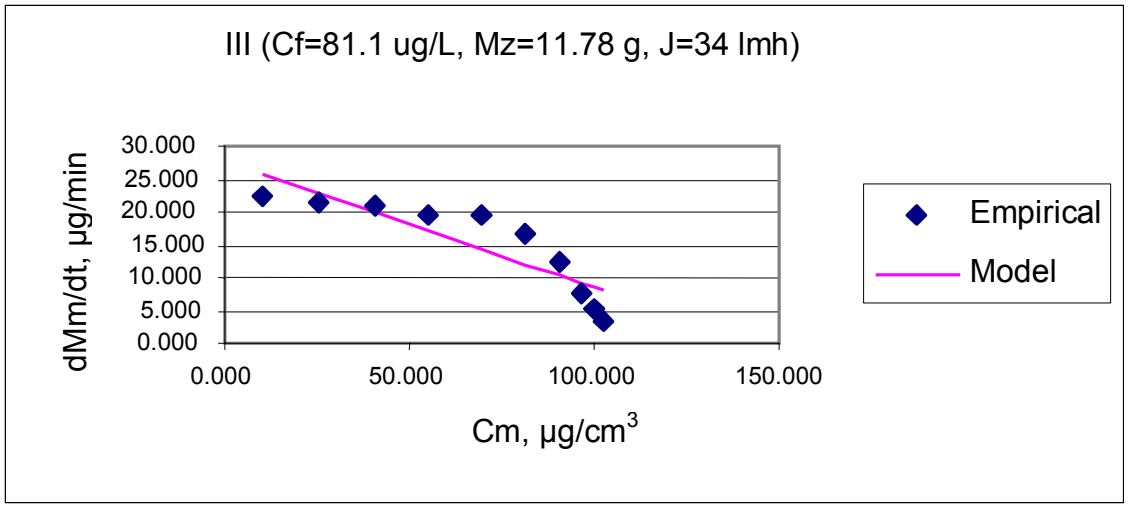

Figure 59 - Freundlich model of case III (81.1 ug/L of arsenic, 11.78 g of zeolite, and a water flux rate of 34 L/(m^2 h))

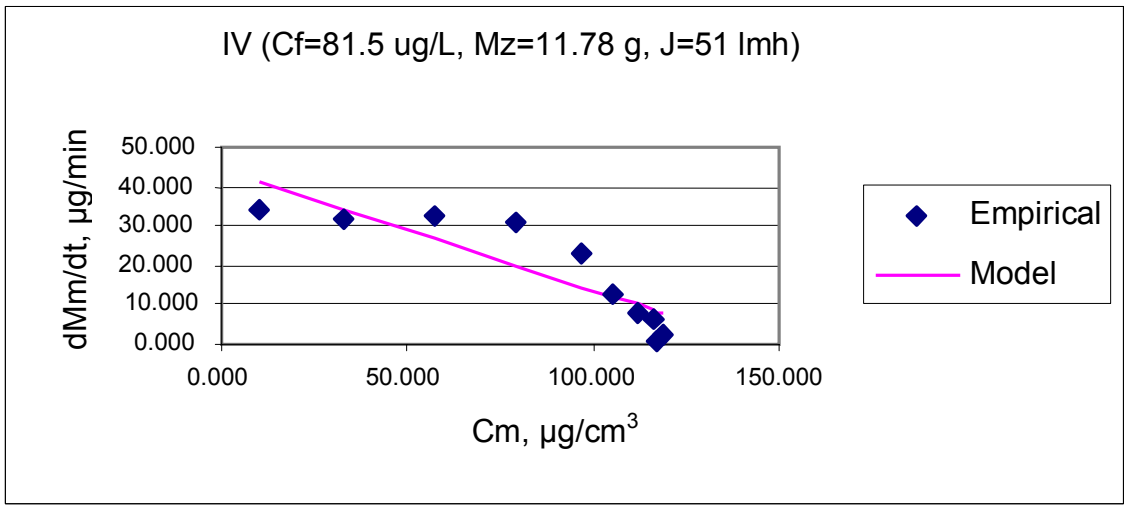

Figure 60 - Freundlich model of case IV (81.5 ug/L of arsenic, 11.78 g of zeolite, and a water flux rate of 51 L/(m^2 h))

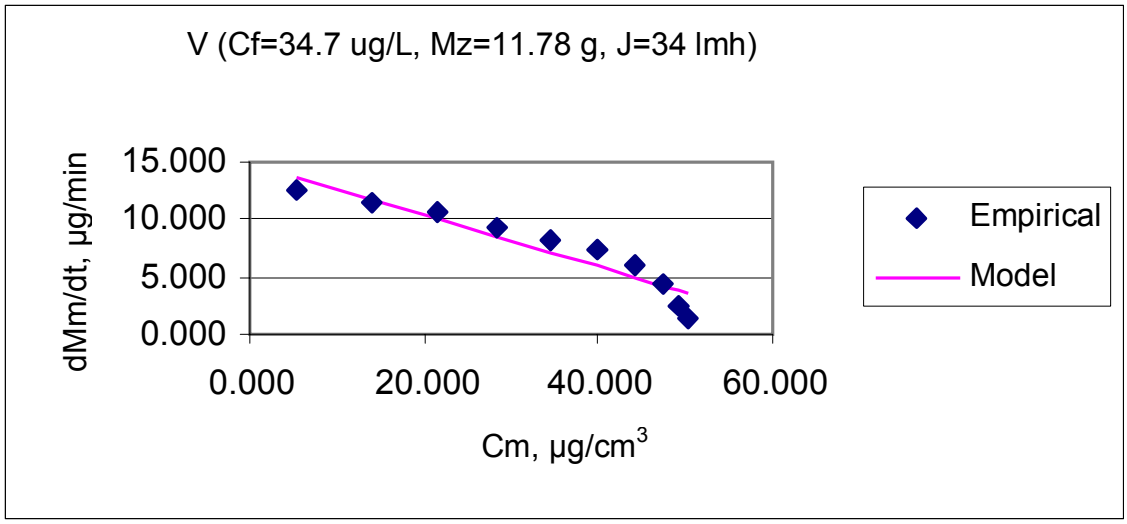

Figure 61 - Freundlich model of case V (34.7 ug/L of arsenic, 11.78 g of zeolite, and a water flux rate of 34 L/(m^2 h))

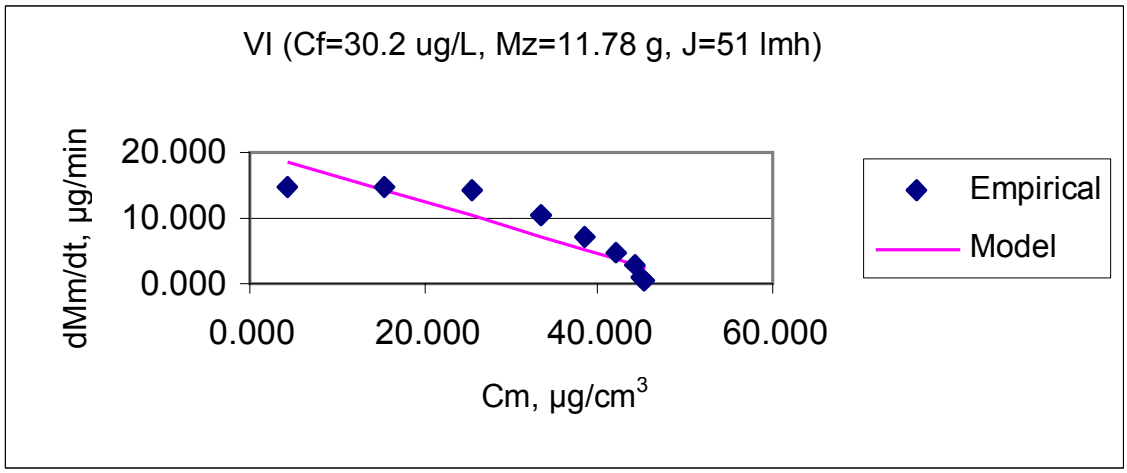

Figure 62 - Freundlich model of case VI (30.2 ug/L of arsenic, 11.78 g of zeolite, and a water flux rate of 51 L/(m^2 h))

Non-Linear Curve Fit Model of Zeolite/Membrane System

Based on the major differences between the Freundlich Model and the empirical data a Non-Linear Curve Fit Model was used to fit the data. Origin, a multi-regression analysis program from OriginLab, was used to develop a mathematical model which best represented the data. This model is based on the following:

$$\frac{dM_M}{dt} = y_0 + Ae^{\frac{-C_M}{\tau}}$$

Where: y_0 is the initial change in molar mass inside the zeolite

A is the rate of this change in molar mass inside the zeolite

And $e^{\frac{-C_M}{\tau}}$ represents the acceleration of change in molar mass uptake inside the zeolite

Figures 63 through 74 demonstrate how well a Non-Linear Curve Fit Model fits all cases; however, the curve fitting parameters are not based on any science and lend no information as to how operational parameters such as flux, zeolite mass and arsenic concentration effect the reaction. Despite numerous attempts to correlate the operational and curve fitting parameters, none was found which provided a consistent pattern.

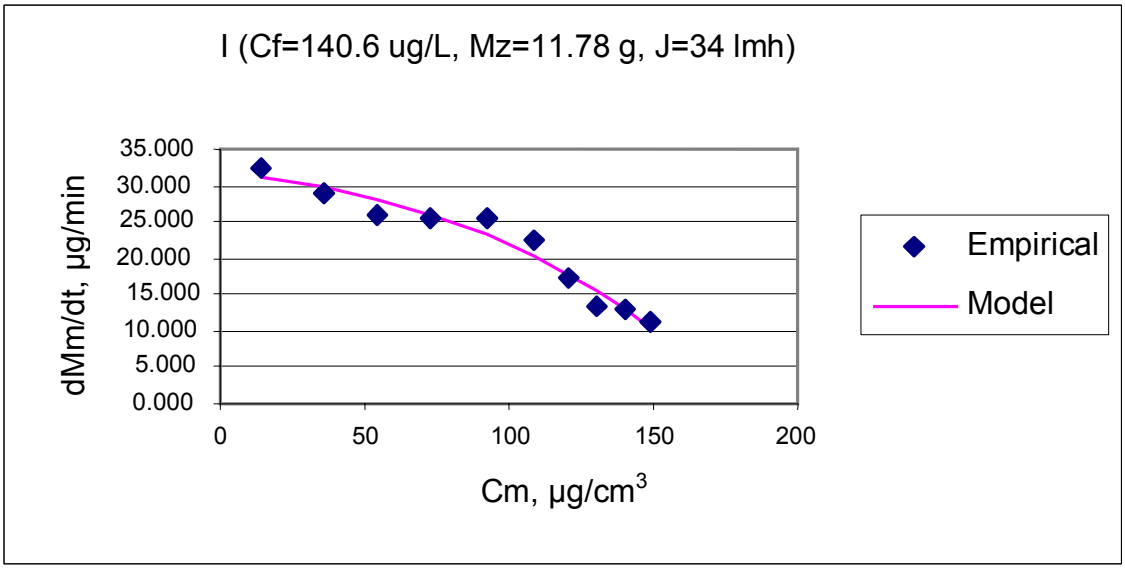

Figure 63 – Non-linear curve fit model of case I (140.6 ug/L of arsenic, 11.78 g of zeolite, and a water flux rate of 34 L/(m^2 h))

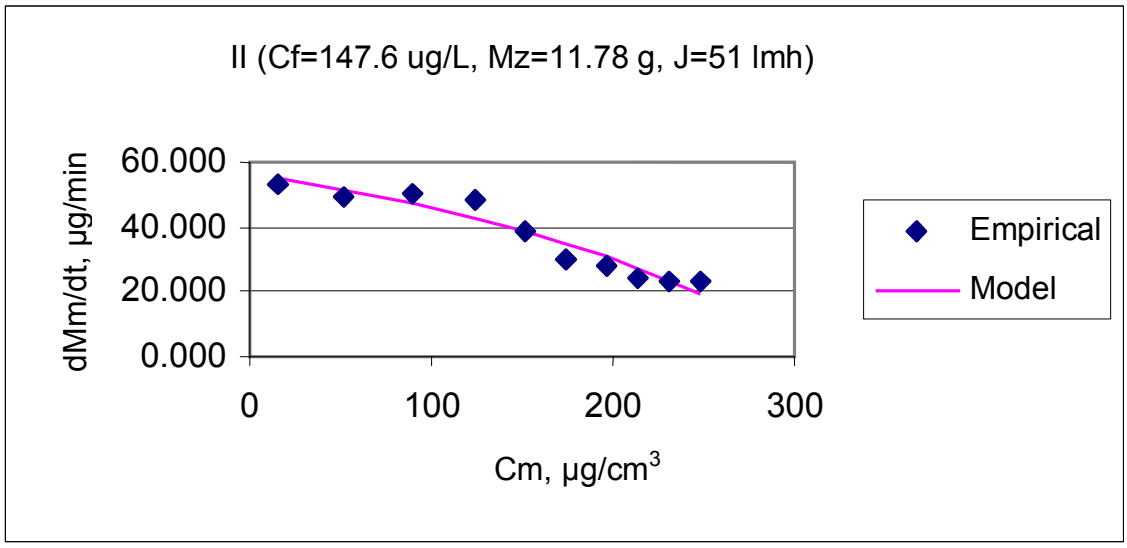

Figure 64 - Non-linear curve fit model of case II (147.6 ug/L of arsenic, 11.78 g of zeolite, and a water flux rate of 51 L/(m^2 h))

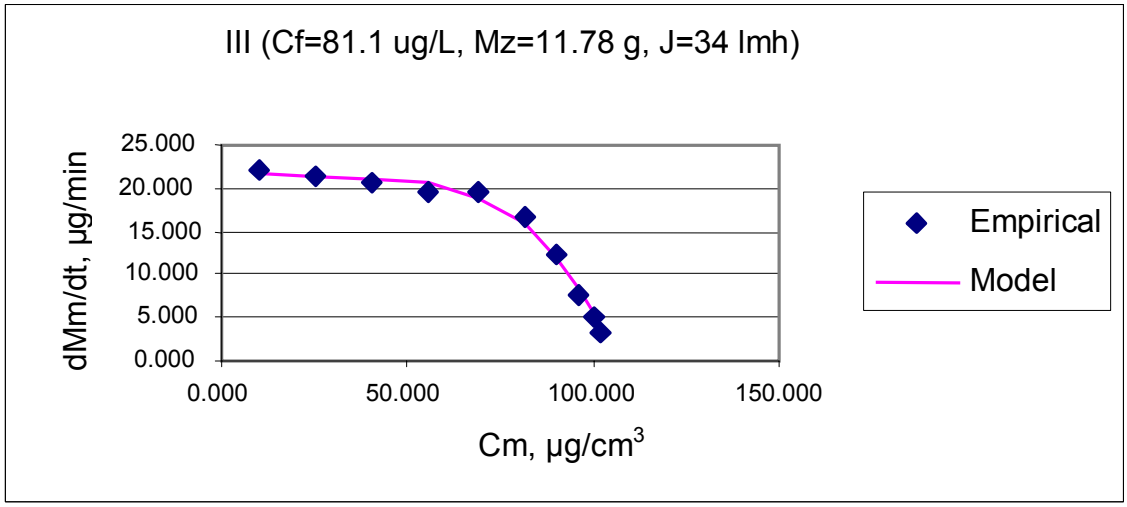

Figure 65 - Non-linear curve fit model of case III (81.1 ug/L of arsenic, 11.78 g of zeolite, and a water flux rate of 34 L/(m^2 h))

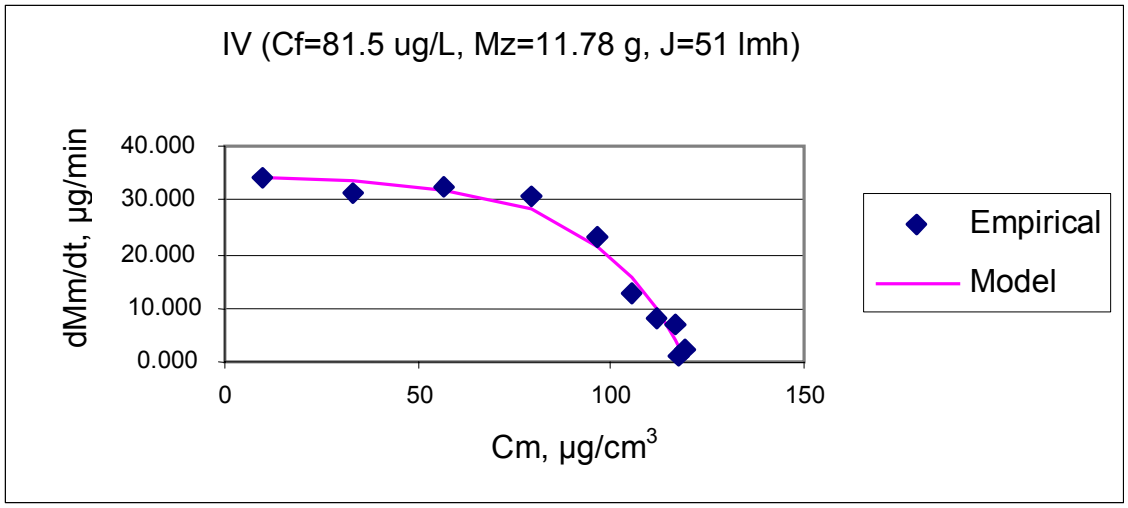

Figure 66 - Non-linear curve fit model of case IV (81.5 ug/L of arsenic, 11.78 g of zeolite, and a water flux rate of 51 L/(m^2 h))

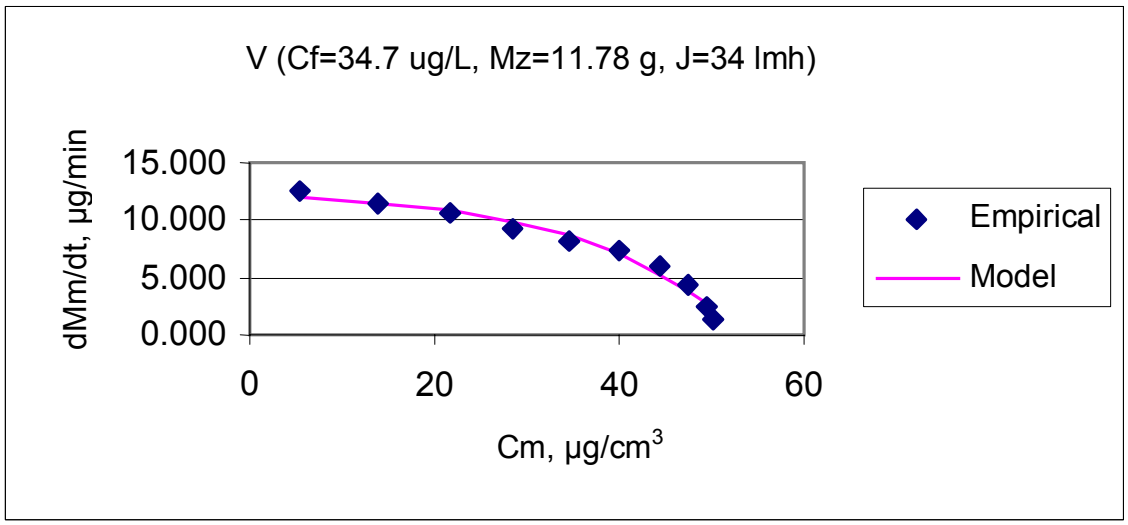

Figure 67 - Non-linear curve fit model of case V (34.7 ug/L of arsenic, 11.78 g of zeolite, and a water flux rate of 34 L/(m^2 h))

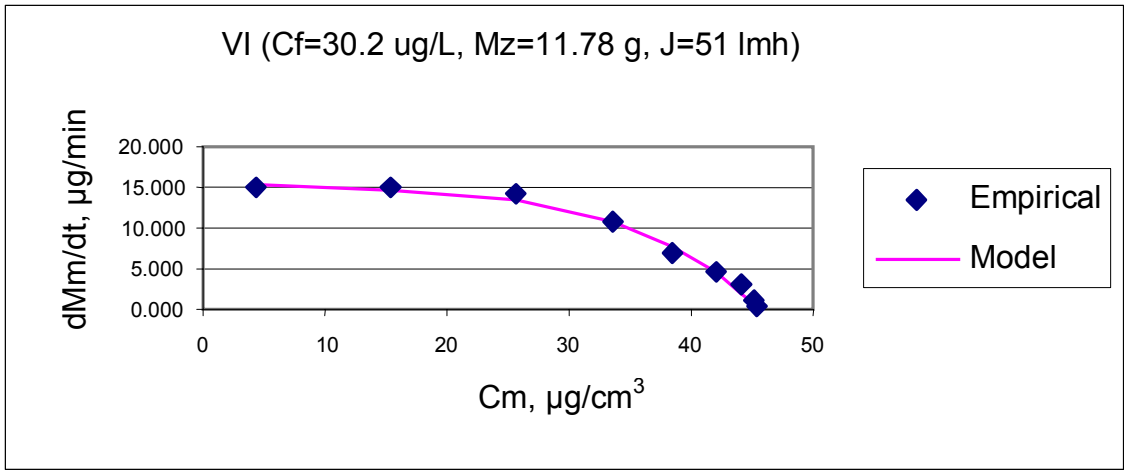

Figure 68 - Non-linear curve fit model of case VI (30.2 ug/L of arsenic, 11.78 g of zeolite, and a water flux rate of 51 L/(m^2 h))

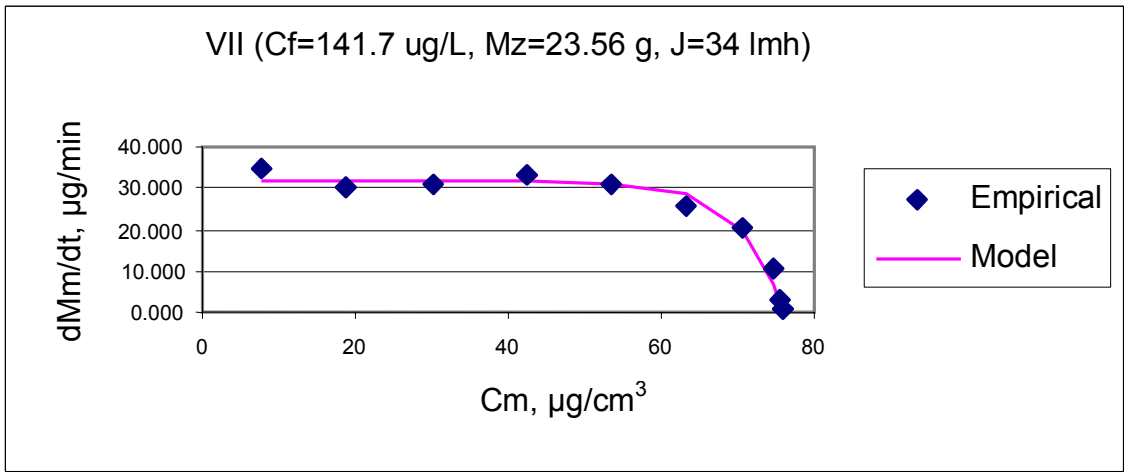

Figure 69 - Non-linear curve fit model of case VII (141.7 ug/L of arsenic, 23.56 g of zeolite, and a water flux rate of 34 L/(m^2 h))

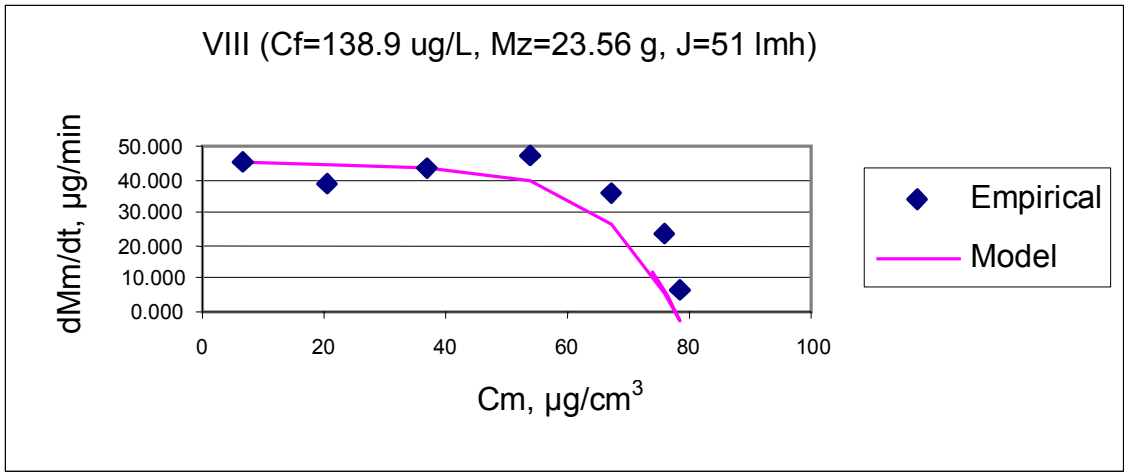

Figure 70 - Non-linear curve fit model of case VIII (138.9 ug/L of arsenic, 23.56 g of zeolite, and a water flux rate of 51 L/(m^2 h))

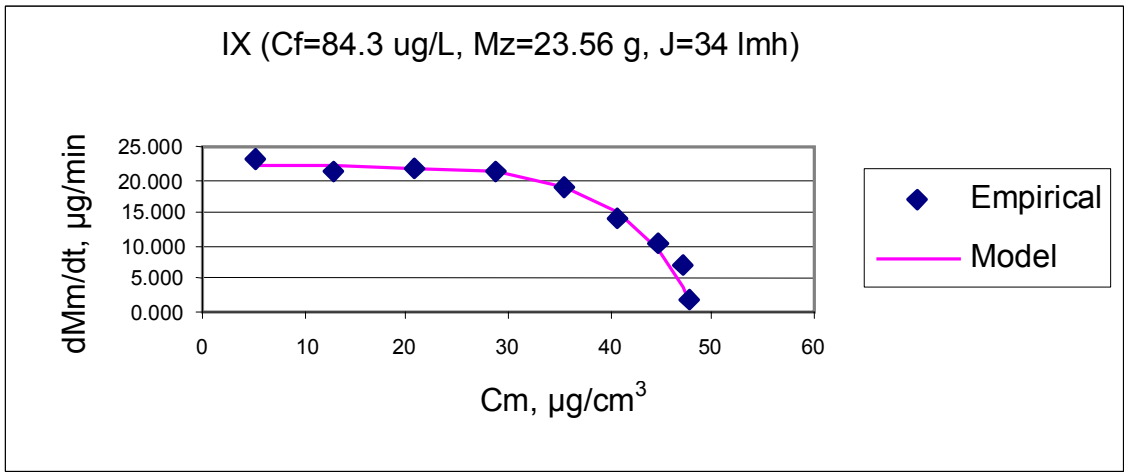

Figure 71 - Non-linear curve fit model of case IX (84.3 ug/L of arsenic, 23.56 g of zeolite, and a water flux rate of 34 L/(m^2 h))

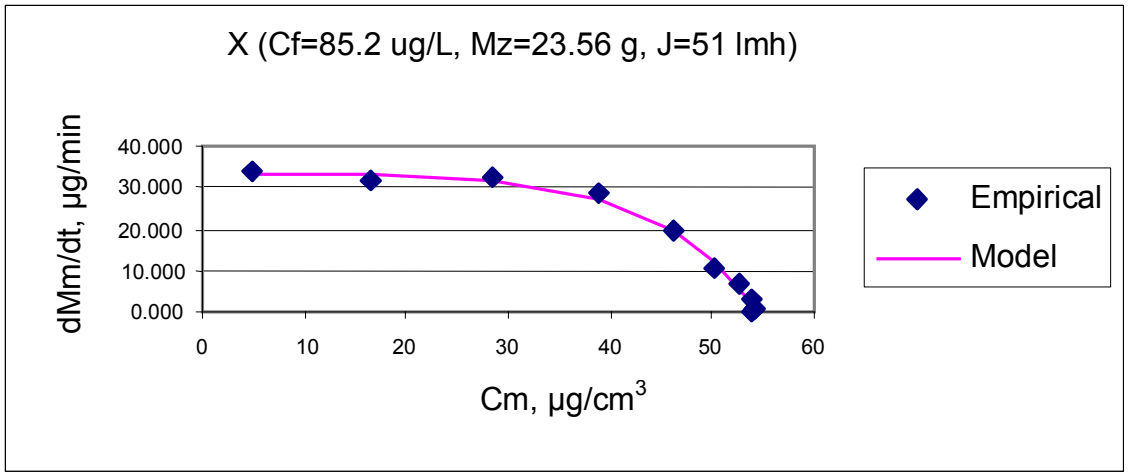

Figure 72 - Non-linear curve fit model of case X (85.2 ug/L of arsenic, 23.56 g of zeolite, and a water flux rate of 51 L/(m^2 h))

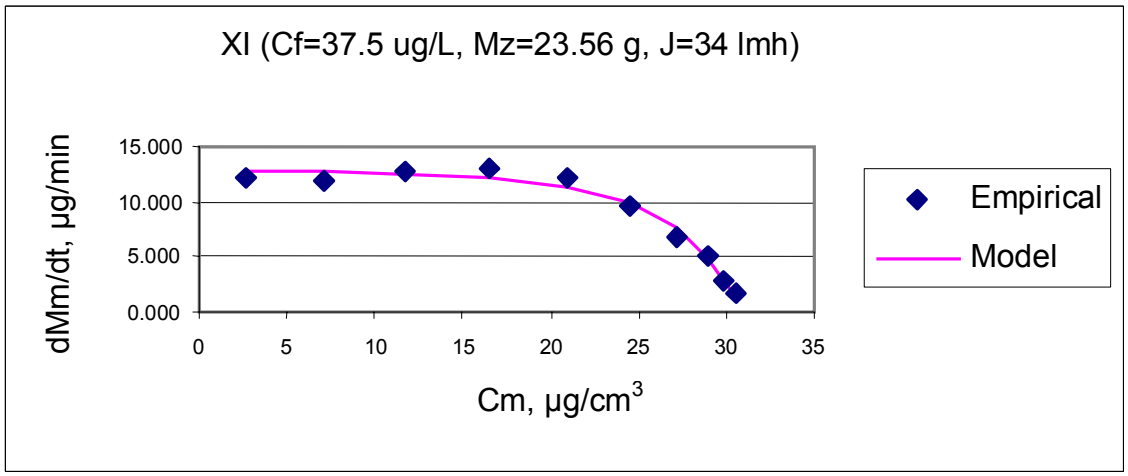

Figure 73 - Non-linear curve fit model of case XI (37.5 ug/L of arsenic, 23.56 g of zeolite, and a water flux rate of 34 L/(m^2 h))

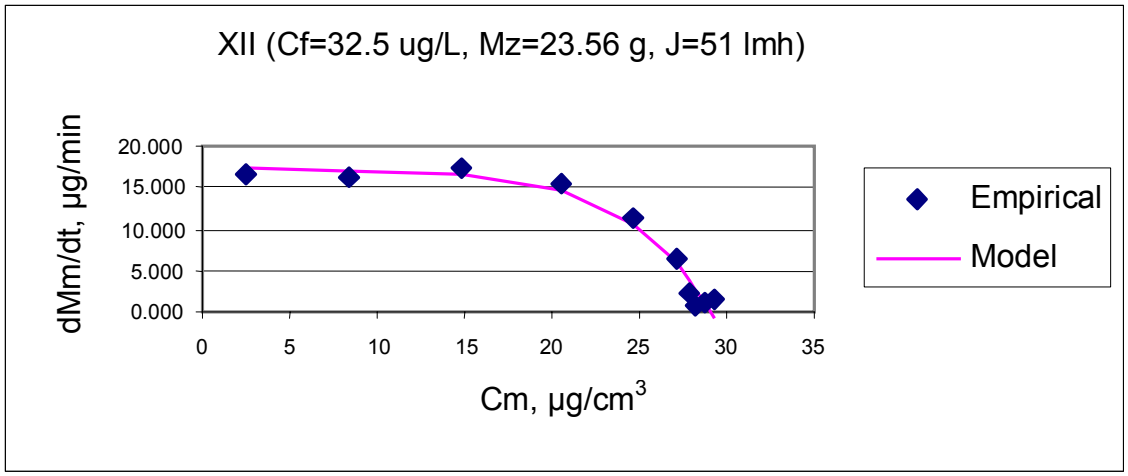

Figure 74 - Non-linear curve fit model of case XII (32.5 ug/L of arsenic, 23.56 g of zeolite, and a water flux rate of 51 L/(m^2 h))

Irreversible Adsorption Model of Zeolite/Membrane System

Since the known models had not been able to:

1. accurately predict the arsenic adsorption or
2. the curve fitting parameters had no correlation to the operational conditions governing the systems such as zeolite mass, flux rate, and initial arsenic concentration

A new model which had not previously been applied in the literature review was studied.

Based on literature review, which found that the zeolite did not leach arsenic, it was concluded that an irreversible adsorption model may provide an adequate description of the reaction. This model, which is exponential in nature, is based on the operational conditions of the system. The basis for this model was found in *Diffusion Mass Transfer in Fluid Systems*, by E. L. Cussler, 1997. The model and the conditions for the zeolite/membrane system are described as follows:

For an irreversible adsorption model, the saturation time can be estimated as:

$$t_{sat} = \frac{C_{z,sat}(1-\varepsilon)}{kaC_f}$$

Where: $C_{z,sat}$ is the saturation concentration in the zeolite

ε is the solution volume per bed volume

k is the mass transfer coefficient

a is the zeolite area per bed volume

and C_f is the feed arsenic concentration

After the initial portion of the cake is saturated, this wave front pushes through the zeolite at a velocity, v_{sat} which is related to the feed velocity, v. The relation between the two velocities is shown below.

$$C_f vA(t - t_{sat}) = C_{z,sat}(1-\varepsilon)v_{sat}A(t - t_{sat})$$

Simplifying this equation we arrive at an equation for this saturated velocity as:

$$v_{sat} = v\left(\frac{C_f}{C_{z,sat}(1-\varepsilon)}\right)$$

where:

$C_f = C_{z,sat}$ *when* $C_{z,sat} >> C_f$

and

$$v_{sat} = v\left(\frac{1}{(1-\varepsilon)}\right) \quad when \quad v_{sat} << v$$

Using this saturation velocity we can determine the depth of the saturation zone, δ_{sat}, through the following equation:

$$\delta_{sat} = \left(\frac{vC_f t}{C_{z,sat}(1-\varepsilon)} \right) - \frac{v}{ka}$$

Having the saturated area now well defined, the model must focus on the adsorption area where saturation has yet to occur. Writing a mass balance on the system provides that the

[arsenic accumulated] = [arsenic flow in – out] – [arsenic adsorbed]

This can be viewed differentially as:

$$\varepsilon \frac{\partial C}{\partial t} = -v \frac{\partial C}{\partial z} - ka\left(C - C^*\right)$$

With the assumption that the adsorption process is irreversible $C^* = 0$. This is true for this case due to the time constraints of the model prior to reaching equilibrium. Also assuming that the concentration of arsenic inside the zeolite is much greater than that in the solute, we can drop the left side of the equation. This results in the following simplification:

$$ka(C) = -v \frac{\partial C}{\partial z}$$

Using the boundary conditions provided by the saturation depth of:

$z = \delta_{sat}$ $C = C_f$

we can integrate and solve for the estimated concentration in the adsorption zone.

$$\frac{C}{C_f} = e^{\frac{-ka}{v}(z-\delta_{sat})}$$

Using this equation, the equation for the saturation depth, and the boundary conditions related to the breakthrough into the permeate stream of

$z = \delta$ $C = C_p$

we arrive at the final mathematical model for the estimated permeate concentration based on the feed concentration, zeolite cake layer, porosity of the cake layer, and the mass transfer coefficient as:

$$C_p = C_f e^{\left(-1+\frac{ka\delta}{v}\left(\frac{C_f vt}{C_{z,sat}(1-\varepsilon)\delta}-1\right)\right)}$$

For the model, δ was estimated as 0.002 cm and 0.004 cm when 11.78 and 23.56 g of zeolite were added to the reactor, respectively. These were based on Choi (Choi et al., 2000) basic model of microspheres in microfiltration. Monte Carlo Simulations, based on experimental data of particle radius, performed by Kim and Hoek, were used to

estimate a homogeneous cake layer with a porosity of 60% (Kim, 2002). The resulting equation for determining the cake layer thickness was:

$$\delta_c = \left(\frac{m_p}{\rho_p (1-\varepsilon) A_m} \right) = \text{volume of cake per area of membrane}$$

Where: m_p = total dried mass of cake, 11.78 or 23.56 g

ρ_p = density of particle, 1.73 g/cm^3

ε = cake porosity, 60%

And A_m = membrane area, 0.85 m^2 or 8500 cm^2

Although all experiments were carried out for the same duration, the time to reach saturation varied substantially. The permeate data was analyzed and t_{sat} was set when the permeate concentration reached the feed concentration or when this permeate concentration reached near steady state. The resulting t_{sat} data was:

Table 20 - Saturation times for each zeolite/membrane case

Case	I	II	III	IV	V	VI	VII	VIII	IX	X	XI	XII
Saturation Time, Min	33	32	48	37	48	42	43	32	43	37	43	32

Using these values, the feed concentration, and the flux rate, the saturation concentration inside the zeolite, $C_{z,sat}$ was determined to be:

Table 21 - Saturation concentrations inside the zeolite for each zeolite/membrane case

Case	I	II	III	IV	V	VI	VII	VIII	IX	X	XI	XII
$C_{z,sat}$, ug/cm^3	121.0	195.8	102.4	116.7	50.3	45.3	75.7	78.2	47.9	53.8	29.9	27.9

Using the saturation concentrations shown in Table 21, ka were determined and are presented in Table 22.

Table 22 - ka values for each zeolite/membrane case

Case	I	II	III	IV	V	VI	VII	VIII	IX	X	XI	XII
ka, min^{-1}	8.8	14.3	10.5	12.5	12.1	12.7	4.5	4.5	4.7	5.4	6.8	7.7

Using these values the permeate concentration was predicted. The following graphs, Figures 75 – 86, correspond to models of the zeolite/Membrane Cases based on the matrix sets provided above.

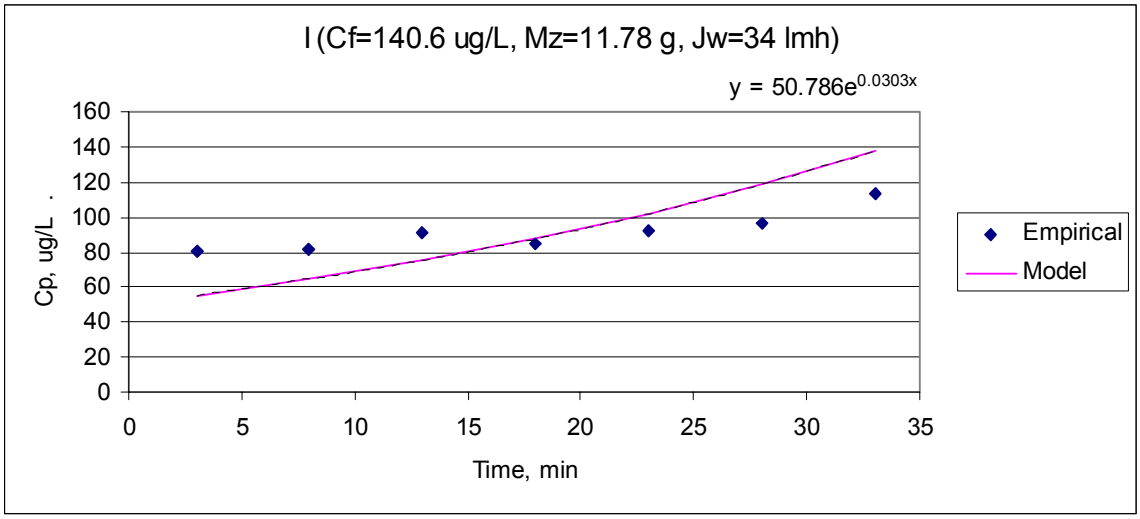

Figure 75 – Irreversible adsorption model of case I (140.6 ug/L of arsenic, 11.78 g of zeolite, and a water flux rate of 34 L/(m^2 h))

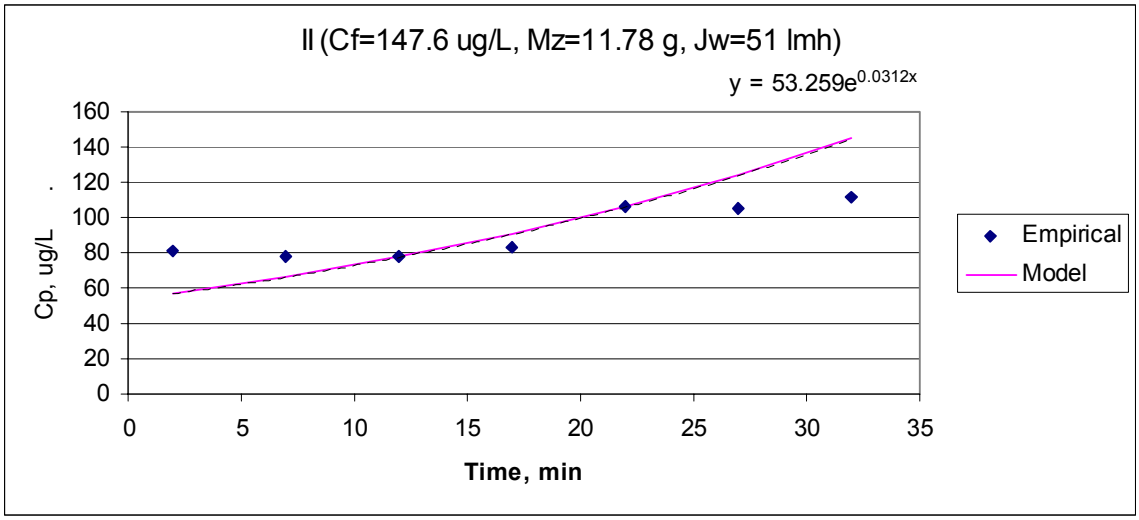

Figure 76 - Irreversible adsorption model of case II (147.6 ug/L of arsenic, 11.78 g of zeolite, and a water flux rate of 51 L/(m^2 h))

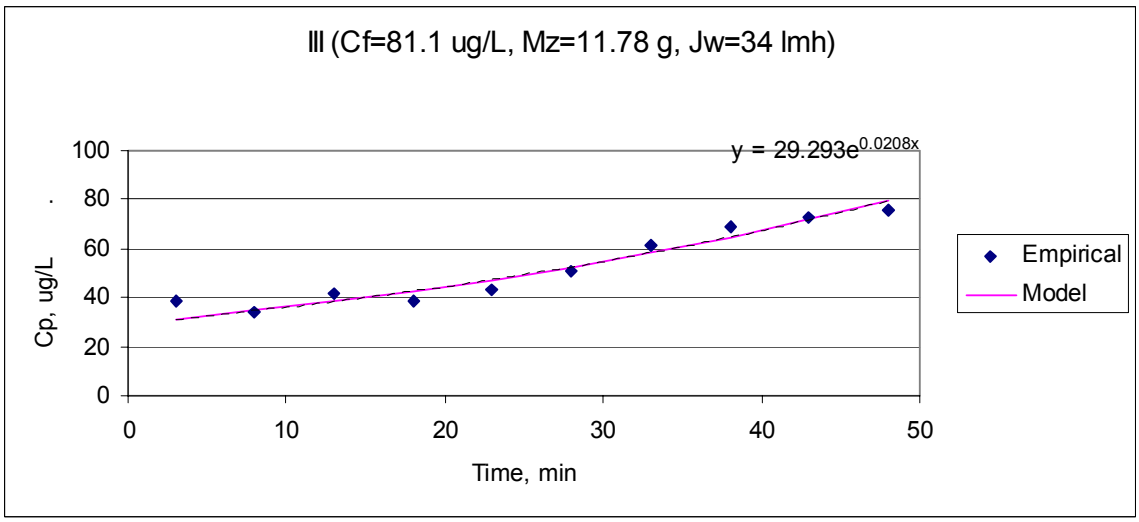

Figure 77 - Irreversible adsorption model of case III (81.1 ug/L of arsenic, 11.78 g of zeolite, and a water flux rate of 34 L/(m^2 h))

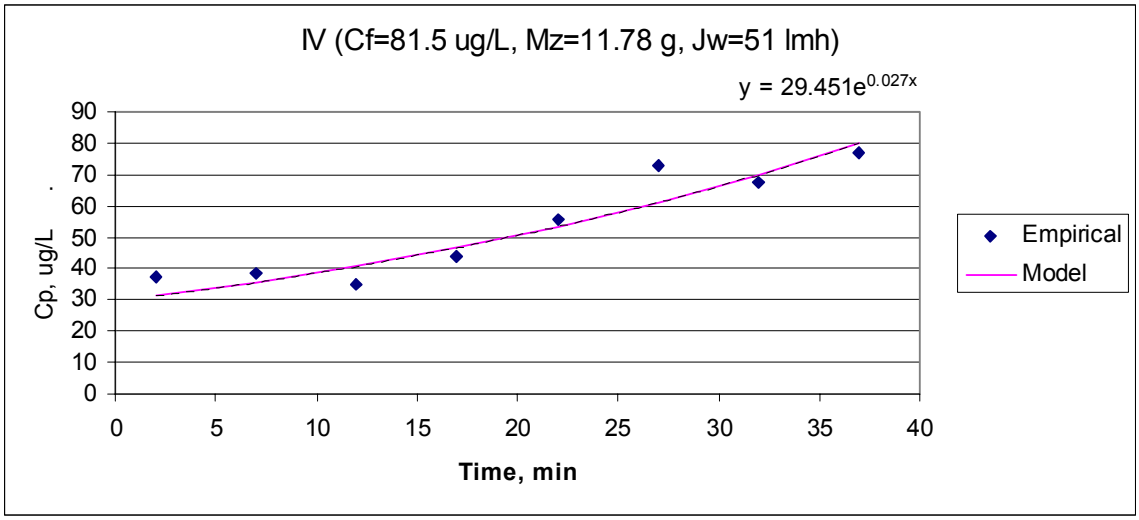

Figure 78 - Irreversible adsorption model of case IV (81.5 ug/L of arsenic, 11.78 g of zeolite, and a water flux rate of 51 L/(m^2 h))

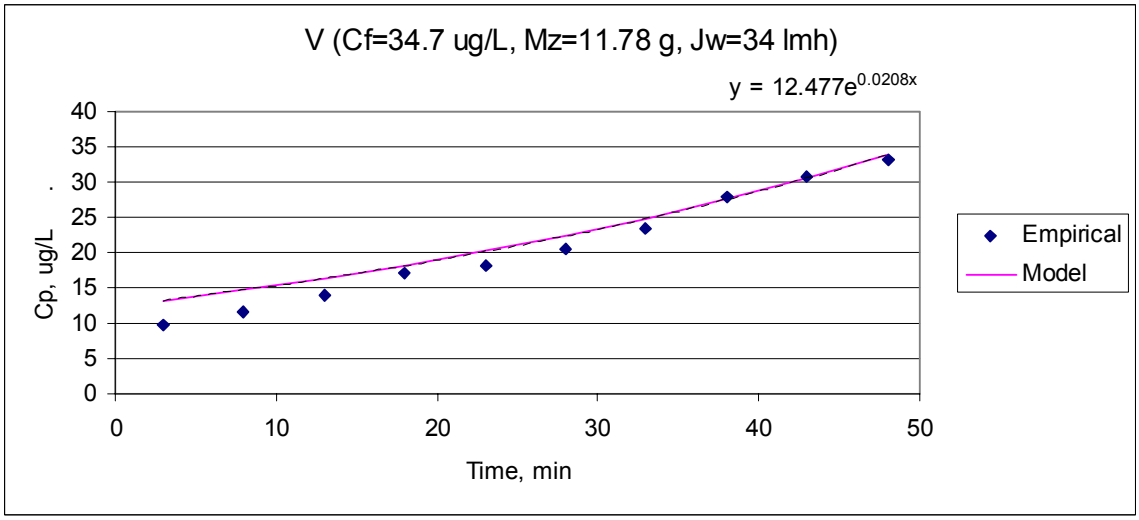

Figure 79 - Irreversible adsorption model of case V (34.7 ug/L of arsenic, 11.78 g of zeolite, and a water flux rate of 34 L/(m^2 h))

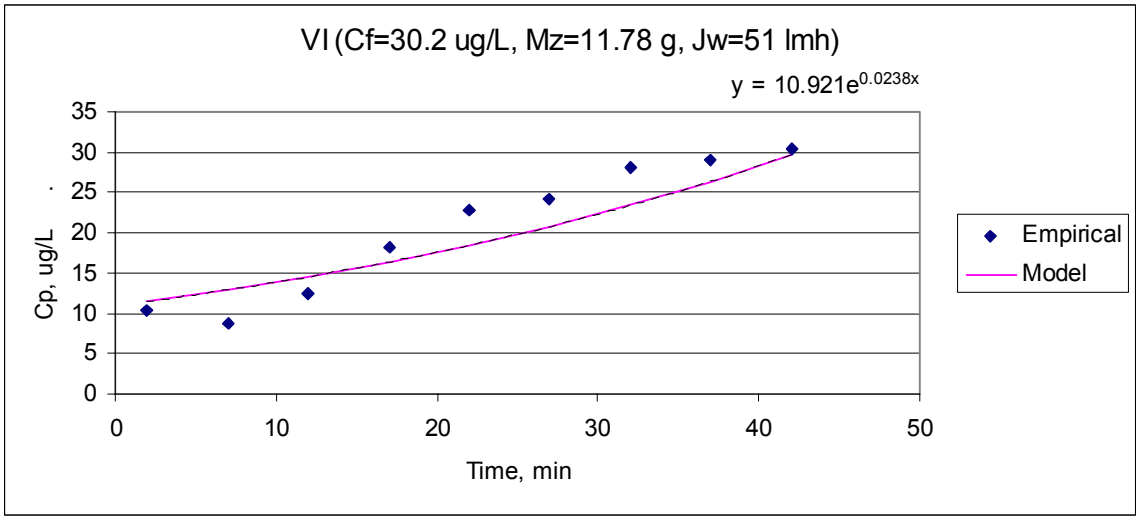

Figure 80 - Irreversible adsorption model of case VI (30.2 ug/L of arsenic, 11.78 g of zeolite, and a water flux rate of 51 L/(m^2 h))

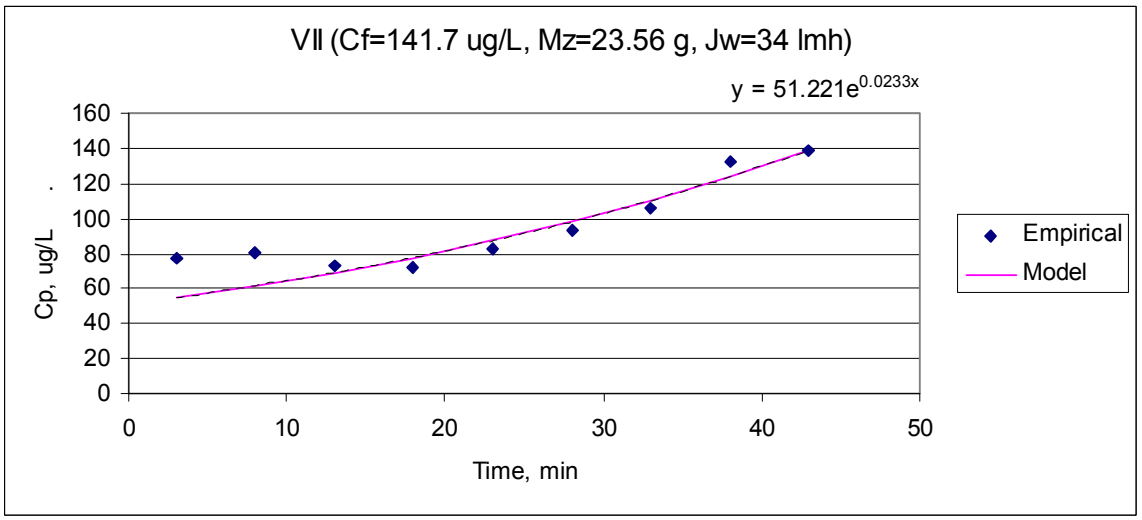

Figure 81 - Irreversible adsorption model of case VII (141.7 ug/L of arsenic, 23.56 g of zeolite, and a water flux rate of 34 L/(m^2 h))

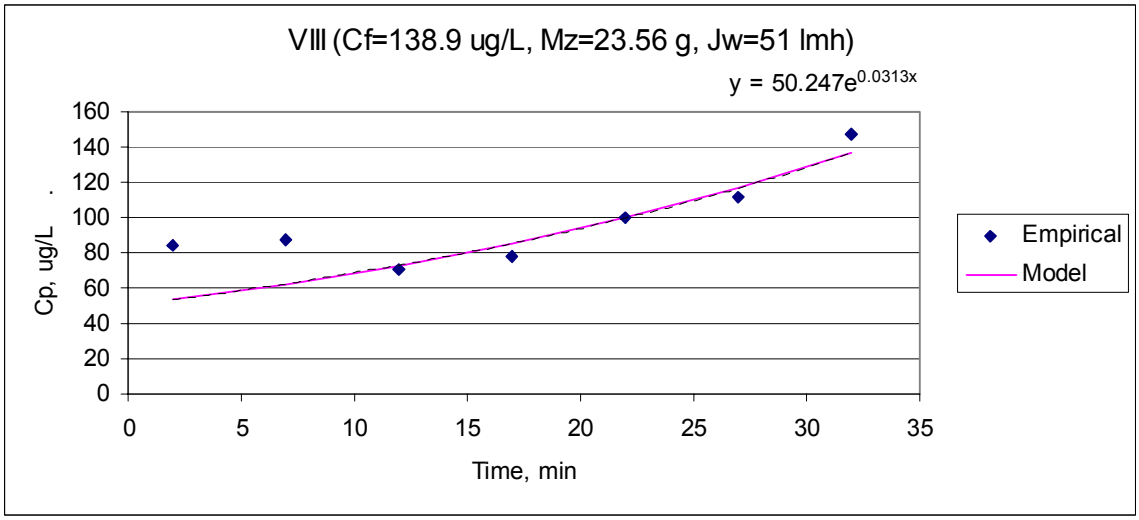

Figure 82 - Irreversible adsorption model of case VIII (138.9 ug/L of arsenic, 23.56 g of zeolite, and a water flux rate of 51 L/(m^2 h))

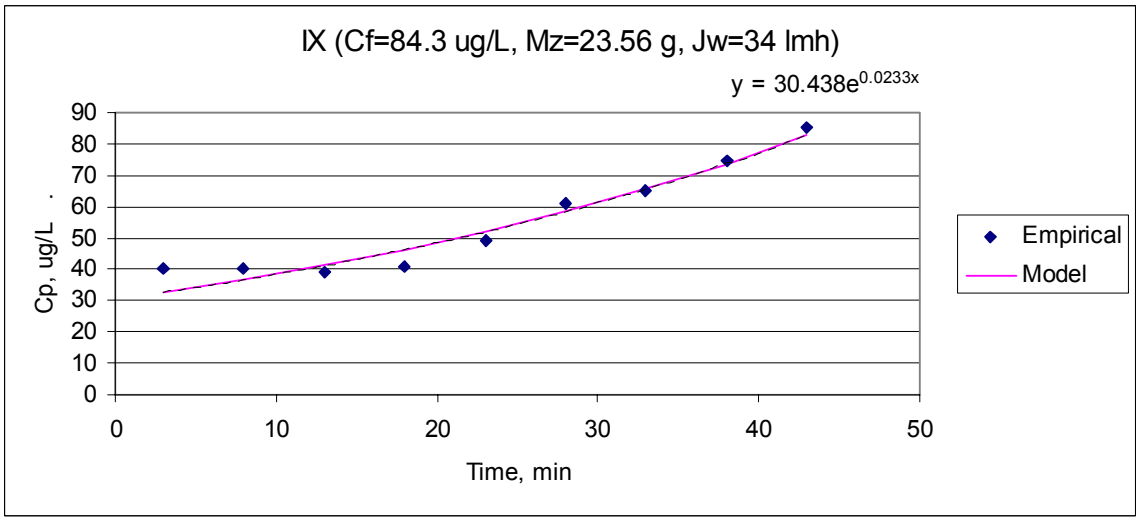

Figure 83 - Irreversible adsorption model of case IX (84.3 ug/L of arsenic, 23.56 g of zeolite, and a water flux rate of 34 L/(m^2 h))

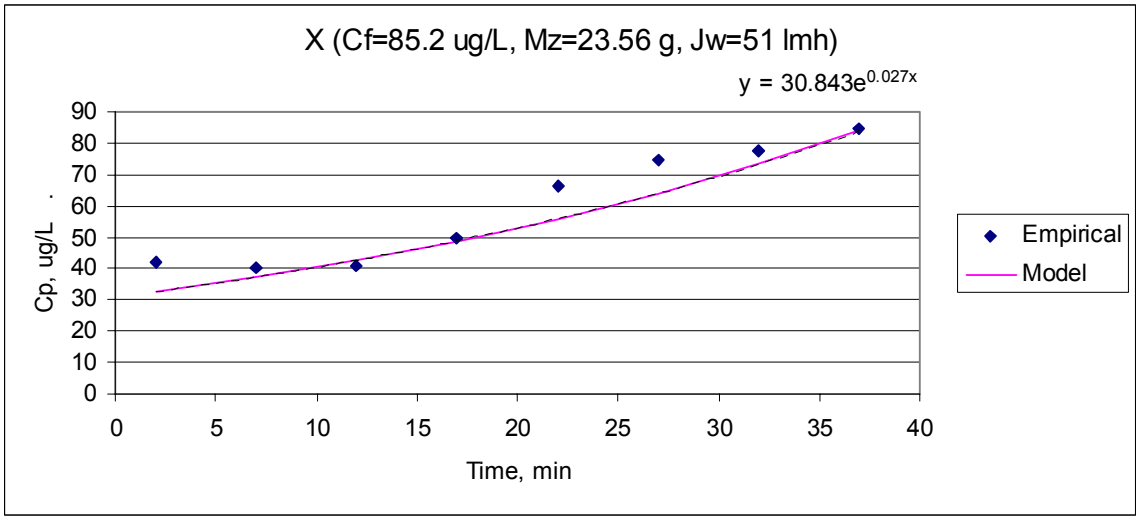

Figure 84 - Irreversible adsorption model of case X (85.2 ug/L of arsenic, 23.56 g of zeolite, and a flux water rate of 51 L/(m^2.h))

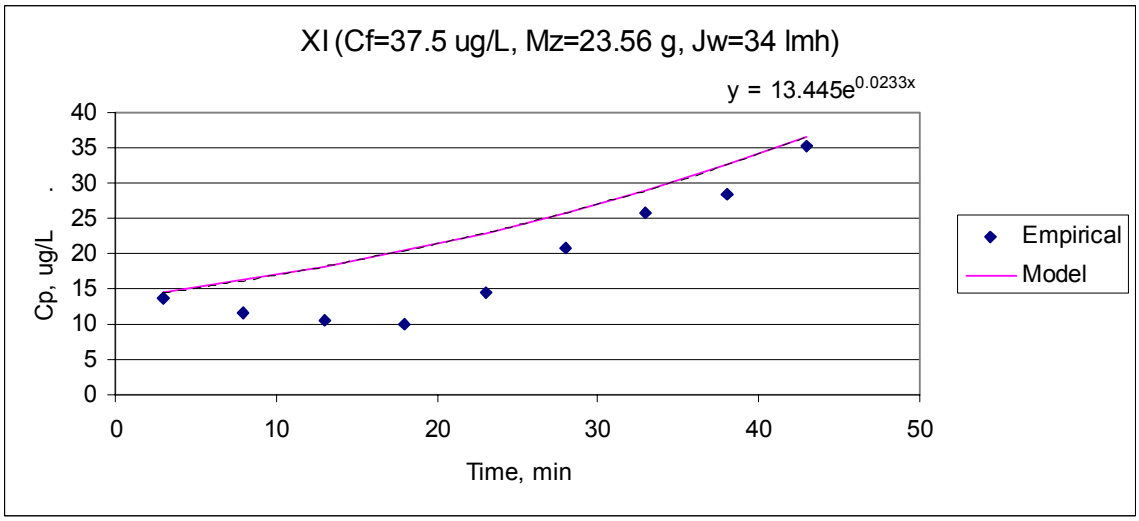

Figure 85 - Irreversible adsorption model of case XI (37.5 ug/L of arsenic, 23.56 g of zeolite, and a water flux rate of 34 L/(m^2 h))

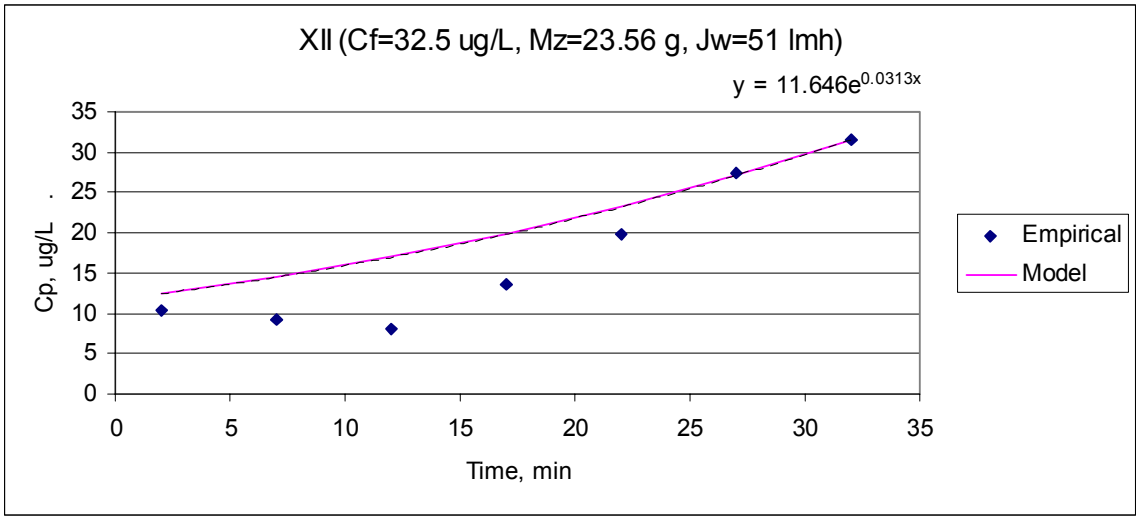

Figure 86 - Irreversible adsorption model of case XII (32.5 ug/L of arsenic, 23.56 g of zeolite, and a water flux rate of 51 L/(m^2 h))

An Analysis of Variance, ANOVA, conducted on all 12 Data sets with a 0.001 significance difference, showed no significant differences between the actual and modeled data.

If a plot is made of the actual permeate concentration versus the modeled permeate concentration the resulting graph show a near 1:1 correlation for nearly all of the data points.

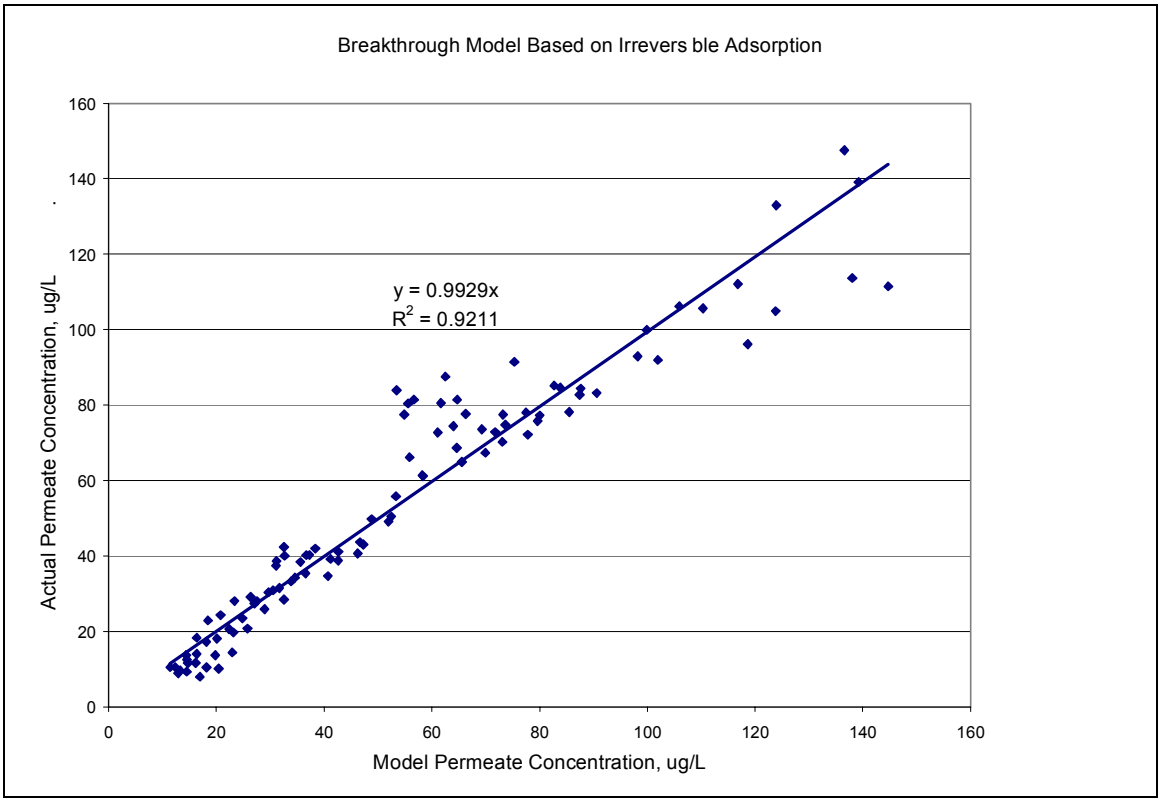

Figure 87 - Composite breakthrough comparison of actual versus modeled data for all runs

Summarizing all of the models from their individual graphs into the form:

$$C_p = \alpha\, e^{\beta t}$$

Where: C_P represents the predicted permeate arsenic concentration at some time

α represents the predicted initial permeate concentration

β represents the rate of change in permeate concentration and is inversely related to time

and t represents the time from the beginning of the cycle

We arrive at Table 23 for all sets of data.

Table 23 - Operational conditions and correlation coefficients for all cases

Case	Flux, l/(m^2.h)	Mass, g	Arsenic feed concentration, µg/L	α	β
I	34	11.78	140.6	50.786	0.0303
II	51	11.78	147.6	53.289	0.0312
III	34	11.78	81.1	29.293	0.0208
IV	51	11.78	81.5	29.451	0.027
V	34	11.78	34.7	12.477	0.0208
VI	51	11.78	30.2	10.921	0.0238
VII	34	23.56	141.7	51.221	0.0233
VIII	51	23.56	138.9	50.247	0.0313
IX	34	23.56	84.3	30.438	0.0233
X	51	23.56	85.2	30.843	0.027
XI	34	23.56	37.5	13.445	0.0233
XII	51	23.56	32.5	11.646	0.0313

A definitive prediction of α may be found by plotting α vs. the arsenic feed concentration, C_f as shown below.

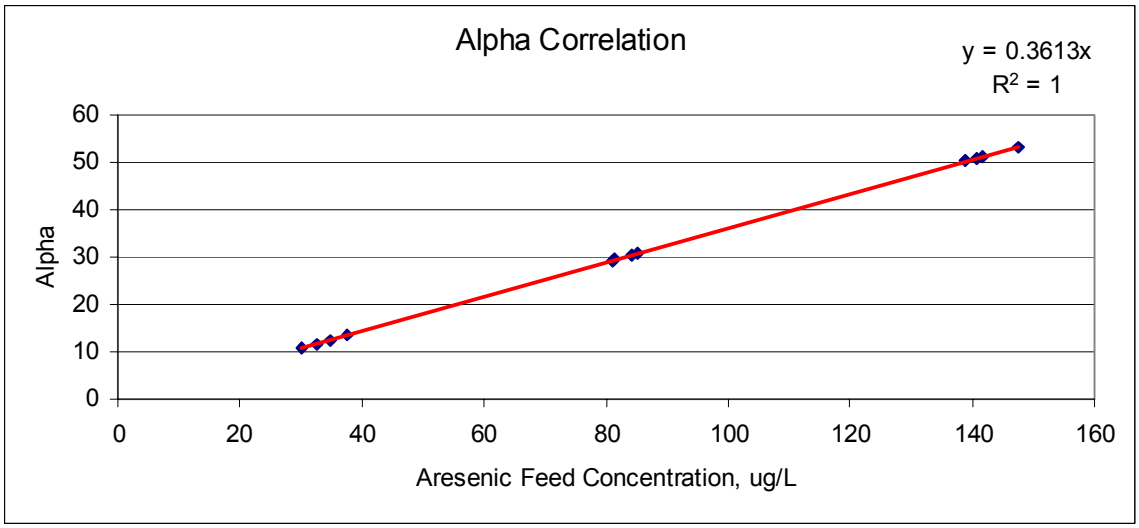

Figure 88 - Alpha correlation to arsenic feed concentration

Accordingly, for this reactor, regardless of flux rate or mass of zeolite, the α value is simply 36.13% of the feed concentration.

Since β must have units inversely related to time, we looked at several possibilities; however, the best fit for this data results in a nearly perfect correlation to the saturation time.

Table 24 - Saturation times and beta values for all cases

Case	t_{sat}, min	$1/t_{sat}$, 1/min	β
I	33	0.03030	0.0303
II	32	0.03125	0.0312
III	48	0.02083	0.0208
IV	37	0.02703	0.027
V	48	0.02083	0.0208
VI	42	0.02381	0.0238
VII	43	0.02326	0.0233
VIII	32	0.03125	0.0313
IX	43	0.02326	0.0233
X	37	0.02703	0.027
XI	43	0.02326	0.0233
XII	32	0.03125	0.0313

Plotting β vs. the saturation time and the inverse saturation time results in the following graphs.

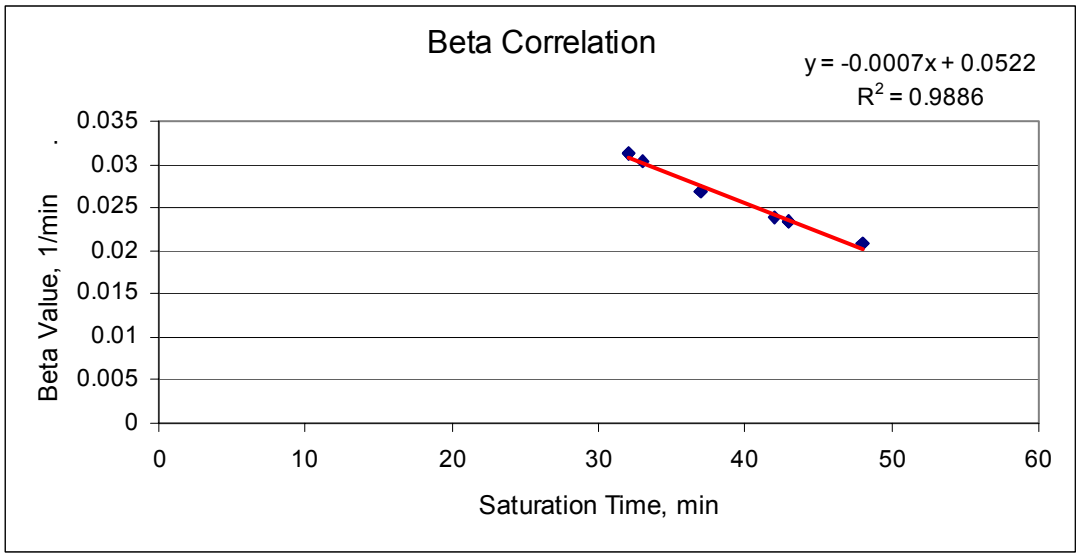

Figure 89 - Beta correlation to saturation time

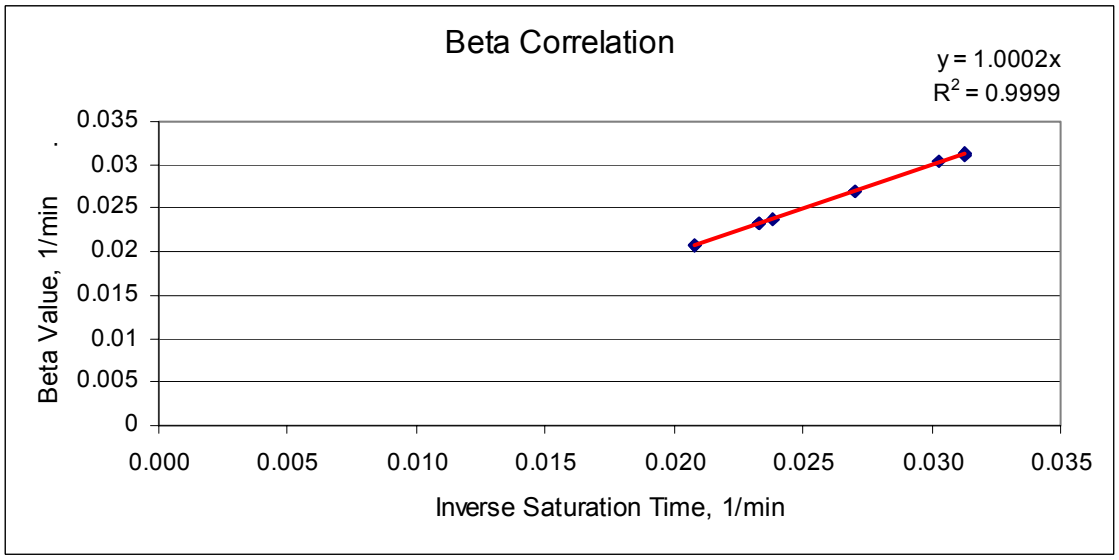

Figure 90 - Beta correlation to the inverse saturation time

For the experiments conducted, β ranged from 0.021 to 0.031. The first β correlation graph demonstrates that if the saturation time were infinitely small the β value would approach 0.0522.

Unfortunately, the saturation time used to predict β is an experimental number and can not be sampled like the feed concentration which is used to predict α. Therefore an estimation to predict the saturation time is necessary. Figure 91 is a graph of the actual saturation time versus the estimated saturation time t_{est}.

$$t_{sat} \quad vs. \quad t_{est}$$

where

$$t_{est} = 30\ \text{min} + \frac{(Q_{\max})\left(\frac{60\,\text{min}}{h}\right)}{J_w(C_f)(S.A.)}$$

where

$Q_{\max} = 150000\ ug/g$

$J_w = Water\ Flux$

$C_f = Arsenic\ Feed\ Concentration$

$S.A. = Specific\ Surface\ Area = 521\ m^2/g$

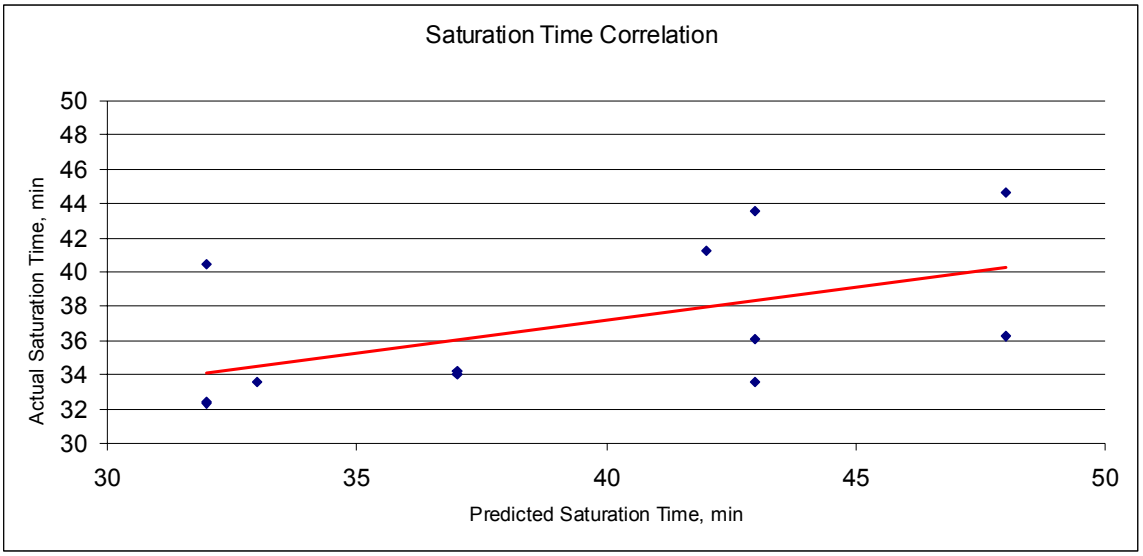

Figure 91 - Correlation of saturation time to operational parameters

Limitations of Irreversible Adsorption Model

While the model accurately predicts the initial arsenic permeate concentration and its change over time; there exist several limitations of its use due to operational conditions tested or assumptions contained within the model. These being:

1. Operational Limitations
    a. Arsenic feed concentration does not change over time
    b. Arsenic feed concentrations range from 30 to 150 µg/L of As(III)
    c. The feed water containing the arsenic has a conductivity of approximate 500 µS/cm, which is similar to the Florida groundwater used
    d. The chabazite has the same diameter and has been treated with ferrous sulfate as described in the methods section
    e. The modified zeolite is bulk fed into the reactor at a rate of 0.25 to 1.0 g/L of water to be treated over the cycle length
    f. The membrane used has a maximum pore size which is smaller than the diameter of the modified zeolite
    g. The membrane reactor is run in dead-end filtration at a flux rate between 34 and 51 liters per square meter per hour.

2. Model Assumptions
    a. The reaction is irreversible
    b. The concentration inside the zeolite is greater than that in the bulk fluid
    c. The zeolite behaves similarly to a microsphere when forming the cake so that its porosity is expected to be approximately 60%
    d. The cake layer is homogeneous

Practical Application of Irreversible Adsorption Model

A design engineer may successfully implement this model if the following is known:

1. The feed arsenic concentration
2. The design permeate flux of the system
3. A pilot test run to confirm saturation time

An example calculation follows:

Conditions:

1. The feed arsenic concentration, C_f, is 100 µg/L of As(III)
2. The design permeate water flux of the system, J_w, is 40 L/(m2.h)

The first step involves estimating the saturation time, t_{sat}, which is as follows:

$$t_{est} = 30\ \text{min} + \frac{(Q_{\max})\left(\frac{60\,\text{min}}{h}\right)}{J_w(C_f)(S.A.)}$$

$$t_{est} = 30\ \text{min} + \frac{\left(\frac{150000ug}{g}\right)\left(\frac{60\,\text{min}}{h}\right)}{\left(\frac{40L}{m^2 * h}\right)\left(\frac{100\mu g}{L}\right)\left(\frac{521m^2}{g}\right)} = 34.3\,\text{min}$$

Taking the inverse of the saturation time provides β, the rate of increase on permeate concentration.

$$\beta = \frac{1}{t_{sat}} = \frac{1}{34.3} = 0.0291 \text{ min}^{-1}$$

The next step is estimating the initial permeate concentration, α, which is as follows:

$$\alpha = 0.3613 * C_f = 0.3613 * 100 \mu g / L = 36.13 \mu g / L$$

Based on the values of α and β and the model prediction of:

$$C_p = \alpha e^{\beta t}$$

or

$$C_p = (36.13 \mu g / L) e^{(0.0291 \text{ min}^{-1}) * t}$$

The resulting breakthrough curve over time is estimated by the following figure:

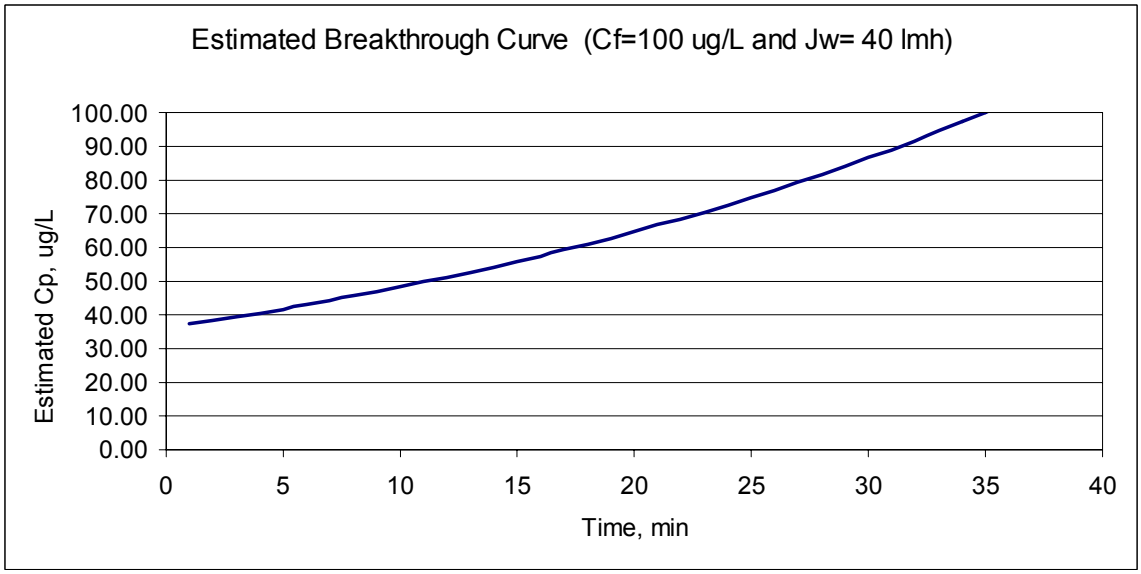

Figure 92 - Estimated breakthrough curve for example model calculation

Once the design engineer has developed the estimate breakthrough curve, a pilot system should be run within the design limitations provided previously. By sampling throughout

the initial filtration cycle a true saturation time can be found. This saturation time can then be used to refine the predicted breakthrough curve.

CONCLUSIONS AND FUTURE WORK

The development of a mathematical model to describe the adsorption of arsenic by a modified zeolite on a membrane substrate led to several significant results which culminated in the final successful outcome of the research. This model needed to determine either the rate of change of adsorption onto the zeolite or the change in permeate concentration of arsenic.

Initially, a natural zeolite was obtained and modified through the use of copper chloride, ferrous chloride, and ferrous sulfate. Kinetic and equilibrium studies of arsenic adsorption on this modified zeolite led to the creation of adsorption isotherms which characterized this process not only in de-ionized water, but also in dechlorinated tap, and a natural groundwater. It was concluded from this work that the ferrous sulfate modified zeolite demonstrated the greatest affinity for arsenic adsorption. Future research related to the modification process such as ferrous sulfate concentration and contact time may lead to an increase in the maximum adsorption capacity.

Conclusions may also be drawn from these studies regarding the water in which the arsenic exists. Waters with conductivities of 500 μS/cm and greater were much more efficient at arsenic removal. This is most likely attributed to the ionic mobility of the arsenic in such waters. While experiments where chlorides were increased into the water demonstrated little change in arsenic adsorption, experiments of sulfates showed a significant initial change in arsenic adsorption when levels were increased above 100 mg/L. This precarious change led to a further experiment where it is concluded that the sulfate lowers the peak height of the GFAA in a linear correlation to the sulfate dosed. It can be concluded therefore that sulfates have an interference with this method.

The adsorption of arsenic by the zeolite/membrane reactor was preceded by characterization of the membranes operational and rejection qualities. The membrane was found to have no inherent rejection of arsenic without the addition of the zeolite

adsorbent. This is attributed to the large pore size of the membrane compared to the effective size of the arsenic molecule. Flux decline tests were used to determine the permeability of the membrane which was found to be 10 gfd/psi. This baseline figure aided in the determination of the amount of cake which was permissible in the reactor without adding significant headloss to the system. This value was found to be approximately 25 g and coupled with the flux of the system allowed for the reactor to be operated within the equilibrium adsorption isotherm tested levels. These values are assumed to be conditional on the Hydranautics membrane used and the flux rate tested. Further work implementing various membranes and the use of a cross flow rate could increase these values to allow for greater contact time thereby enhancing adsorption and decreasing the arsenic permeate concentration.

Twelve different cases were run which encompassed three different arsenic feed concentrations, two flux rates, and two zeolite masses. All 12 cases exhibited were successful at removing the arsenic, but at various efficiencies and for various amounts of time. The resulting behaviors were analyzed and both Langmuir and Freundlich models were applied to determine if it was capable of predicting the process profile. While both models had some ability to fit the data, it was not possible to correlate the curve fitting parameters to the operational conditions. It can therefore be concluded that while the arsenic adsorption for a given operational condition may follow a traditional isotherm curve, changing the operational conditions erratically changes the fitting parameters. Use of Origin, a curve fitting data program, fit the data extremely well, but the curve fitting parameters used had no significant scientific meaning and could not be found based on the operational conditions. While these three models deal with the mass in the system as well as the feed concentration, they do not include the boundary conditions of the governing system. Consequently, the model does not include all of the operating conditions which are necessary for predicting the permeate concentration profile under varying conditions.

Further research into the model of the 12 cases led to the discovery of a theoretical exponential model based on the Irreversible Adsorption Model as described by Cussler (1997). This model implemented the operational and boundary conditions governing the

system and fit all cases extremely well. The coefficients, α and β, of all 12 cases were analyzed for their correlation to the operational conditions and it was found that α was approximately 36% of the initial arsenic feed concentration and β was equal to the inverse of the cake saturation time. While the arsenic feed concentration is easily measured the cake saturation time is an empirical number. A prediction of β, which did not range outside of 0.021 to 0.031, can be found by using the following equation:

$$t_{est} = 30\ \text{min} + \frac{(Q_{\max})\left(\frac{60\,\text{min}}{h}\right)}{J_w(C_f)(S.A.)}$$

While the correlation is not perfect it does provide a general trend to the time to reach saturation. Although this value is necessary for prediction of system operation, it should be noted that the system itself would regenerate after every backwash. This knowledge coupled with a single cycle of sampling would lead to the saturation time for the operational conditions. This time could therefore be used to predict the effective cycle time versus permeate arsenic concentration for all future cycles. Through the use of this model, a utility could develop a sequential backwashing schedule of multiple filters to meet the combined filtrate arsenic MCL of 10 µg/L.

Using the current design, a plant which operated at a flux rate of 25 L/(m2.h) and had an influent arsenic concentration of 20 µg/L could meet the new MCL prior to needing backwashing. While these are possible operating conditions, optimization of the system could expand the possible applications of this model. Future research, such as a more comprehensive understanding of the saturation time and optimization of the system operational parameters, could lead to a significant increase in the adsorption potential of the zeolite/membrane reactor. This optimization, as well as a cost analysis of the process, could lead to a legitimate alternative to costly arsenic removal processes which are currently being implemented throughout the world.

REFERENCES

Aiello R., Colella C., Nastro A. (1979) Natural Chabazite for Iron and Manganese Removal from Water. *The Properties and Applications of Zeolites*. R.P Townsend (ed.), London, 259-268.

Armbruster T. (2001) Clinoptilolite-heulandite: application and basic research. *Zeolites and Mesoporous Materials at the Dawn of the 21st Century*. Galarnau, A., et al. (ed.) 13-27.

Banerjee K., et al. "Optimization of Process Parameters for Arsenic Treatment with Granular Ferric Hydroxide." http://www.idswater.com/Common/Paper/Paper_114/Water%20Template.htm.

Bonnin D. (1997) Arsenic Removal from water utilizing Natural zeolites, Proceedings. AWWA Annual Conference. 421.

Borgono J.M., Greiber R. (1972) Epidemiological study of arsenism in the city of Antofagasta. *Trace Substances in Environmental Health*. 5, 13-24.

Breck D. W. (1979) Potential Uses of Natural and Synthetic Zeolites in Industry. *The Properties and Applications of Zeolites*. R.P Townsend (ed.), London, 391-400.

Buswell, A.M. (1943) "War problems in analysis and treatment." *AWWA Journal*. 35(10), 1303.

Csanady M. and Straub I. (1998) "Health damage due to water pollution in Hungary." Dhaka Arsenic Conference.

Chon H., Woo S.I., Park S.E. (1996) *Recent Advances and New Horizons in Zeolite Science and Technology*. Elsevier, New York. 267-273.

Clifford D., Ghurye G., and Tripp A. (1998) Arsenic Ion Exchange Process with Reuse of Spent Brine. 1998 Annual AWWA Conference. Denver, Colorado.

Clifford, D. and Lin C.C. (1995) "Ion Exchange, Activated Alumina, and Membrane Processes for Arsenic Removal from Groundwater," Proceedings of the 45th Annual Environmental Engineering Conference, University of Kansas.

Choi S. W., et al. (2000) "Modeling of the Permeate Flux during Microfiltration of BSA-Adsorbed Microspheres in a Stirred Cell." *Journal of Colloid and Interface Science*, 228.2, 270-278.

Croal L. R., Gralnick J.A., Malasarn D., and Newman D.K. (2004) "The Genetics of Geochemisty." *Annual Review of Genetics*. 38.1, 175-206.

Cussler E.L. (1997) *Diffusion Mass Transfer in Fluid Systems*. Cambridge University Press. 317-319.

Diamadopoulos E., Ioannidis S., and Sakellaropoulos G.P. (1993) "As(V) removal from aqueous solutions by fly ash." *Water Research*. 27(12), 1773–1777.

Dictionary.com. http://dictionary.reference.com (accessed September 2006).

Driehaus W., Jekel M. R., and Hilderbrandt U. (1998) "Granular ferric hydroxide a new adsorbent for the removal of arsenic from natural water." *Journal of Water Supply Research and Technology-AQUA*, 47 (1), 30-35.

Dutta A., Chaudhuri M. (1991) "Removal of Arsenic from groundwater by lime softening with powdered coal additive." *Journal of Water Supply Research and Technology-AQUA*, 40 (1), 25-29.

Elizalde-Gonza'lez M.P. and Mattusch J. (2001) "Sorption on Natural Solids for Arsenic Removal." *Chemical Engineering Journal*. 81, 187-195.

Endres J., et al. (2000) "The Removal of Fe. Zn, Cu, and Pb from Wastewaters Using Chabazite Zeolites Produced from Southern Brazilian Coal Ashes." *Fundacao de Ciencia e Tecnologia*. Porto Alegre, Brazil.

Exter, M., et al. (1996) "Zeolite-Based Membranes Preparation, Performance and Prospects." *Recent Advances and New Horizons in Zeolite Science and Technology*. Chon, H. et al. (ed.), Elsevier, New York. 421-423.

Faibish R.S., Elimelech M., and Cohen Y. (1998) "Effect of Interparticle Electrostatic Double Layer Interactions on Permeate Flux Decline in Crossflow Membrane Filtration of Colloidal Suspensions: An Experimental Investigation." *Journal of Colloid and Interface Science*, 204.1, 77-86.

Ferguson J.F., and Gavis J. (1972) "A review of arsenic cycle in natural waters." *Journal of Water Research*, 6, 1259-1274.

Ficek, K.J. (1994) "Potassium Permanganate and Manganese Greensand for Removal of Metals," Water Quality Association Convention.

Gulledge J.H. and O'Conner J.T. (1973) "Removal of Arsenic (V) from Water by Adsorption on Aluminum and Ferric Hydroxides." *AWWA Journal*, 65(8), 548-552.

Guisnet M., Gilson J. (ed.) (2002) *Zeolites for Cleaner Technologies*. Imperial College Press, pp. 3, 15, 347.

Harris T.V., Zones S.I. (1994) "A study of Guest/Host Energetics for the Synthesis of Cage Structures NON and CHA." *Zeolites and Related Microporous Materials: State of the Art 1994*. Weitkamp, J. et al. (ed.) Elsevier, New York. 29-30.

Hering J.G., and Chiu V.Q. (1998) "The Chemistry of Arsenic: Treatment and Implications of Arsenic Speciation and Occurrence," AWWA Inorganic Contaminants Workshop, San Antonio, TX.

Hong S., Faibish R.S., and Elimelech M. (1997) "Kinetics of Permeate Flux Decline in Crossflow Membrane Filtration of Colloidal Suspensions." *Journal of Colloid and Interface Science*. 196.2, 267-77.

Huang C.P. and Fu P.L. (1984) "Treatment of Arsenic (V)-containing Water by the Activated Carbon Process." *Journal of Water Pollution Control Federation*. 56(3), 233.

Joshi A. and Chaudhuri M. (1996) "Removal of arsenic from ground water by iron oxide-coated sand." *Journal of Environmental Engineering*, 122(8), 769- 772.

Joshida I., Kobayshi H., and Veno, K. (1976) "Selective adsorption of arsenic ions on silica gel impregnated with ferric hydroxide." *Analytical Letters*, 9, 1125–1129.

Kim A. and Hoek E. (2002) "Cake Structure in Dead End Membrane Filtration: Monte Carlo Simulations." *Environmental Engineering Science*. 19(6), 373-386.

Kipling M.D. (1977) Arsenic. *The Chemical Environment*. Glasgow, Blackie, 93–120.

Kirkov G. N. and Petrova N., (1994) "Influence of crystalline seeds on the zeolitization of volcanic ashes: a calorimetric study." *Zeolites and Related Microporous Materials: State of the Art 1994*. Weitkamp, J. et al. (ed.) Elsevier, New York. 291-294.

Kumar A., et al. (2001) "Development of Iron Oxide Coated Sand" Department of Civil, Architectural and Environmental Engineering, Drexel University, 3141 Chestnut Street, Philadelphia, PA 19104, U.S.A.; ak385@drexel.edu.

Li Q., et al. (2003) "Three-Component Competitive Adsorption Model for Flow-through PAC Systems. 1. Model Development and Verification with a PAC/membrane System." *Environmental Science & Technology*. 37.13, 2997-3004.

Lackovic J.A., Nikolaidis N.P., and Dobbs G. (2000) "Inorganic arsenic removal by zero-valent iron." *Environmental Engineering Science*. 17(1), 29-39.

Lorenzen L., Vandeventer J., and Landi W. (1995) "Factors Affecting the Mechanism of the Adsorption of Arsenic Species on Activated Carbon." *Minerals Engineering*. 8(4-5), 557-569.

Lu FJ. (1990) "Blackfoot disease: arsenic or humic acid?" *Lancet*. 336(8707), 115-116.

Matsui Y., Yuasa A., and Ariga K. (2001) "Removal of a Synthetic Organic Chemical by PAC-UF Systems--I: Theory and Modeling." *Water Research*. 35.2, 455-63.

Mallevialle J., Odendaal P.E., and Weisner M., eds. (1996) *Water Treatment Membrane Processes*. New York: McGraw-Hill, 2.1 – 2.16.

McNeill L. and Edwards, M. (1994) "Arsenic Removal via softening." *Critical Issues in Water and Wastewater treatment: National Conference on Environmental Engineering*. pp 640-645.

Meharg A., (2005) "Venomous Earth - How Arsenic Caused The World's Worst Mass Poisoning." *Macmillan Science*.

Matsukata M., Nishiyama, N., Ueyama, K. (1994) "Preparation of a thin zeolitic membrane." *Zeolites and Related Microporous Materials: State of the Art 1994*. Weitkamp, J. et al. (ed.) Elsevier, New York. 1187.

Megamin Inc., *Zeolites*. (2003). http://www.megamin.hr/zeolit.htm.

National Research Council (NRC) (1999). "Arsenic in drinking water." National Academy Press, Washington, D.C.

NAS (1977) "Medical and biologic effects of environmental pollutant: Arsenic." Washington, DC, National Academy of Sciences.

Occelli M., Gould S., and Stucky, G. (1994) "The Study of the Surface Topography of Microporous Materials Using Atomic Force Microscopy." *Zeolites and Related Microporous Materials: State of the Art 1994*. Weitkamp, J. et al. (ed.) Elsevier, New York. 488.

Ouki S.K., and Kavannagh, M. (1999) "Treatment of Metals-Contaminated Wastewaters by Use of Natural Zeolites." *Water Science and Technology*. 39(10-11), 115-122.

Penrose W.R. (1974). CRC Critical Review of Environmental Control 4, 465.

Pontius F.W., Brown K.G., and Chen C. (1994) "Health Implications of Arsenic in Drinking Water." *AWWA Journal*. 86(9), 52-63.

Rajakovic L.V. (1992) "Sorption of Arsenic onto Activated Carbon Impregnated with Metallic Silver and Copper," *Separation Science Technology,* 27(11), 1423-33.

Reddad Z., et al. "Cadmium and Lead Adsorption by a Natural Polysaccharide in MF Membrane Reactor: Experimental Analysis and Modelling." *Water Research*. 37(16) 3983-3991.

Sancha A.M. (1999) "Removal of arsenic from drinking water supplies." Proceedings, IWSA XXII World Congress and Exhibition, Buenos Aires, Argentina.

Seff K. (1996) "What can be in the channels and cavities of zeolites?" *Recent Advances and New Horizons in Zeolite Science and Technology*. Chon, H. et al. (ed.), Elsevier, New York. 267-273.

Shim S., Navrotsky A., Gaffney T., MacDougall J. (1999) "Chabazite: Energetics of hydration, enthalpy of formation, and effect of cations on stability." *American Mineralogist*. 84, 1870-1882.

Simms J. and Azizian F. (1997). "Pilot Plant Trials on the Removal of Arsenic from Potable Water Using Activated Alumina," Proceedings AWWA Water Quality Technology Conference.

Smith A.H., Hopenhayn-Rich C., Bates M.N., Goeden H.M, Hertz-Picciotto I., Duggan H.M., Wood R., Kosnett M.J., and Smith M.T. (1992) "Cancer risks from arsenic in drinking water." *Environmental Health Perspective*. 97, 259-267.

Sorg T. J. and Logsdon G. S. (1978) "Treatment Technology to Meet the Interim Primary Drinking Water Regulations for Inorganics: Part 2." *AWWA Journal*. 70(7), 379-393.

Subramanian K.S., Viraraghavan T., Phommavong T. and Tanjore S. (1997) "Manganese greensand for removal of arsenic in drinking water." *Water Quality Research Journal of Canada*. 32(3), 551-561.

USEPA (2000) "Technologies and Costs for Removal of Arsenic from Drinking Water." EPA 815-R-00-028, Prepared by Malcolm Pirnie, Inc.

USEPA (2000) "Proposed Arsenic in Drinking Water Rule Regulatory Impact Analysis." EPA 815-R-00-013, Developed by Abt Associate Inc.

USEPA (2000) "Technologies and Costs for Removal of Arsenic from Drinking Water." EPA 815-R-00-028, Prepared by Malcolm Pirnie, Inc.

Vagliasindi F.G.A., and Benjamin, M. (1998) "Arsenic Removal and its Speciation in Adsorption Reactors." American Water Works Association Annual Conference and Exposition, Dallas, Texas.

Vahter M. and Marafante E. (1998) "In vivo methylation and detoxification of arsenic." *Royal Society of Chemistry*. 66, 105-119.

Vakharkar, A. (2005) *Adsorption Studies For Arsenic Removal Using Modified Chabazite*. University of South Florida.

Virta R. (1996) *Zeolites*. http://minerals.usgs.gov/minerals/pubs/commodity/zeolites/.

Weber W.J., McGinley P.M., and Katz L.E. (1991) "Sorption phenomena in subsurface systems: Concepts, models, and effects on contaminant fate and transport." *Water Research*. 499-528.

Welch A.H., West John D.B., Helsel D.R., and Wanty R.B. (2000) "Arsenic in ground water of the United States-- occurrence and geochemistry" *Ground Water*. 38(4), 589-604.

Wikipedia. http://en.wikipedia.org/wiki/Main_Page (accessed September 2006).

APPENDICIES

Appendix A – Arsenic Standards and Analysis

Preparation of Arsenic Trioxide Standard Solution

1. Arsenic trioxide solution required for equilibrium studies was prepared using instruction given in the "Standard Methods for Water and Wastewater, 19th Edition, 1995".
2. Stock As(III) Solution: Dissolved 1.320 g of arsenic trioxide As_2O_3 in water containing 4gms of NaOH. It was then diluted to 1 L to get 1 g/L of As(III) solution.
3. Intermediate As(III) Solution: Diluted 10 ml of stock As solution to 1000ml with water containing 5 ml of concentrated HCl to get 1 mg/L of As(III) solution.
4. Standard As(III) Solution: Dilute 10 ml of intermediate As(III) solution to 1000 ml of water containing the same concentration of acid used for sample preservation to get 100 µg/L of As(III) solution.

Arsenic Analysis

Arsenic analysis was conducted using the graphite furnace atomic absorption spectrometry method as described by ASTM 2972-93C. A description of this method is included below:

Graphite Furnace Atomic Absorption Spectrometry (GFAA)
(EPA 200.9, SM 3113 B, ASTM 2972-93 C, SW-846 7060A)

In the graphite furnace atomic absorption spectrometry technique, a small volume of sample (typically 5 to 50 µL) is injected into a graphite tube positioned in the optical path of an atomic absorption spectrophotometer. An electrical furnace is used to heat the tube sequentially through drying, charring, and finally, an atomization step. A light beam from a hollow cathode lamp or electrode less discharge lamp (EDL) containing the element of interest is directed through the tube, into a monochromator, and into a detector that measures the amount of light absorbed by the free ground state atoms. The amount of light absorbed by the free ground state atoms is directly proportional to the concentration of the analyte in solution within the linear calibration range of the instrument. Because

the greater percentage of analyte atoms are vaporized and dissociated within the light beam passing through the graphite tube, greater analytical sensitivity is obtained and lower detection limits are possible as compared with flame atomic absorption. The limit of detection can be extended by increasing the injection volume or by using a multi-injection technique. These techniques effectively increase the total amount of analyte placed in the tube resulting in greater absorbance. ASTM 2972-93 C utilizes standard graphite tubes and "off-the-wall-atomization." The major highlights of this method are described below:

1. Method Used: ASTM 2972-93 C
2. Lamp Used: UltrAA high intensity cathode lamp
3. Matrix Modifier: 150 mg/L as NiNO3
4. Wavelength: 193.7nm
5. Standards: 10, 20 and 50 ppb
6. Measurement mode: Peak Height

Appendix B – Determination of Order of Reaction

Integral method used for determining rate order of kinetic and equilibrium reactions, taken from the Master's Thesis of Ashutosh Vakharkar, University of South Florida, 2005.

Procedure: The integral method of analysis always puts a particular rate equation to the test by integrating and comparing the predicted concentration versus time curve with the experimental concentration versus time data. The integral method is especially useful for fitting simple reaction types corresponding to elementary reactions. To find a rate equation using the integral method lets consider the following example: Reactant A decomposes in a batch reactor.

$$A \rightarrow \text{Products}$$

The composition of A in the reactor is measured at various times. To find a rate equation that fits the data, start by guessing the simplest rate form, or first order kinetics. This means a plot of ln (Cao/Ca) versus time should give a straight line through the origin. If this plot fails to give us a straight line, it means that first order kinetics cannot reasonably represent the data and another rate form must be guessed. Proceed to guess the rate equation to be second order. This suggests that a plot of 1/Ca versus time should give a straight line. If this plot gives a straight line then the equation is of the second order with the intercept representing the initial concentration and slope representing the rate constant, k. If this plot fails to give a straight line then the second order kinetic form is rejected as well and fractional method should be used as calculations with higher order such as third order rate form are tedious and not recommended.

Appendix B - (Continued)

Rate Determination for Modified Chabazite with Different Salts In De-ionized Water

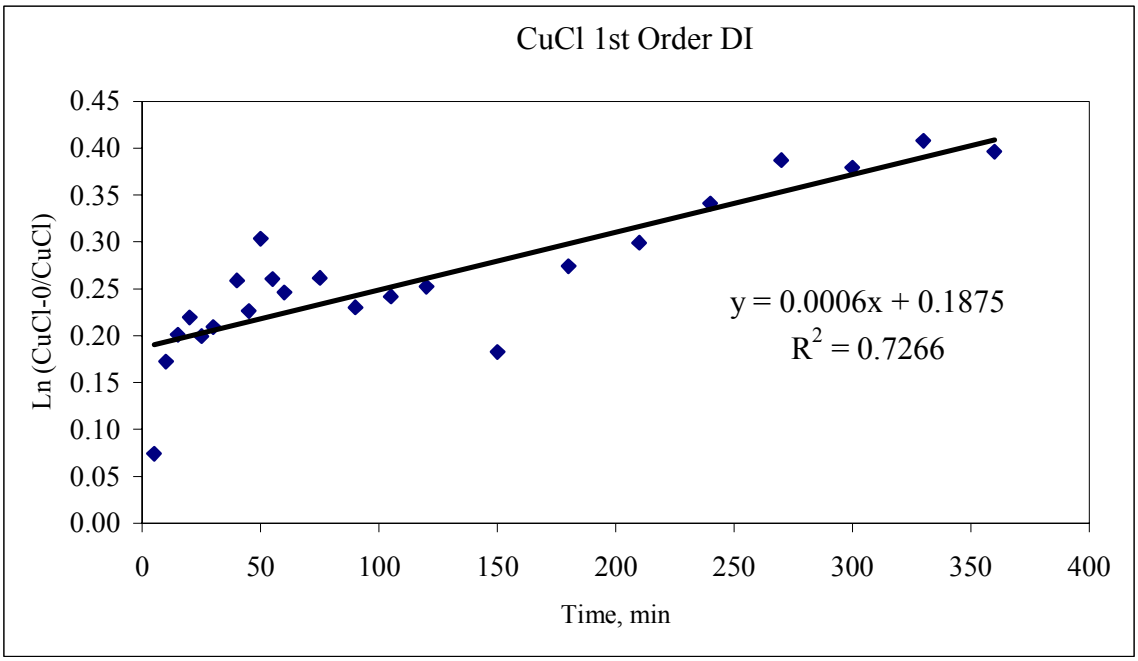

Figure 93 - Kinetic rate for copper (I) modified chabazite in de-ionized water, 1st order

Appendix B - (Continued)

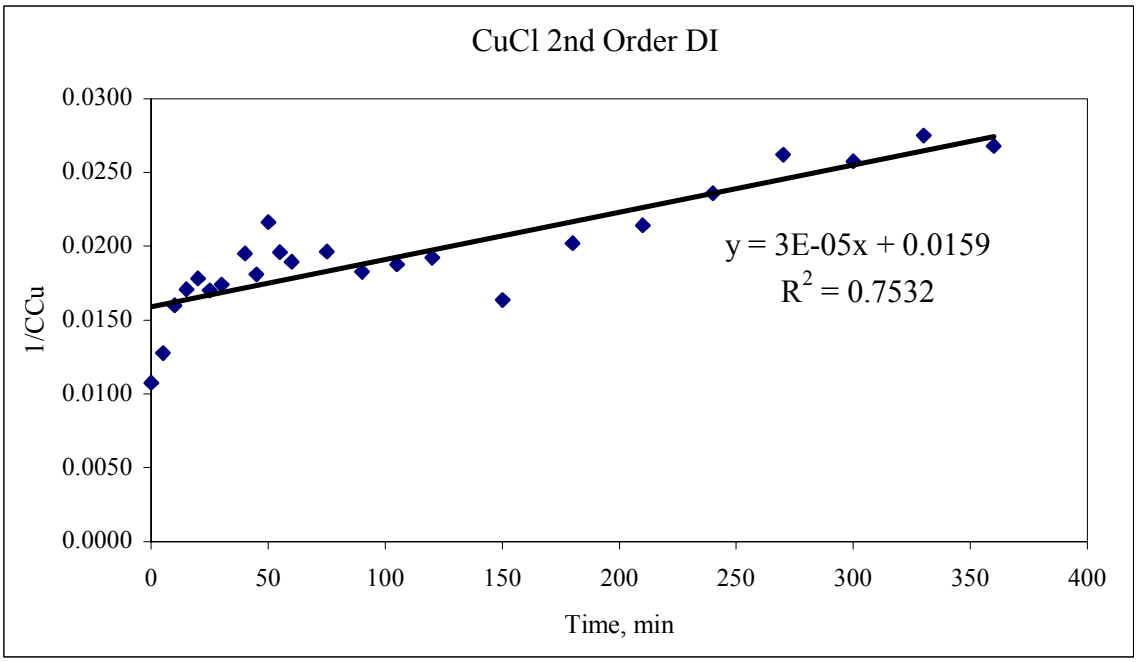

Figure 94 - Kinetic rate for copper (I) modified chabazite in de-ionized water, 2nd order

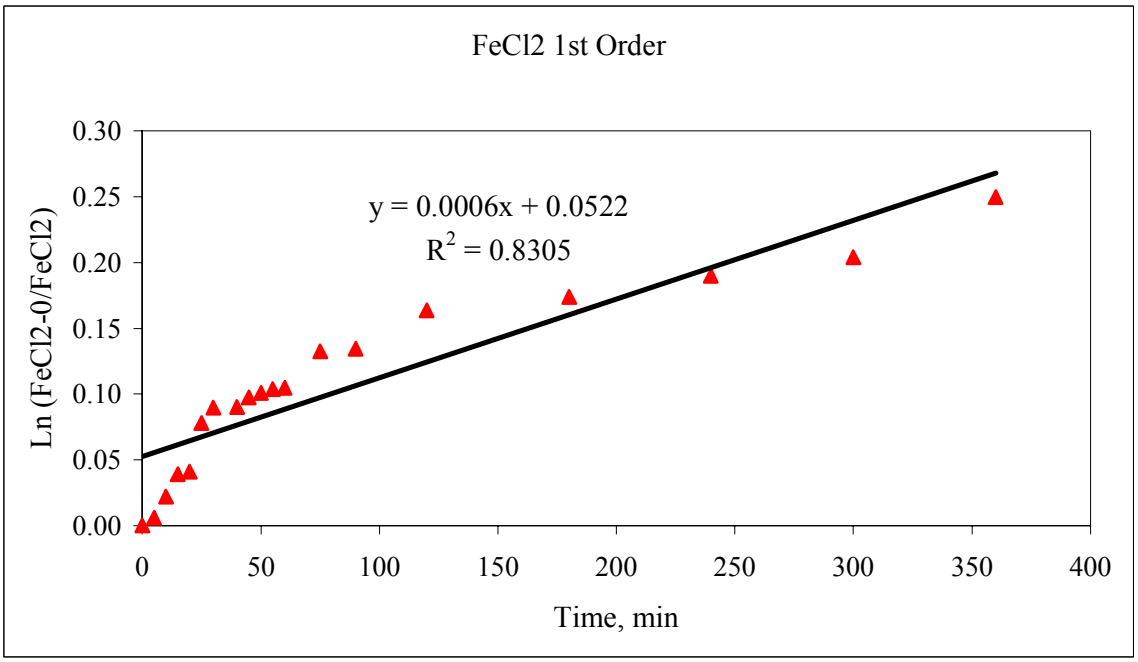

Figure 95 - Kinetic rate for ferrous chloride modified chabazite in de-ionized water, 1st order

Appendix B - (Continued)

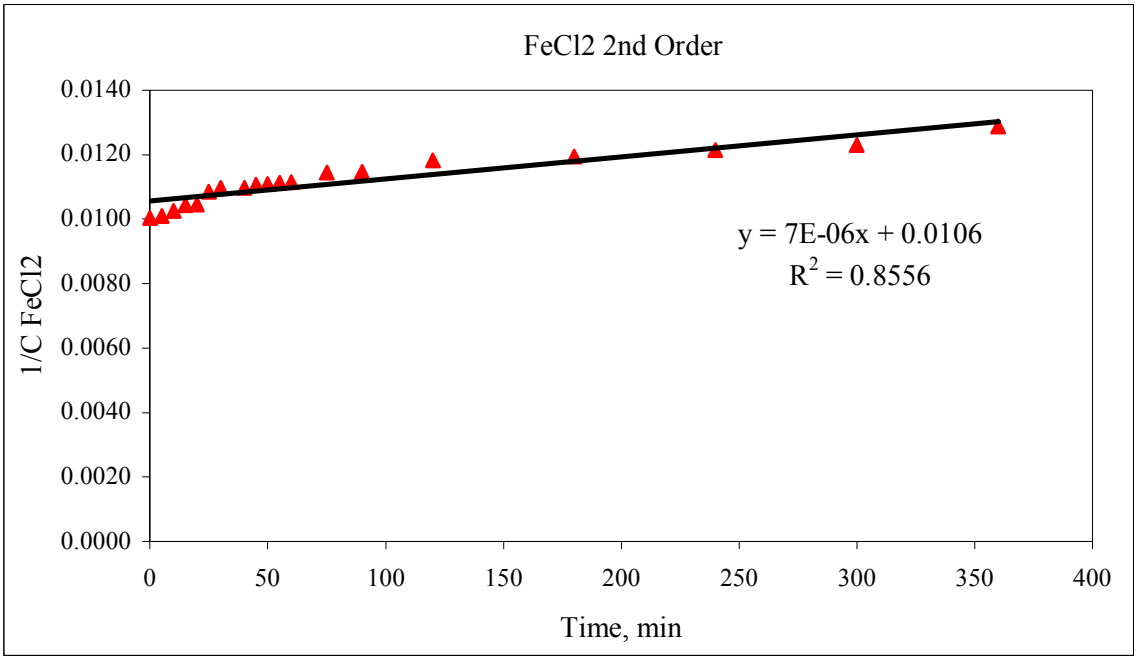

Figure 96 - Kinetic rate for ferrous chloride modified chabazite in de-ionized water, 2nd order

Appendix B - (Continued)

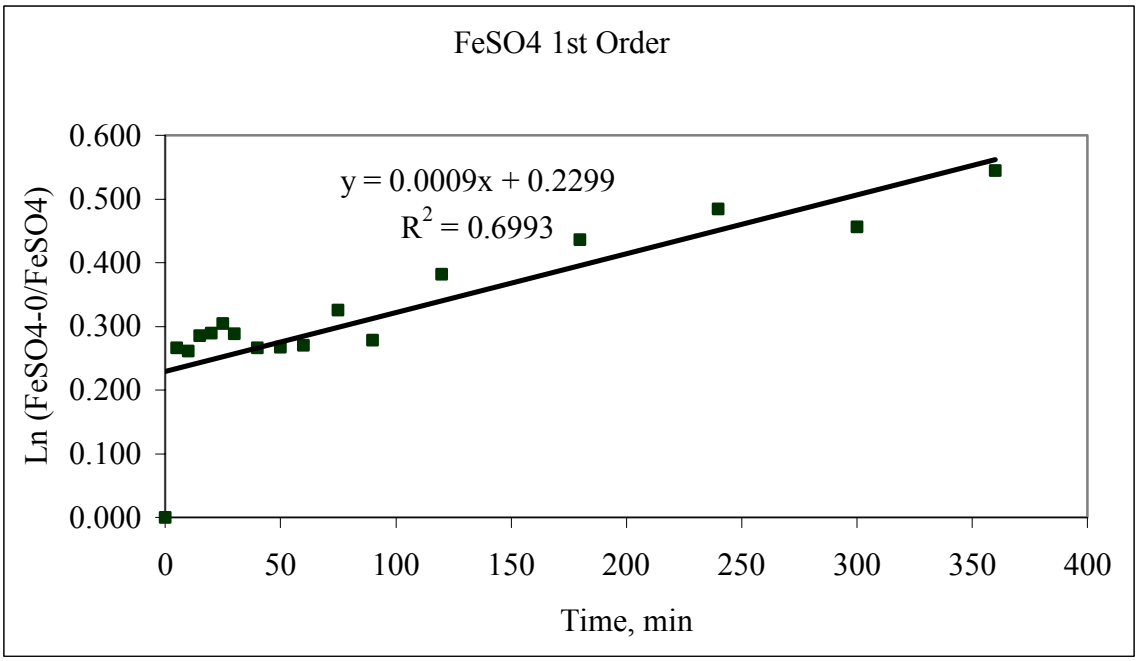

Figure 97 - Kinetic rate for ferrous sulfate modified chabazite in de-ionized water, 1st order

Appendix B - (Continued)

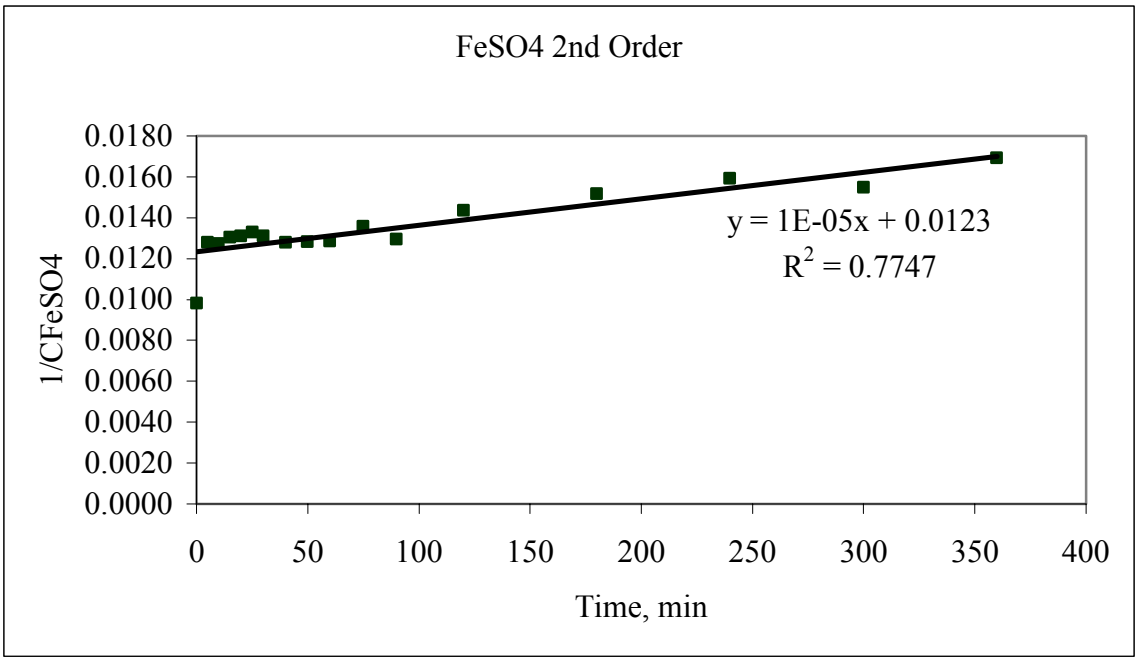

Figure 98 - Kinetic rate for ferrous sulfate modified chabazite in de-ionized water, 2nd order

Appendix B - (Continued)

Rate Determination with Chloride Salts of Different Metals In Tap Water

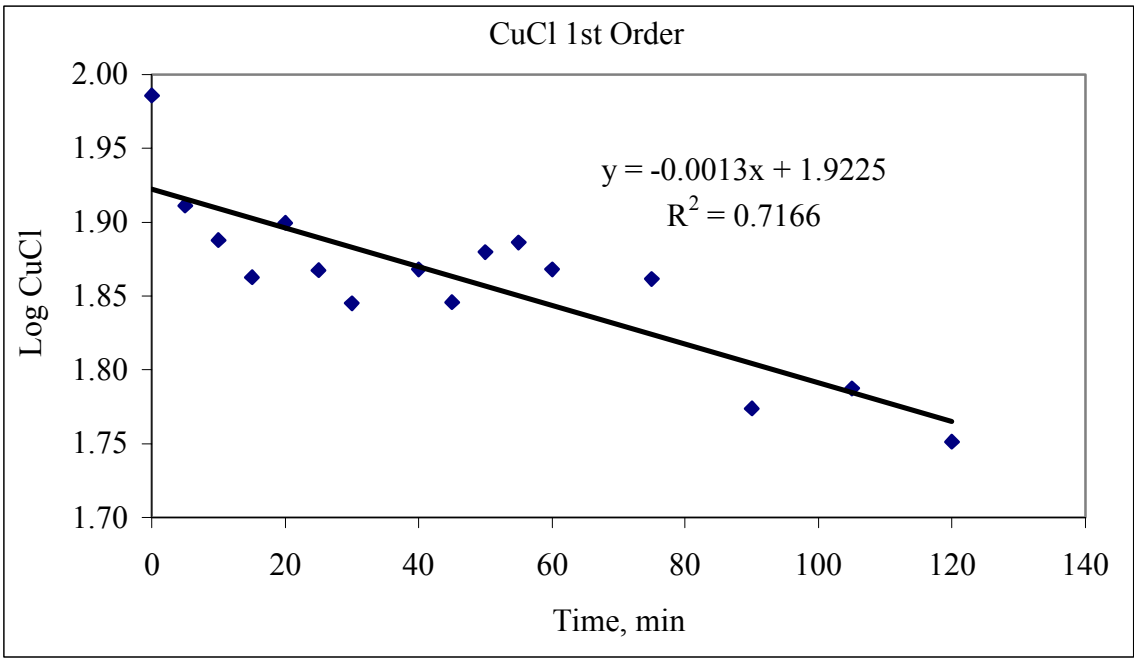

Figure 99 - Kinetic rate for copper (I) chloride modified chabazite in tap water, 1st order

Appendix B - (Continued)

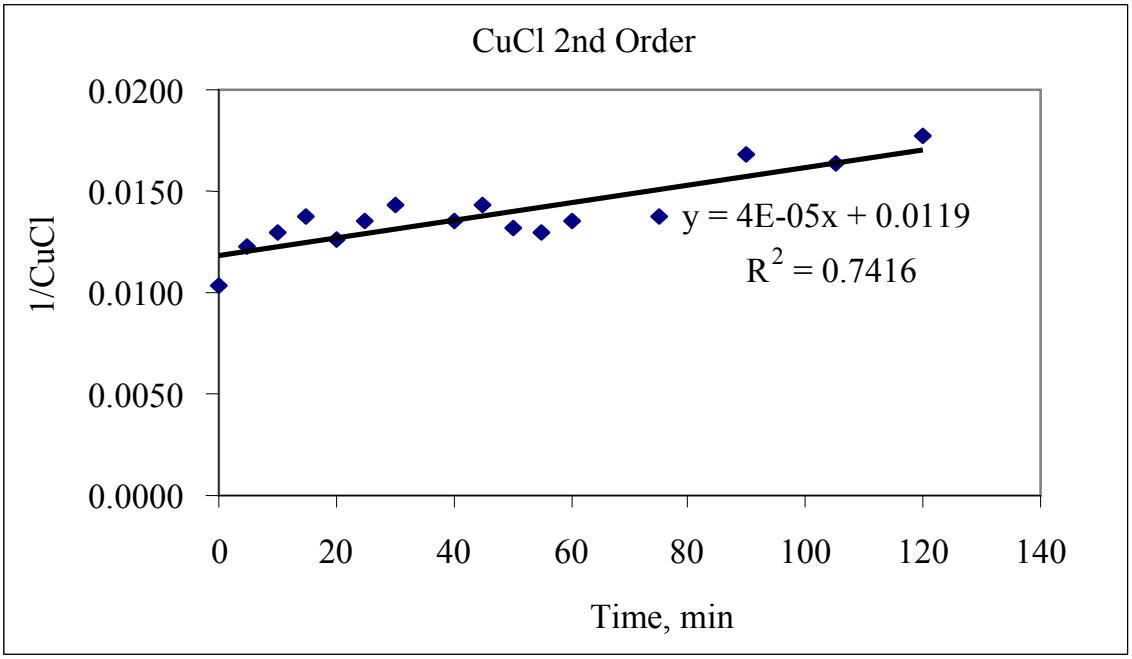

Figure 100 - Kinetic rate for copper (I) chloride modified chabazite in tap water, 2nd order

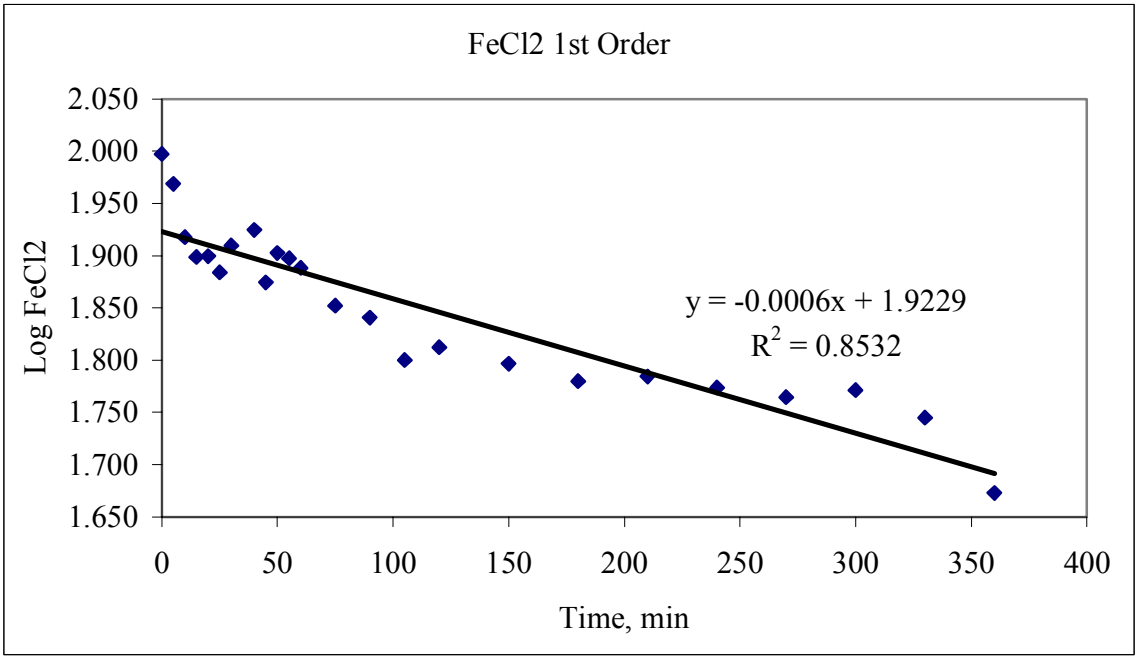

Figure 101 - Kinetic rate for ferrous chloride modified chabazite in tap water, 1st order

Appendix B - (Continued)

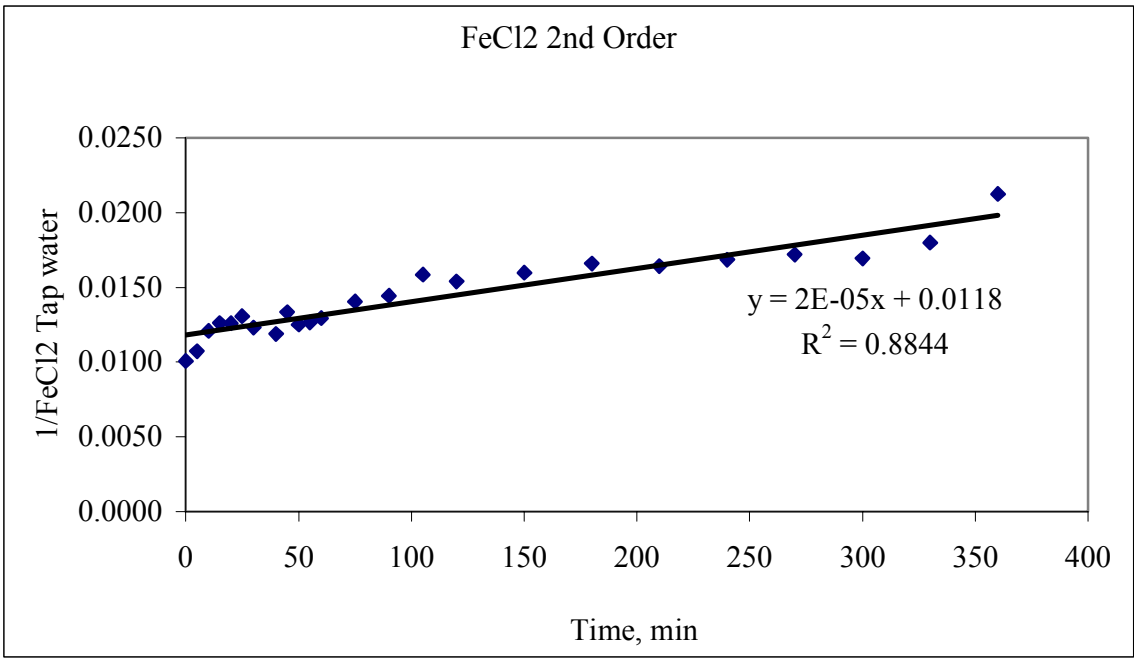

Figure 102 - Kinetic rate for ferrous chloride modified chabazite in tap water, 2nd order

Appendix B - (Continued)

Rate Determination with Different Salts of Same Metal in Tap Water

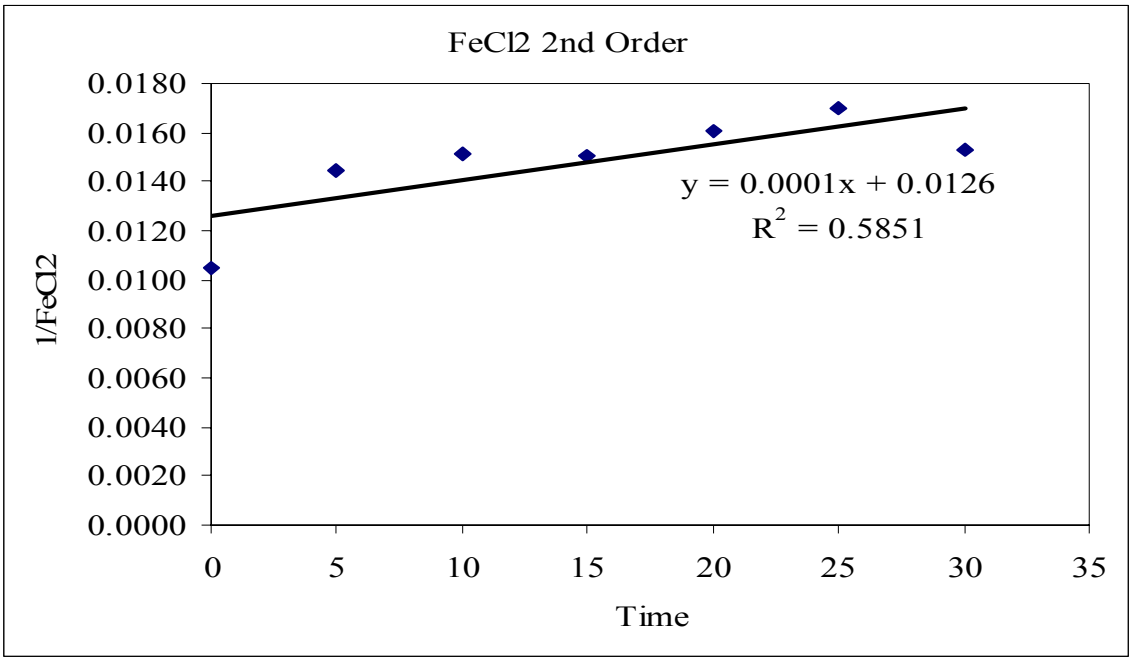

Figure 103 - Kinetic rate for ferrous chloride modified chabazite in dechlorinated tap water

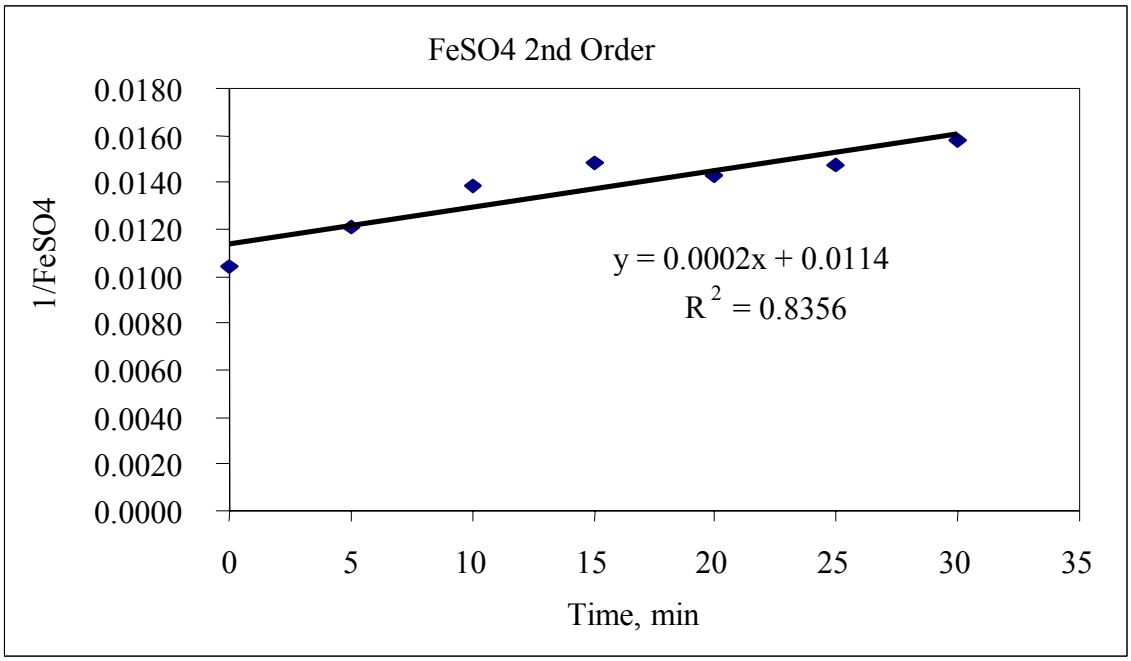

Figure 104 - Kinetic rate for ferrous sulfate modified chabazite in dechlorinated tap water

Appendix B - (Continued)

Rate Determination for Ferrous Modified Chabazite in Different Source Waters

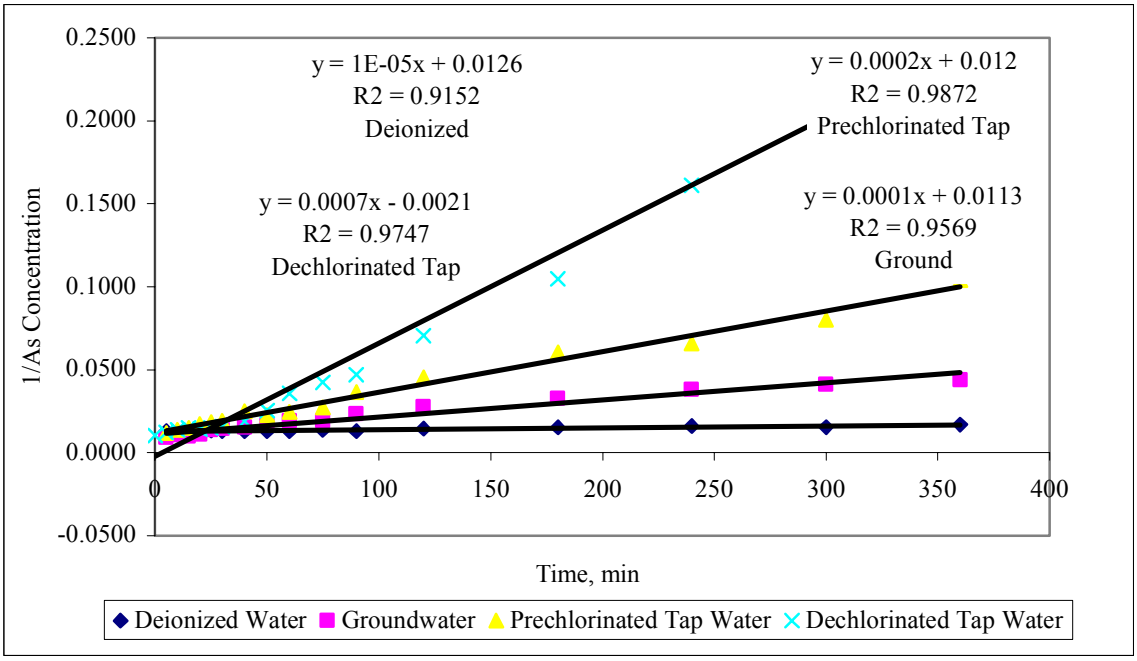

Figure 105 - Kinetic rate determination for ferrous sulfate modified chabazite in different source waters

Appendix C – Operational Conditions Versus Arsenic Breakthrough

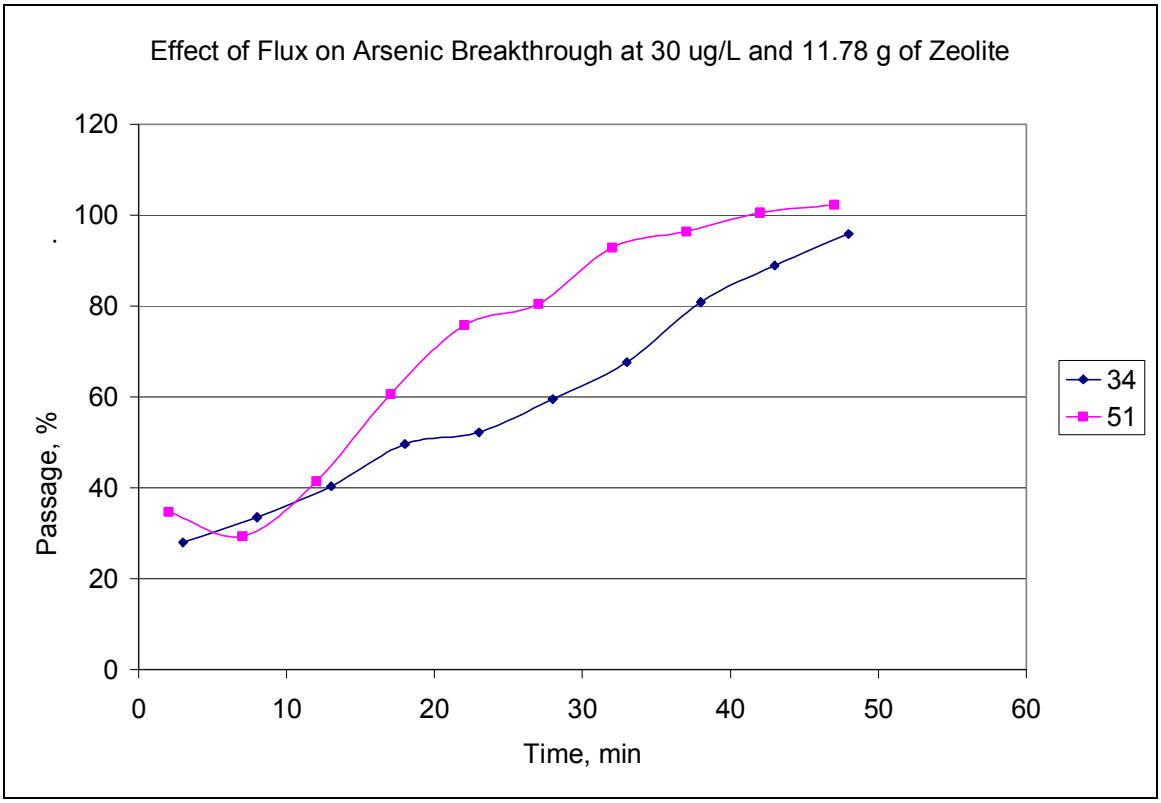

Figure 106 - Effect of flux on arsenic breakthrough at 30 µg/L and 11.78 g of zeolite

Appendix C - (Continued)

Figure 107 - Effect of flux on arsenic breakthrough at 80 µg/L and 11.78 g of zeolite

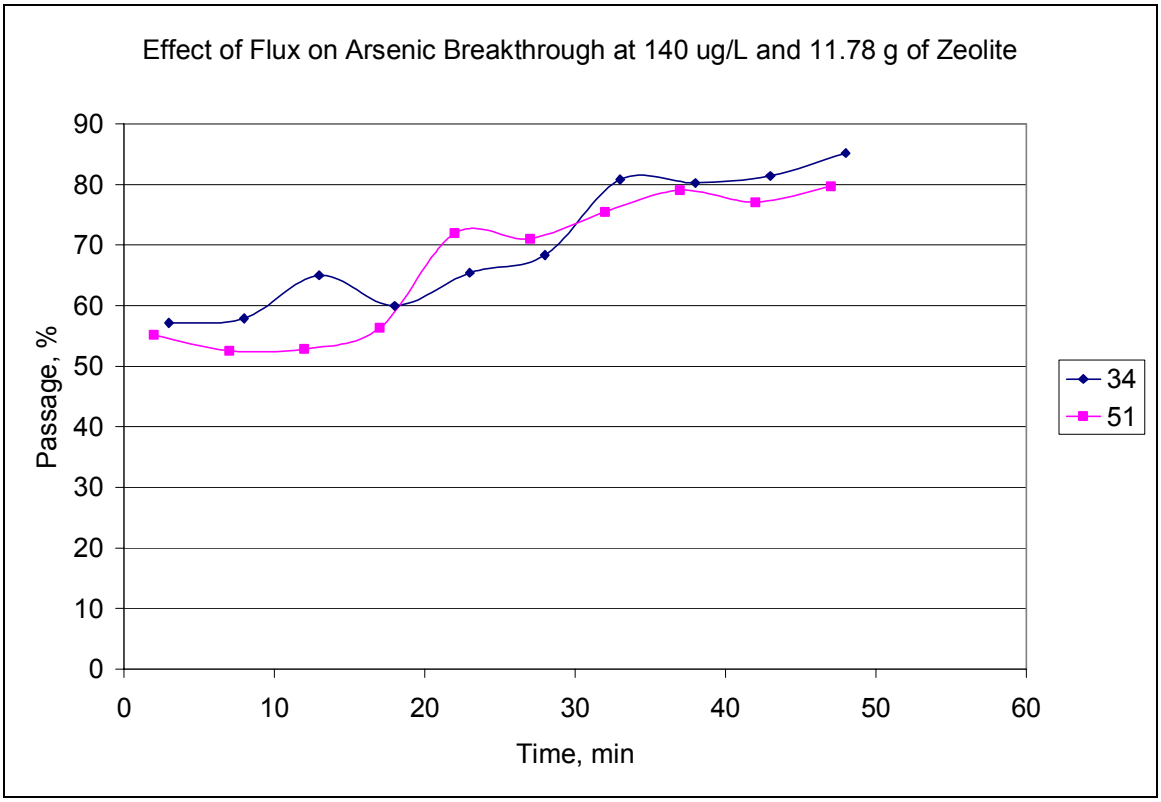

Figure 108 - Effect of flux on arsenic breakthrough at 140 µg/L and 11.78 g of zeolite

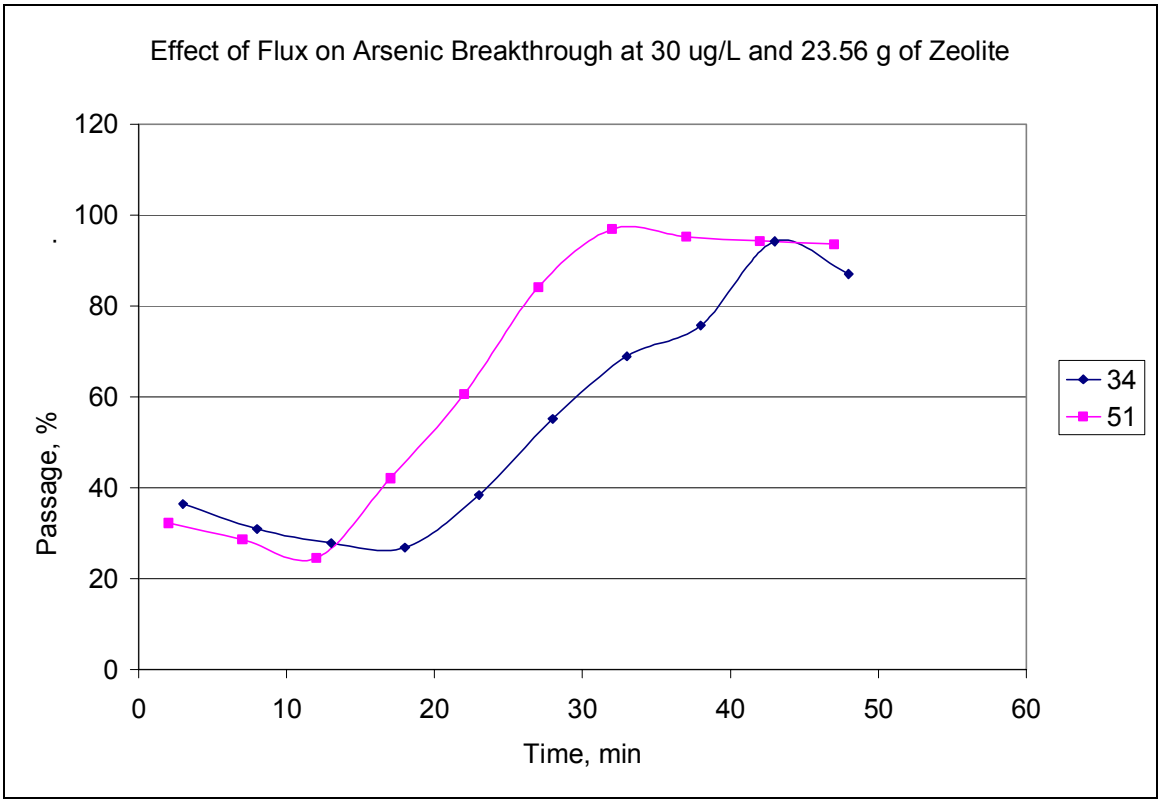

Figure 109 - Effect of flux on arsenic breakthrough at 30 µg/L and 23.56 g of zeolite

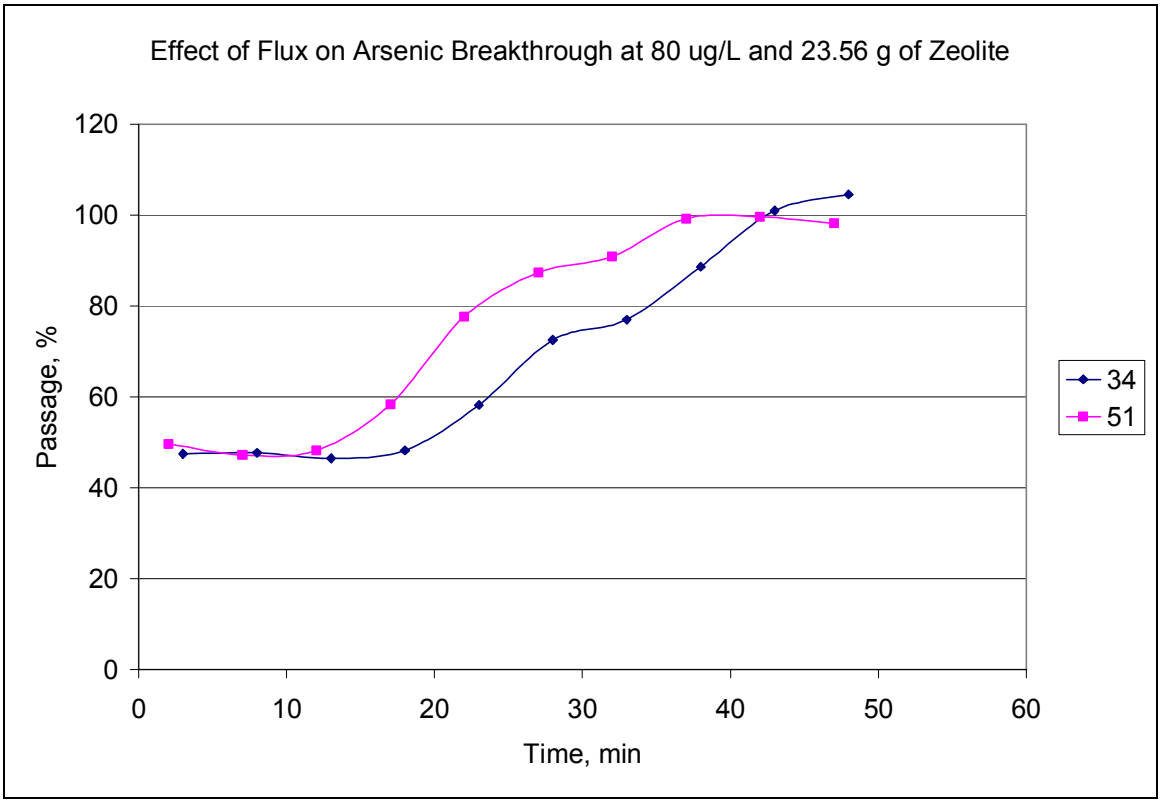

Figure 110 - Effect of flux on arsenic breakthrough at 80 µg/L and 23.56 g of zeolite

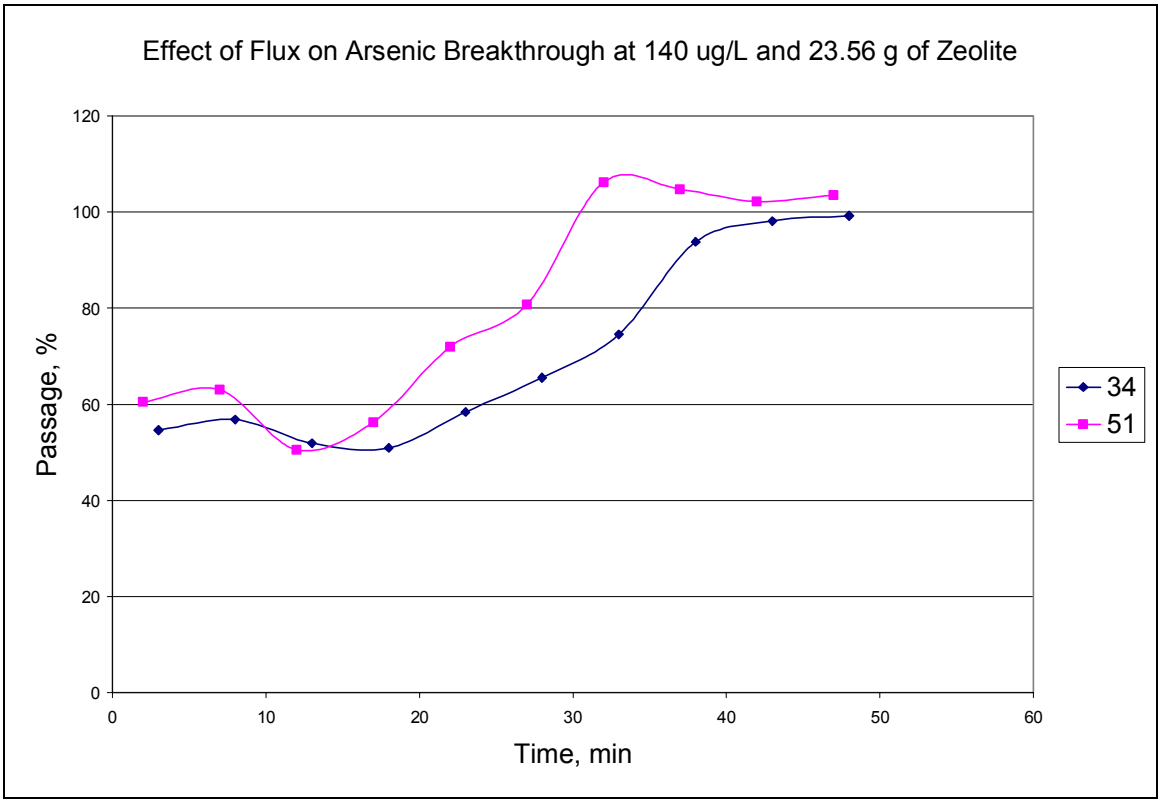

Figure 111 - Effect of flux on arsenic breakthrough at 140 µg/L and 23.56 g of zeolite

Appendix C - (Continued)

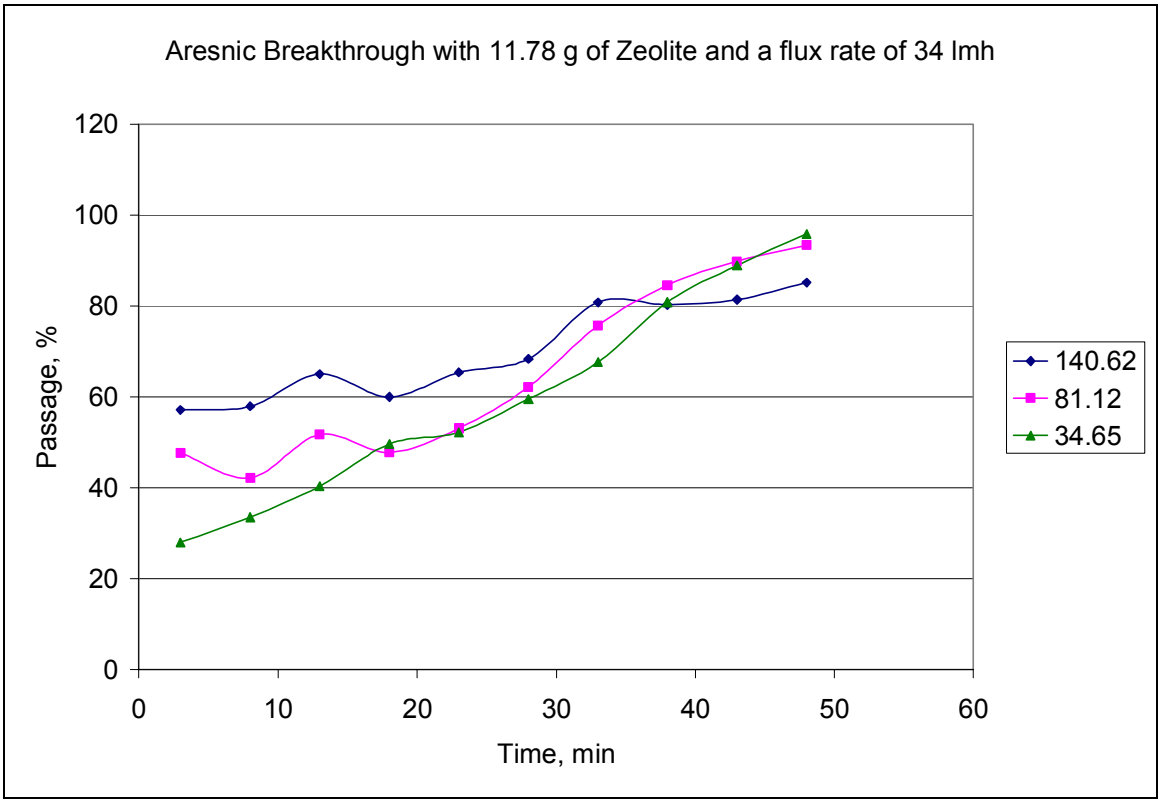

Figure 112 - Arsenic breakthrough with 11.78 g of zeolite and a flux rate of 34 L/(m2.h)

Appendix C - (Continued)

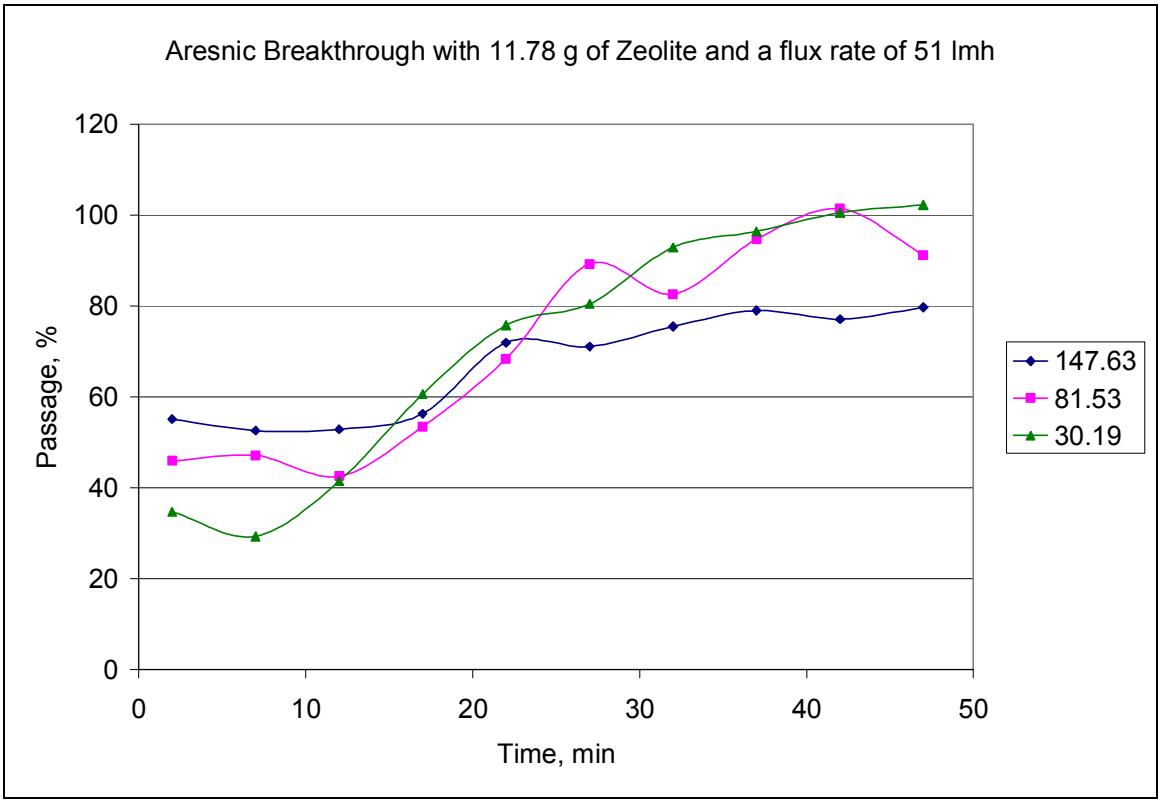

Figure 113 - Arsenic breakthrough with 11.78 g of zeolite and a flux rate of 51 L/(m2.h)

Appendix C - (Continued)

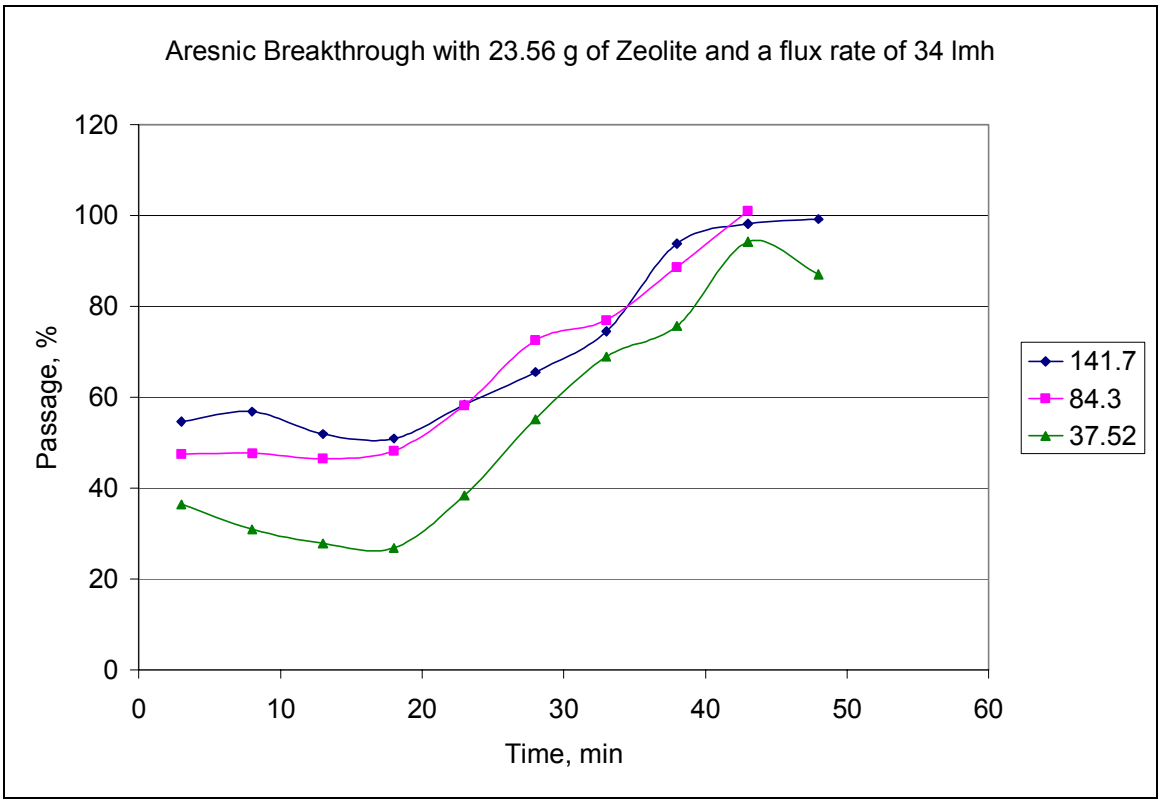

Figure 114 - Arsenic breakthrough with 23.56 g of zeolite and a flux rate of 34 L/(m2.h)

Appendix C - (Continued)

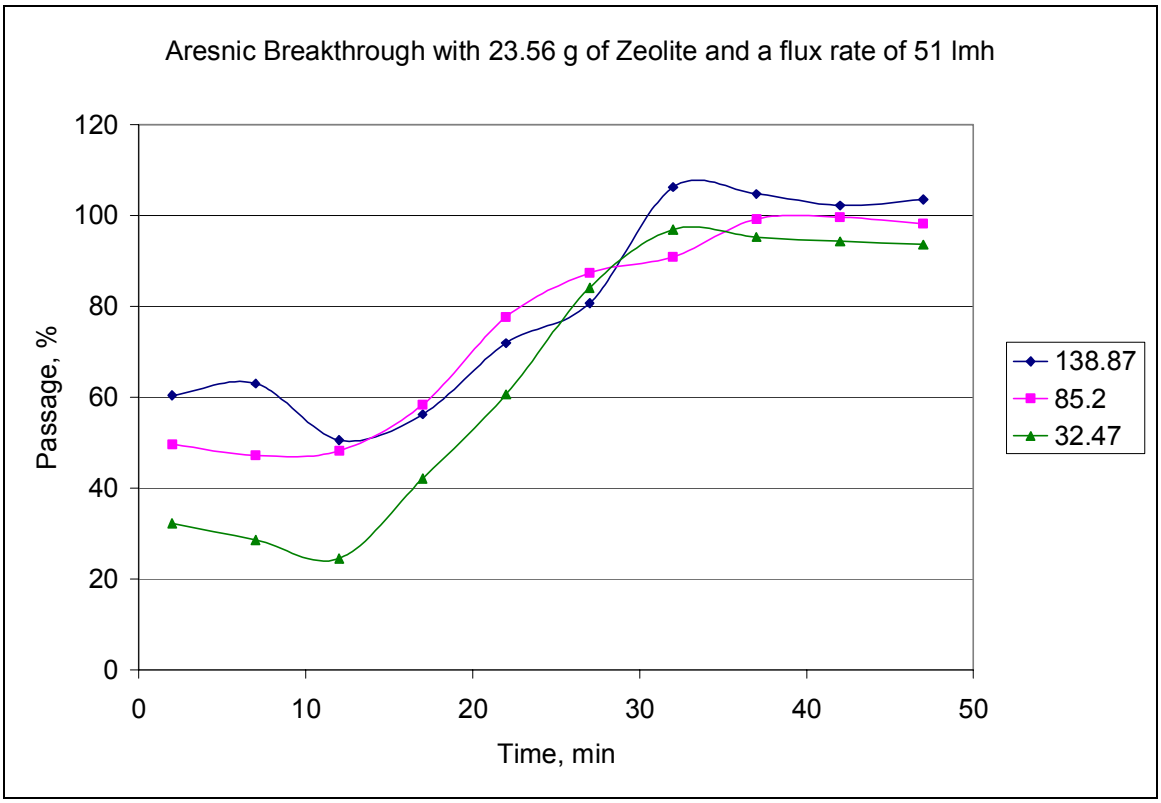

Figure 115 - Arsenic breakthrough with 23.56 g of zeolite and a flux rate of 51 L/(m2.h)

Appendix D – Analysis of Variance of Irreversible Adsorption Model

An Analysis of Variance, ANOVA, was conducted on all 12 Data sets with Data1_A referring to the actual permeate concentration and Data1_B referring to the modeled permeate concentration. Data Sets 2-12 are denoted similarly. A one way ANOVA with a 0.001 significance difference, showed no significant differences between the actual and modeled data.

One-Way ANOVA

Summary Statistics

Dataset	N	Mean	SD	SE
Data1_A	7	91.33	11.46469	4.33324
Data1_B	7	91.70371	29.70622	11.2279

Null Hypothesis: The means of all selected datasets are equal
Alternative Hypothesis: The means of one or more selected datasets are different

ANOVA

Source	DoF	Sum of Squares	Mean Square	F Value	P Value
Model	1	0.488801454	0.488801454	0.00096	0.97574
Error	12	6083.39174	506.949312		

At the 0.001 level,
the population means are not significantly different.

Levene's Test for Equal Variance

Source	DoF	Sum of Squares	Mean Square	F Value	P Value
Model	1	1450367.43	1450367.43	4.79245	0.04908
Error	12	3631631.11	302635.926		

At the 0.001 level,
the population variations are not significantly different.

Appendix D - (Continued)

Brown-Forsythe's Test for Equal Variance

Source	DoF	Sum of Squares	Mean Square	F Value	P Value
Model	1	823.915819	823.915819	5.03918	0.04441
Error	12	1962.02378	163.501981		

At the 0.001 level,
the population variations are not significantly different.

Means Comparison using Bonferroni Test

Dataset	Mean	Difference between Means	Simultaneous Confidence Intervals		Significant at 0.001 Level
Data1_A	91.33		Lower Limit	Upper Limit	
Data1_B	91.70371	-0.37371	-52.33847	51.59105	No

Means Comparison using Scheffe' Test

Dataset	Mean	Difference between Means	Simultaneous Confidence Intervals		Significant at 0.001 Level
Data1_A	91.33		Lower Limit	Upper Limit	
Data1_B	91.70371	-0.37371	-52.33846	51.59104	No

Means Comparison using Tukey Test

Dataset	Mean	Difference between Means	Simultaneous Confidence Intervals		Significant at 0.001 Level
Data1_A	91.33		Lower Limit	Upper Limit	
Data1_B	91.70371	-0.37371	-52.34055	51.59314	No

One-Way ANOVA

Summary Statistics

Dataset	N	Mean	SD	SE
Data2_A	7	91.82429	14.93564	5.64514
Data2_B	7	95.08445	31.74337	11.99787

Null Hypothesis: The means of all selected datasets are equal
Alternative Hypothesis: The means of one or more selected datasets are different

Appendix D - (Continued)

ANOVA

Source	DoF	Sum of Squares	Mean Square	F Value	P Value
Model	1	37.2003374	37.2003374	0.06045	0.80994
Error	12	7384.28909	615.357424		

At the 0.001 level,
the population means are not significantly different.

Levene's Test for Equal Variance

Source	DoF	Sum of Squares	Mean Square	F Value	P Value
Model	1	1582836.85	1582836.85	4.14175	0.06454
Error	12	4585995.50	382166.292		

At the 0.001 level,
the population variations are not significantly different.

Brown-Forsythe's Test for Equal Variance

Source	DoF	Sum of Squares	Mean Square	F Value	P Value
Model	1	560.283966	560.283966	2.50768	0.13928
Error	12	2681.13077	223.427564		

At the 0.001 level,
the population variations are not significantly different.

Means Comparison using Bonferroni Test

Dataset	Mean	Difference between Means	Simultaneous Confidence Intervals		Significant at 0.001 Level
Data2_A	91.82429		Lower Limit	Upper Limit	
Data2_B	95.08445	-3.26016	-60.51213	53.9918	No

Appendix D - (Continued)

Means Comparison using Scheffe' Test

Dataset	Mean	Difference between	Simultaneous Confidence Intervals		Significant at 0.001
Data2_A	91.82429	Means	Lower Limit	Upper Limit	Level
Data2_B	95.08445	-3.26016	-60.51212	53.99179	No

Means Comparison using Tukey Test

Dataset	Mean	Difference between	Simultaneous Confidence Intervals		Significant at 0.001
Data2_A	91.82429	Means	Lower Limit	Upper Limit	Level
Data2_B	95.08445	-3.26016	-60.51442	53.99409	No

One-Way ANOVA

Summary Statistics

Dataset	N	Mean	SD	SE
Data3_A	10	52.565	15.68677	4.96059
Data3_B	10	52.08903	16.27358	5.14616

Null Hypothesis: The means of all selected datasets are equal
Alternative Hypothesis: The means of one or more selected datasets are different

ANOVA

Source	DoF	Sum of Squares	Mean Square	F Value	P Value
Model	1	1.13272015	1.13272015	0.00443	0.94764
Error	18	4598.13749	255.452083		

At the 0.001 level,
the population means are not significantly different.

Levene's Test for Equal Variance

Source	DoF	Sum of Squares	Mean Square	F Value	P Value
Model	1	1424.58061	1424.58061	0.03375	0.85629
Error	18	759771.765	42209.5425		

Appendix D - (Continued)

At the 0.001 level,
the population variations are not significantly different.

Brown-Forsythe's Test for Equal Variance

Source	DoF	Sum of Squares	Mean Square	F Value	P Value
Model	1	0.00186373386	0.00186373386	0.00002	0.99624
Error	18	1471.31501	81.7397227		

At the 0.001 level,
the population variations are not significantly different.

Means Comparison using Bonferroni Test

Dataset	Mean	Difference between Means	Simultaneous Confidence Intervals Lower Limit	Upper Limit	Significant at 0.001 Level
Data3_A	52.565				
Data3_B	52.08903	0.47597	-27.555	28.50693	No

Means Comparison using Scheffe' Test

Dataset	Mean	Difference between Means	Simultaneous Confidence Intervals Lower Limit	Upper Limit	Significant at 0.001 Level
Data3_A	52.565				
Data3_B	52.08903	0.47597	-27.55501	28.50694	No

Means Comparison using Tukey Test

Dataset	Mean	Difference between Means	Simultaneous Confidence Intervals Lower Limit	Upper Limit	Significant at 0.001 Level
Data3_A	52.565				
Data3_B	52.08903	0.47597	-27.55533	28.50726	No

One-Way ANOVA

Summary Statistics

Dataset	N	Mean	SD	SE
Data4_A	8	53.40125	17.18722	6.0766
Data4_B	8	52.31271	17.13565	6.05837

Appendix D - (Continued)

Null Hypothesis: The means of all selected datasets are equal
Alternative Hypothesis: The means of one or more selected datasets are different

ANOVA

Source	DoF	Sum of Squares	Mean Square	F Value	P Value
Model	1	4.73964148	4.73964148	0.01609	0.90086
Error	14	4123.21852	294.515608		

At the 0.001 level,
the population means are not significantly different.

Levene's Test for Equal Variance

Source	DoF	Sum of Squares	Mean Square	F Value	P Value
Model	1	9.59645533	9.59645533	0.00020	0.98898
Error	14	679485.957	48534.7112		

At the 0.001 level,
the population variations are not significantly different.

Brown-Forsythe's Test for Equal Variance

Source	DoF	Sum of Squares	Mean Square	F Value	P Value
Model	1	4.55535871	4.55535871	0.06493	0.80257
Error	14	982.194122	70.1567230		

At the 0.001 level,
the population variations are not significantly different.

Means Comparison using Bonferroni Test

Dataset	Mean	Difference between Means	Simultaneous Confidence Intervals Lower Limit	Upper Limit	Significant at 0.001 Level
Data4_A	53.40125				
Data4_B	52.31271	1.08854	-34.43955	36.61662	No

Appendix D - (Continued)

Means Comparison using Scheffe' Test

Dataset	Mean	Difference between	Simultaneous Confidence Intervals		Significant at 0.001
Data4_A	53.40125	Means	Lower Limit	Upper Limit	Level
Data4_B	52.31271	1.08854	-34.43956	36.61664	No

Means Comparison using Tukey Test

Dataset	Mean	Difference between	Simultaneous Confidence Intervals		Significant at 0.001
Data4_A	53.40125	Means	Lower Limit	Upper Limit	Level
Data4_B	52.31271	1.08854	-34.44358	36.62065	No

One-Way ANOVA

Summary Statistics

Dataset	N	Mean	SD	SE
Data5_A	10	20.672	8.08523	2.55677
Data5_B	10	22.18756	6.93181	2.19203

Null Hypothesis: The means of all selected datasets are equal
Alternative Hypothesis: The means of one or more selected datasets are different

ANOVA

Source	DoF	Sum of Squares	Mean Square	F Value	P Value
Model	1	11.4845469	11.4845469	0.20251	0.65807
Error	18	1020.78815	56.7104530		

At the 0.001 level,
the population means are not significantly different.

Levene's Test for Equal Variance

Source	DoF	Sum of Squares	Mean Square	F Value	P Value
Model	1	1215.07472	1215.07472	0.49589	0.49032
Error	18	44105.3778	2450.29877		

Appendix D - (Continued)

At the 0.001 level,
the population variations are not significantly different.

Brown-Forsythe's Test for Equal Variance

Source	DoF	Sum of Squares	Mean Square	F Value	P Value
Model	1	4.07846833	4.07846833	0.24647	0.62558
Error	18	297.853475	16.5474153		

At the 0.001 level,
the population variations are not significantly different.

Means Comparison using Bonferroni Test

Dataset	Mean	Difference between Means	Simultaneous Confidence Intervals		Significant at 0.001 Level
Data5_A	20.672		Lower Limit	Upper Limit	
Data5_B	22.18756	-1.51556	-14.72288	11.69177	No

Means Comparison using Scheffe' Test

Dataset	Mean	Difference between Means	Simultaneous Confidence Intervals		Significant at 0.001 Level
Data5_A	20.672		Lower Limit	Upper Limit	
Data5_B	22.18756	-1.51556	-14.72288	11.69177	No

Means Comparison using Tukey Test

Dataset	Mean	Difference between Means	Simultaneous Confidence Intervals		Significant at 0.001 Level
Data5_A	20.672		Lower Limit	Upper Limit	
Data5_B	22.18756	-1.51556	-14.72304	11.69193	No

One-Way ANOVA

Summary Statistics

Dataset	N	Mean	SD	SE
Data6_A	9	20.53667	8.31463	2.77154
Data6_B	9	19.32247	6.23627	2.07876

Appendix D - (Continued)

Null Hypothesis: The means of all selected datasets are equal
Alternative Hypothesis: The means of one or more selected datasets are different

ANOVA

Source	DoF	Sum of Squares	Mean Square	F Value	P Value
Model	1	6.63421185	6.63421185	0.12283	0.73056
Error	16	864.193017	54.0120636		

At the 0.001 level,
the population means are not significantly different.

Levene's Test for Equal Variance

Source	DoF	Sum of Squares	Mean Square	F Value	P Value
Model	1	3251.86131	3251.86131	1.93966	0.18276
Error	16	26824.1150	1676.50718		

At the 0.001 level,
the population variations are not significantly different.

Brown-Forsythe's Test for Equal Variance

Source	DoF	Sum of Squares	Mean Square	F Value	P Value
Model	1	15.5135949	15.5135949	0.90549	0.35547
Error	16	274.125052	17.1328157		

At the 0.001 level,
the population variations are not significantly different.

Means Comparison using Bonferroni Test

Dataset	Mean	Difference between Means	Simultaneous Confidence Intervals		Significant at 0.001 Level
Data6_A	20.53667		Lower Limit	Upper Limit	
Data6_B	19.32247	1.21419	-12.69571	15.1241	No

Appendix D - (Continued)

Means Comparison using Scheffe' Test

Dataset	Mean	Difference between	Simultaneous Confidence Intervals		Significant at 0.001
Data6_A	20.53667	Means	Lower Limit	Upper Limit	Level
Data6_B	19.32247	1.21419	-12.69572	15.12411	No

Means Comparison using Tukey Test

Dataset	Mean	Difference between	Simultaneous Confidence Intervals		Significant at 0.001
Data6_A	20.53667	Means	Lower Limit	Upper Limit	Level
Data6_B	19.32247	1.21419	-12.6959	15.12429	No

One-Way ANOVA

Summary Statistics

Dataset	N	Mean	SD	SE
Data7_A	9	95.20889	25.37694	8.45898
Data7_B	9	91.44089	28.83911	9.61304

Null Hypothesis: The means of all selected datasets are equal
Alternative Hypothesis: The means of one or more selected datasets are different

ANOVA

Source	DoF	Sum of Squares	Mean Square	F Value	P Value
Model	1	63.8901470	63.8901470	0.08659	0.77234
Error	16	11805.4649	737.841555		

At the 0.001 level,
the population means are not significantly different.

Levene's Test for Equal Variance

Source	DoF	Sum of Squares	Mean Square	F Value	P Value
Model	1	125273.732	125273.732	0.25526	0.62028
Error	16	7852278.76	490767.422		

Appendix D - (Continued)

At the 0.001 level,
the population variations are not significantly different.

Brown-Forsythe's Test for Equal Variance

Source	DoF	Sum of Squares	Mean Square	F Value	P Value
Model	1	93.9286065	93.9286065	0.27575	0.60670
Error	16	5450.00508	340.625317		

At the 0.001 level,
the population variations are not significantly different.

Means Comparison using Bonferroni Test

Dataset	Mean	Difference between Means	Simultaneous Confidence Intervals		Significant at 0.001 Level
Data7_A	95.20889		Lower Limit	Upper Limit	
Data7_B	91.44089	3.768	-47.6435	55.1795	No

Means Comparison using Scheffe' Test

Dataset	Mean	Difference between Means	Simultaneous Confidence Intervals		Significant at 0.001 Level
Data7_A	95.20889		Lower Limit	Upper Limit	
Data7_B	91.44089	3.768	-47.64353	55.17953	No

Means Comparison using Tukey Test

Dataset	Mean	Difference between Means	Simultaneous Confidence Intervals		Significant at 0.001 Level
Data7_A	95.20889		Lower Limit	Upper Limit	
Data7_B	91.44089	3.768	-47.6442	55.1802	No

One-Way ANOVA

Summary Statistics

Dataset	N	Mean	SD	SE
Data8_A	7	97.04	26.21415	9.90802
Data8_B	7	89.70611	29.94785	11.31922

Appendix D - (Continued)

Null Hypothesis: The means of all selected datasets are equal
Alternative Hypothesis: The means of one or more selected datasets are different

ANOVA

Source	DoF	Sum of Squares	Mean Square	F Value	P Value
Model	1	188.250775	188.250775	0.23768	0.63467
Error	12	9504.33036	792.027530		

At the 0.001 level,
the population means are not significantly different.

Levene's Test for Equal Variance

Source	DoF	Sum of Squares	Mean Square	F Value	P Value
Model	1	113067.452	113067.452	0.16184	0.69454
Error	12	8383656.13	698638.011		

At the 0.001 level,
the population variations are not significantly different.

Brown-Forsythe's Test for Equal Variance

Source	DoF	Sum of Squares	Mean Square	F Value	P Value
Model	1	97.5265569	97.5265569	0.28555	0.60284
Error	12	4098.42656	341.535546		

At the 0.001 level,
the population variations are not significantly different.

Means Comparison using Bonferroni Test

Dataset	Mean	Difference between Means	Simultaneous Confidence Intervals		Significant at 0.001 Level
Data8_A	97.04		Lower Limit	Upper Limit	
Data8_B	89.70611	7.33389	-57.61875	72.28653	No

Appendix D - (Continued)

Means Comparison using Scheffe' Test

Dataset	Mean	Difference between	Simultaneous Confidence Intervals		Significant at 0.001
Data8_A	97.04	Means	Lower Limit	Upper Limit	Level
Data8_B	89.70611	7.33389	-57.61874	72.28652	No

Means Comparison using Tukey Test

Dataset	Mean	Difference between	Simultaneous Confidence Intervals		Significant at 0.001
Data8_A	97.04	Means	Lower Limit	Upper Limit	Level
Data8_B	89.70611	7.33389	-57.62135	72.28913	No

One-Way ANOVA

Summary Statistics

Dataset	N	Mean	SD	SE
Data9_A	9	55.00444	17.20626	5.73542
Data9_B	9	54.33911	17.13775	5.71258

Null Hypothesis: The means of all selected datasets are equal
Alternative Hypothesis: The means of one or more selected datasets are different

ANOVA

Source	DoF	Sum of Squares	Mean Square	F Value	P Value
Model	1	1.99200584	1.99200584	0.00676	0.93551
Error	16	4718.06536	294.879085		

At the 0.001 level,
the population means are not significantly different.

Levene's Test for Equal Variance

Source	DoF	Sum of Squares	Mean Square	F Value	P Value
Model	1	19.6846527	19.6846527	0.00028	0.98679
Error	16	1114199.61	69637.4756		

Appendix D - (Continued)

At the 0.001 level,
the population variations are not significantly different.

Brown-Forsythe's Test for Equal Variance

Source	DoF	Sum of Squares	Mean Square	F Value	P Value
Model	1	0.291880244	0.291880244	0.00287	0.95794
Error	16	1627.41823	101.713640		

At the 0.001 level,
the population variations are not significantly different.

Means Comparison using Bonferroni Test

Dataset	Mean	Difference between Means	Simultaneous Confidence Intervals		Significant at 0.001 Level
Data9_A	55.00444		Lower Limit	Upper Limit	
Data9_B	54.33911	0.66533	-31.83596	33.16663	No

Means Comparison using Scheffe' Test

Dataset	Mean	Difference between Means	Simultaneous Confidence Intervals		Significant at 0.001 Level
Data9_A	55.00444		Lower Limit	Upper Limit	
Data9_B	54.33911	0.66533	-31.83598	33.16665	No

Means Comparison using Tukey Test

Dataset	Mean	Difference between Means	Simultaneous Confidence Intervals		Significant at 0.001 Level
Data9_A	55.00444		Lower Limit	Upper Limit	
Data9_B	54.33911	0.66533	-31.83641	33.16707	No

One-Way ANOVA

Summary Statistics

Dataset	N	Mean	SD	SE
Data10_A	8	59.49	18.19189	6.4318
Data10_B	8	54.78522	17.94555	6.34471

Appendix D - (Continued)

Null Hypothesis: The means of all selected datasets are equal
Alternative Hypothesis: The means of one or more selected datasets are different

ANOVA

Source	DoF	Sum of Squares	Mean Square	F Value	P Value
Model	1	88.5396517	88.5396517	0.27118	0.61068
Error	14	4570.91391	326.493851		

At the 0.001 level,
the population means are not significantly different.

Levene's Test for Equal Variance

Source	DoF	Sum of Squares	Mean Square	F Value	P Value
Model	1	242.696599	242.696599	0.00430	0.94861
Error	14	789259.170	56375.6550		

At the 0.001 level,
the population variations are not significantly different.

Brown-Forsythe's Test for Equal Variance

Source	DoF	Sum of Squares	Mean Square	F Value	P Value
Model	1	11.4038241	11.4038241	0.18142	0.67663
Error	14	880.041930	62.8601378		

At the 0.001 level,
the population variations are not significantly different.

Means Comparison using Bonferroni Test

Dataset	Mean	Difference between Means	Simultaneous Confidence Intervals		Significant at 0.001 Level
Data10_A	59.49		Lower Limit	Upper Limit	
Data10_B	54.78522	4.70478	-32.70242	42.11197	No

Appendix D - (Continued)

Means Comparison using Scheffe' Test

Dataset	Mean	Difference between	Simultaneous Confidence Intervals		Significant at 0.001
Data10_A	59.49	Means	Lower Limit	Upper Limit	Level
Data10_B	54.78522	4.70478	-32.70244	42.11199	No

Means Comparison using Tukey Test

Dataset	Mean	Difference between	Simultaneous Confidence Intervals		Significant at 0.001
Data10_A	59.49	Means	Lower Limit	Upper Limit	Level
Data10_B	54.78522	4.70478	-32.70666	42.11621	No

One-Way ANOVA

Summary Statistics

Dataset	N	Mean	SD	SE
Data11_A	9	18.95222	9.10479	3.03493
Data11_B	9	24.00321	7.57026	2.52342

Null Hypothesis: The means of all selected datasets are equal
Alternative Hypothesis: The means of one or more selected datasets are different

ANOVA

Source	DoF	Sum of Squares	Mean Square	F Value	P Value
Model	1	114.805956	114.805956	1.63768	0.21889
Error	16	1121.64728	70.1029552		

At the 0.001 level,
the population means are not significantly different.

Levene's Test for Equal Variance

Source	DoF	Sum of Squares	Mean Square	F Value	P Value
Model	1	2328.04464	2328.04464	0.53005	0.47711
Error	16	70274.1177	4392.13236		

Appendix D - (Continued)

At the 0.001 level,
the population variations are not significantly different.

Brown-Forsythe's Test for Equal Variance

Source	DoF	Sum of Squares	Mean Square	F Value	P Value
Model	1	5.50360425	5.50360425	0.16862	0.68679
Error	16	522.239998	32.6399999		

At the 0.001 level,
the population variations are not significantly different.

Means Comparison using Bonferroni Test

Dataset	Mean	Difference between Means	Simultaneous Confidence Intervals Lower Limit	Upper Limit	Significant at 0.001 Level
Data11_A	18.95222				
Data11_B	24.00321	-5.05098	-20.89798	10.79601	No

Means Comparison using Scheffe' Test

Dataset	Mean	Difference between Means	Simultaneous Confidence Intervals Lower Limit	Upper Limit	Significant at 0.001 Level
Data11_A	18.95222				
Data11_B	24.00321	-5.05098	-20.89799	10.79602	No

Means Comparison using Tukey Test

Dataset	Mean	Difference between Means	Simultaneous Confidence Intervals Lower Limit	Upper Limit	Significant at 0.001 Level
Data11_A	18.95222				
Data11_B	24.00321	-5.05098	-20.89819	10.79623	No

One-Way ANOVA

Summary Statistics

Dataset	N	Mean	SD	SE
Data12_A	7	17.12	9.2877	3.51042
Data12_B	7	20.79255	6.94147	2.62363

Appendix D - (Continued)

Null Hypothesis: The means of all selected datasets are equal
Alternative Hypothesis: The means of one or more selected datasets are different

ANOVA

Source	DoF	Sum of Squares	Mean Square	F Value	P Value
Model	1	47.2065867	47.2065867	0.70224	0.41841
Error	12	806.672149	67.2226791		

At the 0.001 level,
the population means are not significantly different.

Levene's Test for Equal Variance

Source	DoF	Sum of Squares	Mean Square	F Value	P Value
Model	1	3728.29263	3728.29263	1.17211	0.30024
Error	12	38170.2036	3180.85030		

At the 0.001 level,
the population variations are not significantly different.

Brown-Forsythe's Test for Equal Variance

Source	DoF	Sum of Squares	Mean Square	F Value	P Value
Model	1	11.4814494	11.4814494	0.42726	0.52566
Error	12	322.464638	26.8720532		

At the 0.001 level,
the population variations are not significantly different.

Means Comparison using Bonferroni Test

Dataset	Mean	Difference between Means	Simultaneous Confidence Intervals		Significant at 0.001 Level
Data12_A	17.12		Lower Limit	Upper Limit	
Data12_B	20.79255	-3.67255	-22.59531	15.25022	No

Appendix D - (Continued)

Means Comparison using Scheffe' Test

Dataset	Mean	Difference between	Simultaneous Confidence Intervals		Significant at 0.001
Data12_A	17.12	Means	Lower Limit	Upper Limit	Level
Data12_B	20.79255	-3.67255	-22.59531	15.25021	No

Means Comparison using Tukey Test

Dataset	Mean	Difference between	Simultaneous Confidence Intervals		Significant at 0.001
Data12_A	17.12	Means	Lower Limit	Upper Limit	Level
Data12_B	20.79255	-3.67255	-22.59607	15.25098	No

Appendix E – Glossary

Adsorbate	A substance that is adsorbed
Adsorbent	A material having capacity or tendency to adsorb another substance
Adsorption	The accumulation of gases, liquids, or solutes on the surface of a solid or liquid
Alkylation	The replacement of a hydrogen atom in an organic compound by an alkyl group
Allosteric	Pertaining to regulation of the rate of an enzymatic process
Allotropic	The existence, especially in the solid state, of two or more crystalline or molecular structural forms of an element
Arsenate	A salt or ester of arsenic acid containing 5 Oxygens
Arsenite	A salt or ester of arsenic acid containing 3 Oxygens
Arsenopyrite	A common mineral, iron arsenic sulfide, FeAsS, occurring in silver-white to steel-gray crystals or masses: an ore of arsenic
Bed	A compact mass of a substance functioning in a reaction as a catalyst or reactant
Cake Layer	A crust or compact mass
Chabazite	A zeolite mineral, essentially a hydrated sodium calcium aluminum silicate, occurring usually in red to colorless rhombohedral crystals
Chemisorption	Adsorption involving a chemical linkage between the adsorbent and the adsorbate
Colloidal	A system in which finely divided particles, which are approximately 10 to 10,000 angstroms in size, are dispersed within a continuous medium in a manner that prevents them from being filtered easily or settled rapidly
Complexation	To form a compound in which independently existing molecules or ions of a nonmetal form coordinate bonds with a metal atom or ion.
Cracking	The process of breaking down certain hydrocarbons into simpler ones of lower boiling points by means of excess heat, distillation under pressure, etc., in order to give a greater yield of low-boiling products than could be obtained by simple distillation
Crossflow	Filtration in which some feed water passes parallel to the surface of filtration without being filtered
Cryosorption	Sorption occurring on a cold surface
Deadend	Filtration in which all feed water is filtered

Appendix E - (Continued)

Dehyroxylating	To remove a hydroxyl group from a compound
Desiccant	A substance, such as calcium oxide or silica gel, that has a high affinity for water and is used as a drying agent
Divalent	Having a valence of two
Enthalpy	A thermodynamic function of a system, equivalent to the sum of the internal energy of the system plus the product of its volume multiplied by the pressure exerted on it by its surroundings
Flux	The rate of flow of fluid, particles, or energy through a given surface
HDTMA	A surfactant, hexadecyltrimethylammonium bromide
Hydrocracking	The process whereby hydrocarbon molecules of petroleum are broken down into kerosene and gasolene by the addition of hydrogen under high pressure in the presence of a catalyst
Isomerization	The conversion of a compound into an isomer of itself
Isotherms	Functions which connect the amount of adsorbate on the adsorbent,
Lumen	A cavity or passage in a tubular shape
Methylate	To replace (one or more hydrogen atoms) with the methyl group
Microfiltration	A filtration process which removes contaminants from a fluid or gas by passage through a microporous membrane. A typical microfiltration membrane pore size range is 0.1-10µm
Monovalent	Having a valence of one; univalent.
Nanofiltration	Variety of membrane filtration in which hydrostatic pressure forces a liquid against a semipermeable membrane. Suspended solids and solutes of high molecular weight (0.001 µm and larger) are retained, while water and low molecular weight solutes pass through the membrane.
Polymer	A chemical compound or mixture of compounds formed by polymerization and consisting essentially of repeating structural units
Potable	Fit or suitable for drinking
ppb	Parts per billion or µg/L
ppm	Parts per million or mg/L
Sieving	To put or force through a sieve; sift
Slurries	A thin mixture of an insoluble substance, as cement, clay, or coal, with a liquid, as water or oil
Smelting	To melt or fuse (ores) in order to separate the metallic constituents

Appendix E - (Continued)

Substrate	An underlying layer; a substratum
Ultrafiltration	Variety of membrane filtration in which hydrostatic pressure forces a liquid against a semipermeable membrane. Suspended solids and solutes of high molecular weight (0.01 µm and larger) are retained, while water and low molecular weight solutes pass through the membrane.
USEPA	United States Environmental Protection Agency

All definitions reproduced from www.Dictionary.com.

ABOUT THE AUTHOR

Miles Beamguard, son of Jim and Dewana Beamguard, grew up in Midlothian, VA. After graduating with a Bachelor in Mechanical Engineering from Georgia Tech in 1996, he hiked the Appalachian Trail from Georgia to Maine. This was the first time he realized the importance of drinking water. After completing the 2160 mile journey, Miles began working in the membrane field for Suez Lyonnaise de Seux. This work in membranes led him to begin consulting for Malcolm Pirnie. After discussing with several colleagues of Dr. Carnahan, Miles decided to pursue his Ph.D. at the University of South Florida. While in school, Miles continued to work in the field and gather practical experience. In the process of working on his Ph.D., Miles has received his Masters and co-developed WHB Environmental, LLC, an independent, WBE, consulting firm. He plans to continue consulting and perhaps teach as an Adjunct Professor in the Tampa area.